

GTL DIESEL WAY FORWARD TO IMPROVE PROPERTIES BY SEPARATING
LIGHT ENDS AND FORMULATING THE SPECIFICATIONS

A Thesis

By

MOSTAFA MOHAMED MOHAMED IBRAHIM SHAHIN

Submitted to the Office of Graduate and Professional Studies of
Texas A&M University
In partial fulfillment of the requirements for the degree of

MASTER OF SCIENCE

Chair of Committee, Nimir Elbashir
Committee Members, Mahmoud M. El-Halwagi
 Ibrahim Hassan

Head of Department, Nazmul Karim

May 2016

Major Subject: Chemical Engineering

Copyright 2016 Mostafa Mohamed Mohamed Ibrahim Shahin

ABSTRACT

Gas-To-Liquid (GTL) Diesel fuel produced from synthetic crudes obtained from natural gas that is converted by the Fisher Tropsch (FT) technology is a promising key player for the mobility industry future along with conventional diesel fuels. The main distinctive properties that distinguish between GTL Diesel and conventional Diesel fuels include density, viscosity, lubricity and Cetane Index. The aim of this study was to identify the effect of the change in GTL Diesel's composition and boiling range on its market specifications, then to develop predictive models for the GTL Diesel properties based on the fuel's composition. The study recommends how the industry can use these data for upgrading the fuel quality based on distribution market demand. Intensive testing to analyze many characteristics for GTL Diesel was done at Texas A&M University at Qatar (TAMUQ), and ORYX GTL Company provided the GTL Diesel samples. The study was divided into two sections; the first section consisted of the experimental and modeling work where multiple GTL Diesel cuts were initially prepared. The properties of the prepared cuts were analyzed for five critical GTL Diesel fuel market specifications: Density, Viscosity (kinematic and dynamic), Flash point, Cetane index and Cold properties (Pour and Cloud points). In the second section, these properties were compared with the original market specifications in order to identify whether an improvement in fuel characteristics is obtained. In the third section, the properties of these fuel cuts are used to generate mathematical models for properties-compositions relationships. Finally, we proposed certain modifications to the existing GTL Plants that will improve the separation of specific quality of fuels and value-added chemicals cut. This study also

identified the potentials for the light cuts obtained from GTL Diesel fuel to be used for the production of Linear Alkyl Benzene (LAB), which is considered as an expensive value-chemical and a feedstock to detergents manufacturing plants.

DEDICATION

To my family, wife and kids.

To my company ORYX GTL.

ACKNOWLEDGEMENTS

I would like to acknowledge my committee chair, Prof. Elbashir, and my committee members, Prof. El-Halwagi, and Prof. Hassan, for their thorough guidance, support and knowledge they shared throughout the journey of the research.

It is my pleasure to recognize my friends, colleagues, and the Chemical Engineering program faculty members for enhancing my valuable time at TAMUQ. I would like to extend my appreciation to all research team members for giving time to my research and helping me in conducting experimental activities necessary to achieve the research target.

Last but not least, I would like to extend my special thanks to my wife for her unlimited support and patience.

NOMENCLATURE

Ar	Aromatic
ASTM	American Society of Testing Materials
BC	Branched Carbon
°C	Degree Celsius
CAS	Chemical Abstracts Service
CFPP	Cloud filter Plug Point
Co	Company
CO	Carbon Monoxide
CP	Cloud Point
CN	Carbon Number
cSt	centi-Stoke
EU	European Union
FBP	Final Boiling Point
FCL	Fuel Characterizations Lab
FP	Flash Point
FT	Fisher Tropsch

GC	Gas Chromatography
GCC	Gulf Cooperation Council
GTL	Gas-to-Liquid
HC	Hydrocarbon
IBP	Initial Boiling Point
i-	<i>iso</i>
LAB	Linear Alkyl Benzene
LPG	Liquefied Petroleum Gas
mb/d	million barrel per day
mPa.S	milli-bar second
mm ² /s	millimeter squared per second
n-	Normal
NG	Natural Gas
PM	Particulate Materials
PP	Pour Point
PPE	Personal Protection Equipment
SPK	Synthetic Paraffinic Kerosene
TAMUQ	Texas A&M University at Qatar

T ₁₀	Temperature at which boils 10% (v/v) according to ASTM D 86.
T ₂₀	Temperature at which boils 20% (v/v) according to ASTM D 86.
T ₅₀	Temperature at which boils 50% (v/v) according to ASTM D 86.
T ₉₀	Temperature at which boils 90% (v/v) according to ASTM D 86.
ULSD	Ultra Low Sulfur Diesel
Wt	Weight

TABLE OF CONTENTS

	Page
ABSTRACT.....	ii
DEDICATION.....	iv
ACKNOWLEDGEMENTS.....	v
NOMENCLATURE.....	vi
TABLE OF CONTENTS.....	ix
LIST OF FIGURES.....	xii
LIST OF TABLES.....	xvii
CHAPTER I INTRODUCTION AND LITERATURE REVIEW	1
1.1 Introduction	1
1.1.1 Diesel Fuel Grades	7
1.1.2 GTL Diesel Grades.....	9
1.2 Literature Review	11
1.3 Industry and Academic Research Consortium Activities in GTL Diesel Fuels....	15
CHAPTER II RESEARCH PROBLEM AND OBJECTIVES	18
2.1 Research Problem.....	18
2.2 Research Objectives	19
CHAPTER III RESEARCH METHODOLOGY	20
CHAPTER IV EXPERIMENTAL SETUP.....	23
4.1 Experiment Design.....	26
4.1.1 GTL Diesel Fractionation.....	29
4.1.2 Atmospheric Distillation Analysis	32
4.1.3 Carbon Distribution.....	32
4.1.4 Density Analysis.....	33
4.1.5 Viscosity Analysis	34
4.1.6 Flash Point Analysis	35
4.1.7 Cloud and Pour Points Analysis	37

CHAPTER V RESULTS AND DISCUSSION	38
5.1 GTL Diesel Fractionation.....	38
5.2 Carbon Distribution for GTL Diesel Heavy Cuts	39
5.3 Carbon Distribution for GTL Diesel Light Cuts	42
5.4 Atmospheric Distillation	42
5.5 Density Analysis	45
5.6 Viscosity Analysis.....	46
5.7 Flash Point Analysis.....	48
5.8 Cloud and Pour Point Analysis	49
5.9 Cetane Index Calculation	51
CHAPTER VI MODELING	54
6.1 Cloud Point Model, using Distillation Data	58
6.1.1 Using Literature Regression Coefficients (Model Testing)	58
6.1.2 Using Estimated LINGO Regression Coefficients (Calibrating Model).....	60
6.2 Modeling the Kinematic Viscosity using Distillation Data	61
6.2.1 Using Literature Regression Coefficients (Model Testing)	61
6.2.2 Using Estimated LINGO Regression Coefficients (Calibrating Model).....	64
6.3 Various Properties Model, using Normal and <i>iso</i> Paraffin Data.....	66
6.3.1 Using Literature Regression Coefficients (Model Testing)	66
6.3.2 Using Estimated LINGO Regression Coefficients (Calibration Model).....	69
6.4 Various Properties Model, using Individual Carbon Number Distribution Data (Empirical Model)	72
6.5 Various Properties Model, using Total Carbon Number Grouping Data (Empirical Model)	76
CHAPTER VII CONCLUSIONS AND RECOMMENDATIONS	80
REFERENCES	87
APPENDIX A– EXPERIMENTS GUIDELINES	90
A.1 Atmospheric Distillation	90
A.2 Density Analysis.....	91
A.3 Viscosity Analysis.....	93
A.4 Flash Point Analysis	95
A.5 Cloud Point and Pour Point Analysis	97
APPENDIX B – EXPERIMENTAL RESULTS	98
B.1 Gas Chromatograph Analysis	100
APPENDIX C – LINGO PROGRAMMING.....	111

APPENDIX D – LINGO CALCULATIONS RESULTS 141

LIST OF FIGURES

	Page
Figure 1.1 Sequence of the GTL process including the Fischer Tropsch synthesis.....	2
Figure 1.2 FT products blend carbon number distribution [21].....	3
Figure 1.3 Global product demand, 2013 and 2040 [4].....	5
Figure 1.4 Non-OPEC other liquids supply by type and region, 2013 and 2040 [4].....	6
Figure 1.5 Research consortium to study GTL diesel effect on emissions and engine performance [17].....	16
Figure 1.6 ORYX GTL consortium to study the effect of GTL Diesel on school buses.....	17
Figure 4.1 Pillars of quality management system.....	27
Figure 4.2 Pillars of data management system.....	27
Figure 4.3 FCL LAB fractionation column sketch.....	31
Figure 4.4 B/R instrument corporation fractionation column and control unit.....	31
Figure 4.5 ASTM D86 atmospheric distillation Petrotest ADU4+.....	32
Figure 4.6 Aglien GC/MS with mass selective detector.....	33
Figure 4.7 Density analyzer Anton Paar DMA 4100.....	34
Figure 4.8 Viscosity analyzer Anton Paar SVM 3000.....	35
Figure 4.9 Flash point automated Pensky-Martens.....	36
Figure 4.10 Cloud and pour point analyzing device.....	37
Figure 5.1 Light to heavy GTL Diesel cuts volume percentage.....	39
Figure 5.2 Overall carbon distributions for heavy cuts.....	40

Figure 5.3	The effect of IBP on GTL Diesel carbon number grouping for heavy cuts.....	41
Figure 5.4	The effect of IBP on carbon number distribution for light cuts.....	42
Figure 5.5	The effect of IBP on D86 distillation data for GTL Diesel cuts.....	43
Figure 5.6	Change of T ₁₀ , T ₂₀ , T ₅₀ and T ₉₀ distillation data with IBP of the cut.....	44
Figure 5.7	Density of GTL Diesel heavy cuts compared with market specification (min. 760 kg/m ³ and max. 780 kg/m ³).....	45
Figure 5.8	Change of GTL Diesel heavy cuts with the change of average boiling range.....	46
Figure 5.9	Kinematic viscosity of heavy GTL Diesel cuts compared with market specification (1.5 to 4.5 cSt).....	47
Figure 5.10	Change of dynamic viscosity of GTL Diesel heavy Cuts with the change of IBP.	48
Figure 5.11	Flash point of GTL Diesel heavy cuts compared with market specification.....	49
Figure 5.12	Cloud point of GTL Diesel heavy cuts compared with market specification.....	50
Figure 5.13	Pour point of GTL Diesel heavy cuts.....	51
Figure 5.14	The impact of IBP change on GTL Diesel heavy cuts calculated Cetane Index.....	53
Figure 6.1	Cloud point calculated using literature regressions and Eq. 6.1 vs. Lab measured at different IBP	59
Figure 6.2	Cloud point calculated vs. measured at different IBP using LINGO regressions.....	60
Figure 6.3	Kinematic viscosity measure vs. calculated using literature regressions coefficients [30].....	63

Figure 6.4	Kinematic viscosity measure vs. calculated using LINGO new regression coefficients.....	64
Figure 6.5	GTL Diesel calculated vs. measured CP using paraffins content and literature regressions [11].....	68
Figure 6.6	GTL Diesel calculated vs. measured density using paraffins content and literature regressions [11].....	68
Figure 6.7	GTL Diesel calculated vs. ASTM Cetane Index using paraffins content and literature regressions [11].....	69
Figure 6.8	Calculated vs. measured cloud point using LINGO new coefficients.....	70
Figure 6.9	Calculated vs. measured density using LINGO new coefficients.....	71
Figure 6.10	Calculated vs. measured dynamic viscosity using LINGO new coefficients.....	71
Figure 6.11	Calculated vs. measured flash point using LINGO new coefficients.....	72
Figure 6.12	Measured vs. calculated cloud point using individual CN at different IBP.....	74
Figure 6.13	Measured vs. calculated density using individual CN at different IBP.....	74
Figure 6.14	Measured vs. calculated dynamic viscosity using individual CN at different IBP.....	75
Figure 6.15	Measured vs. calculated flash point using individual CN at different IBP.....	75
Figure 6.16	Measured vs. calculated cloud point using CN grouping at different IBP.....	77
Figure 6.17	Measured vs. calculated density using CN grouping at different IBP.....	78

Figure 6.18	Measured vs. calculated dynamic viscosity using CN grouping at different IBP.....	78
Figure 6.19	Measured vs. calculated flash point using CN grouping at different IBP.....	79
Figure 7.1	Two possible modifications to existing GTL facility to produce additional products.....	84
Figure A.1	Flash point test finish screen.....	96
Figure B-1	GTL Diesel whole cut GC carbon distribution analysis.....	100
Figure B-2	GTL Diesel cut >130° GC carbon distribution analysis.....	101
Figure B-3	GTL Diesel cut >140° GC carbon distribution analysis	101
Figure B-4	GTL Diesel cut >150° GC carbon distribution analysis	101
Figure B-5	GTL Diesel cut >160° GC carbon distribution analysis	102
Figure B-6	GTL Diesel cut >170° GC carbon distribution analysis	102
Figure B-7	GTL Diesel cut >180° GC carbon distribution analysis	102
Figure B-8	GTL Diesel cut >190° GC carbon distribution analysis	103
Figure B-9	GTL Diesel cut >200° GC carbon distribution analysis	103
Figure B-10	GTL Diesel cut >210° GC carbon distribution analysis	103
Figure B-11	GTL Diesel cut >215° GC carbon distribution analysis	104
Figure B-12	GTL Diesel cut <130° GC carbon distribution analysis	104
Figure B-13	GTL Diesel cut <140° GC carbon distribution analysis	104
Figure B-14	GTL Diesel cut <150° GC carbon distribution analysis	104
Figure B-15	GTL Diesel cut <160° GC carbon distribution analysis	105
Figure B-16	GTL Diesel cut <170° GC carbon distribution analysis	105
Figure B-17	GTL Diesel cut <180° GC carbon distribution analysis	106

Figure B-18	GTL Diesel cut <190° GC carbon distribution analysis	106
Figure B-19	GTL Diesel cut <200° GC carbon distribution analysis	106
Figure B-20	GTL Diesel cut <210° GC carbon distribution analysis	107
Figure B-21	GTL Diesel cut <215° GC carbon distribution analysis	107

LIST OF TABLES

	Page	
Table 1.1	Global product demand, shares and growth, 2013–2040 [4]....	4
Table 1.2	GTL Diesel typical carbon content compared to ULSD [6]....	7
Table 1.3	ASTM D 975 requirements for diesel fuel oils.....	8
Table 1.4	Marketing specification for GTL Diesel.....	10
Table 1.5	Relevant literature in the field of this study.....	12
Table 3.1	GTL Diesel cuts IBP.....	20
Table 3.2	Standard test methods.....	21
Table 4.1	List of chemical used for the experimental activities.....	25
Table 4.2	List of glass wares.....	25
Table 4.3	List of materials / utilities.....	25
Table 4.4	LAB PPE and safety equipment.....	25
Table 4.5	ASTM tests repeatability and reproducibility values.....	28
Table 5.1	Light and heavy cuts percentage volume at different IBP's and 100 mbar	38
Table 6.1	Calculation of cloud point from distillation data.....	59
Table 6.2	Calculation of kinematic viscosity from distillation data, literature regressions coefficients.....	62
Table 6.3	Calculation of kinematic viscosity using distillation data, new regressions coefficients.....	65
Table 6.4	Literature regression coefficients for various properties.....	66

Table 6.5	Calculation of various properties using n, <i>iso</i> paraffins and literatures regressions.....	67
Table 6.6	New estimated regressions coefficients using LINGO for n, <i>iso</i> paraffins.....	70
Table 6.7	Estimated regressions coefficients using LINGO for individual CN.....	73
Table 6.8	Estimated regressions coefficients using LINGO for CN grouping.....	77
Table 7.1	Proposed GTL Diesel new specification formulation.....	82
Table 7.2	GTL Diesel properties prediction equations, standard error....	83
Table B-1	GTL Diesel whole cut analysis.....	98
Table B-2	Carbon distribution for heavy GTL Diesel fractions.....	99
Table B-3	Carbon distribution for light GTL Diesel fractions.....	99
Table B-4	Distillation results for GTL Diesel heavy cuts.....	108
Table B-5	Cloud and pour point results for GTL Diesel heavy cuts.....	108
Table B-6	Dynamic and kinematic viscosity results for GTL Diesel heavy cuts.....	109
Table B-7	Flash point results for GTL Diesel heavy cuts.....	110
Table B-8	Density results for GTL Diesel heavy cuts.....	110
Table D-1	Cloud point calculation using LINGO with various methods...	141
Table D-2	Density calculation using LINGO with various methods.....	141
Table D-3	Dynamic viscosity calculation using LINGO with various methods.....	142
Table D-4	Flash point calculation using LINGO with various methods.....	142

CHAPTER I

INTRODUCTION AND LITERATURE REVIEW

1.1 Introduction

Gas-to-Liquid (GTL) technology is a chemical process to convert natural gas into synthetic crude that can be further processed into hydrocarbon products. The GTL process first reform methane into synthesis gas, a mixture of hydrogen and carbon monoxide, that later converted over a surface of cobalt or iron catalyst into longer chain hydrocarbons similar to those that comprise crude oils. The former conversion technology used is based on the Fischer-Tropsch synthesis.

Franz Fischer and Hans Tropsch developed first Fisher-Tropsch (FT) Technology at the "Kaiser-Wilhelm-Institut für Kohlenforschung" in Mülheim Van der Ruhr (Germany), by the early 1920s; and their technology was patented in 1930 [1]. In the (FT) process, the feedstock can be either solid (coal), liquid (refinery residuals) or gas that either naturally exists (natural gas) or is produced from biomass feedstock. Syngas is produced by reaction of main feed natural gas (NG) and oxygen in a reforming process; the commercial reforming technologies for natural gas could be steam reforming, partial oxidation and auto-thermal reformer.

Nowadays GTL mostly refers to Natural Gas conversion that results in an extremely pure synthetic crude (syncrude) that is virtually free of contaminants such as sulfur, aromatics and metals. The synthetic crude produced from FT can be refined into products such as LPG, naphtha, jet fuel, diesel fuel and lubricant oils, by further

processing into Hydrocracker units. The synthetic crude reacts with hydrogen inside the Hydrocracker units, and then splits using a distillation facility to produce the required hydrocarbon products' slates as shown in Figure 1.1[21].

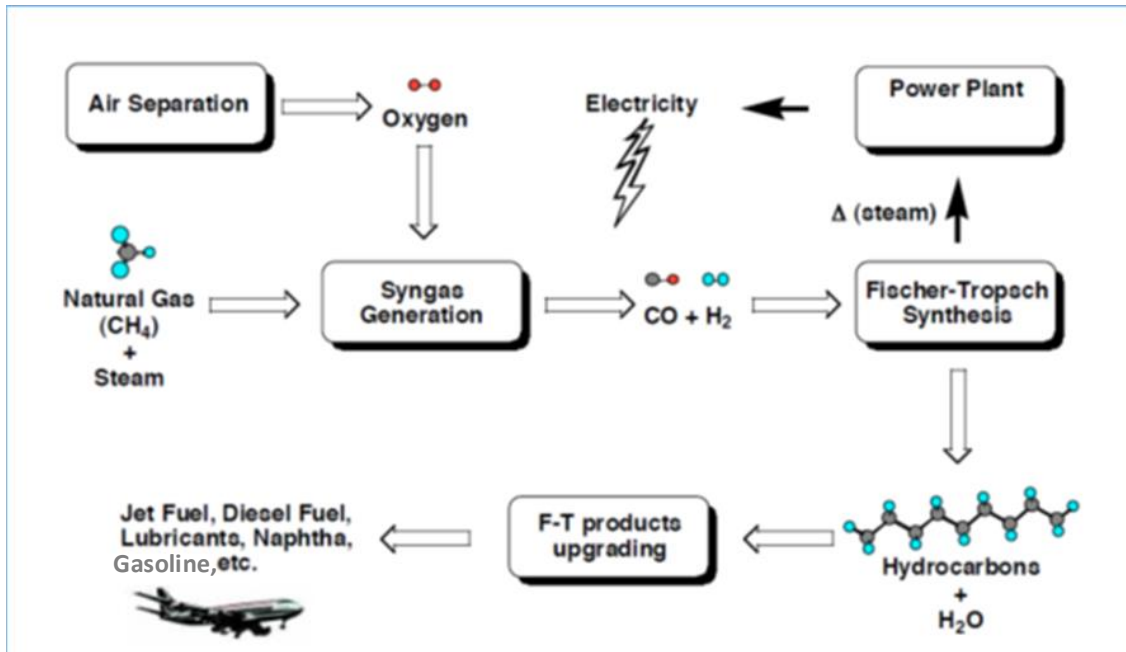


Figure 1.1 Sequence of the GTL process including the Fischer Tropsch synthesis [21]

Typically, the carbon number distribution for FT products ranges from C_1 to C_{60} (boiling range -164°C to 620°C) based on the selectivity of the FT catalyst and media of reaction, as shown in Figure 1.2 [21].

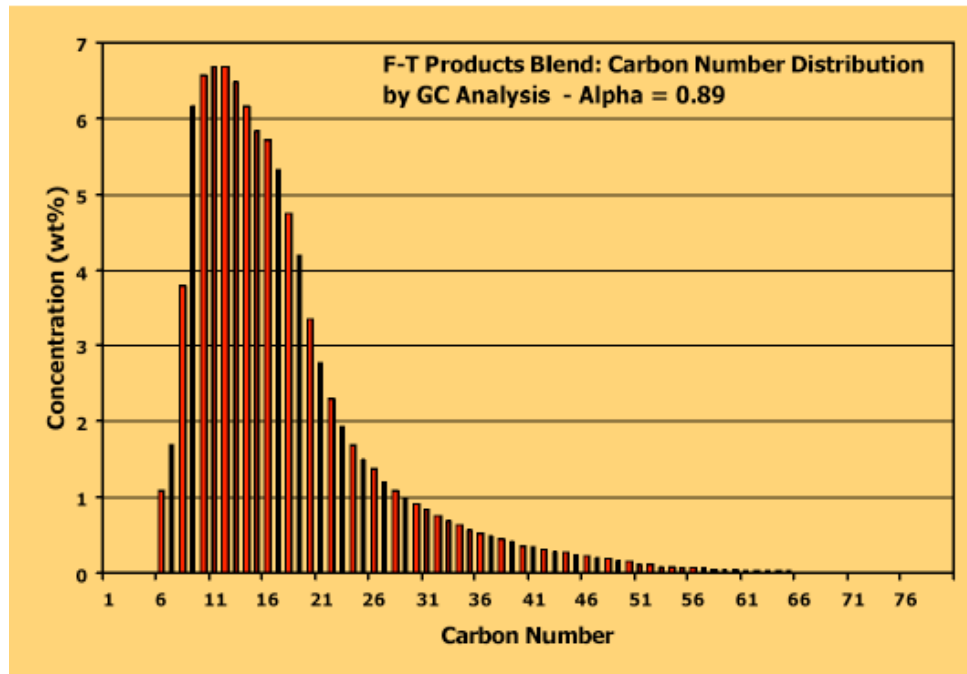


Figure 1.2 FT products blend carbon number distribution [21]

Qatar is a member of Gulf Cooperation Council (GCC) that consists of Bahrain, Kuwait, Oman, Qatar, Saudi Arabia, and the United Arab Emirates; they are all located at the Arab Gulf. Qatar has the world's largest per capita production and proven reserves of both oil and natural gas, its Natural Gas reserve is 871.5 trillion cubic feet (tcf). Also, Qatar is considered the world capital of gas processing technology. Specifically in the GTL field, Qatar in 2003 built the first commercial GTL plant, ORYX GTL, which is a joint venture between Qatar Petroleum (QP) and SASOL. The main synthetic products of the plant are GTL Diesel, Naphtha and LPG. In 2007, ORYX GTL sold its first products to the global market. Since that time, GTL products are satisfying the market needs for GTL Diesel fuel as a blend stock, GTL naphtha as a petrochemical feedstock and LPG as an export fuel.

In 2011, another mega GTL plant was built in Qatar to produce GTL products on a very large scale. Shell Pearl GTL Plant located in Ras Laffan Industrial City is the world's largest GTL plant to turn natural gas into cleaner-burning fuels. Shell is making steady progress in ramping up the production, after selling the first commercial shipment of GTL Gasoil in June 2011. These plants are helping to meet the world's growing demand for cleaner fuels and value-added chemicals [3].

As shown in Table 1.1 and Figure 1.3, the global demand for petroleum products is increasing. Comparing the fuel demands of the years 2013 and 2040, the highest growth rates and shares are for Diesel/Gasoil. Diesel/Gasoil global demand in 2013 was 26.1 million barrel/day (mb/d) and is expected to increase to 36.1 mb/d by 2040[4].

Table 1.1 Global product demand, shares and growth, 2013–2040 [4]

	Global demand mb/d								Growth rates			Shares	
									% p.a.		%		
	2013	2015	2020	2025	2030	2035	2040	2013–2020	2020–2040	2013–2040	2013	2040	
Light products													
Ethane/LPG	10.0	10.3	11.0	11.6	12.1	12.4	12.6	1.4	0.7	0.9	11.1	11.4	
Naphtha	6.0	6.2	6.6	7.1	7.6	8.1	8.8	1.3	1.4	1.4	6.7	7.9	
Gasoline	23.0	23.6	24.6	25.4	25.9	26.3	26.7	1.0	0.4	0.6	25.5	24.0	
Middle distillates													
Jet/Kerosene	6.6	6.8	7.3	7.8	8.2	8.7	9.2	1.4	1.1	1.2	7.4	8.2	
Diesel/Gasoil	26.1	27.1	29.7	31.7	33.3	34.7	36.1	1.9	1.0	1.2	29.0	32.5	
Heavy products													
Residual fuel*	8.0	7.8	7.1	6.9	6.6	6.3	6.0	-1.6	-0.9	-1.1	8.9	5.4	
Other**	10.4	10.4	10.6	10.9	11.2	11.5	11.8	0.3	0.5	0.5	11.5	10.6	
Total	90.0	92.3	96.9	101.3	104.8	108.0	111.1	1.1	0.7	0.8	100.0	100.0	

* Includes refinery fuel oil.
** Includes bitumen, lubricants, petroleum coke, waxes, still gas, sulphur, direct use of crude oil, etc.

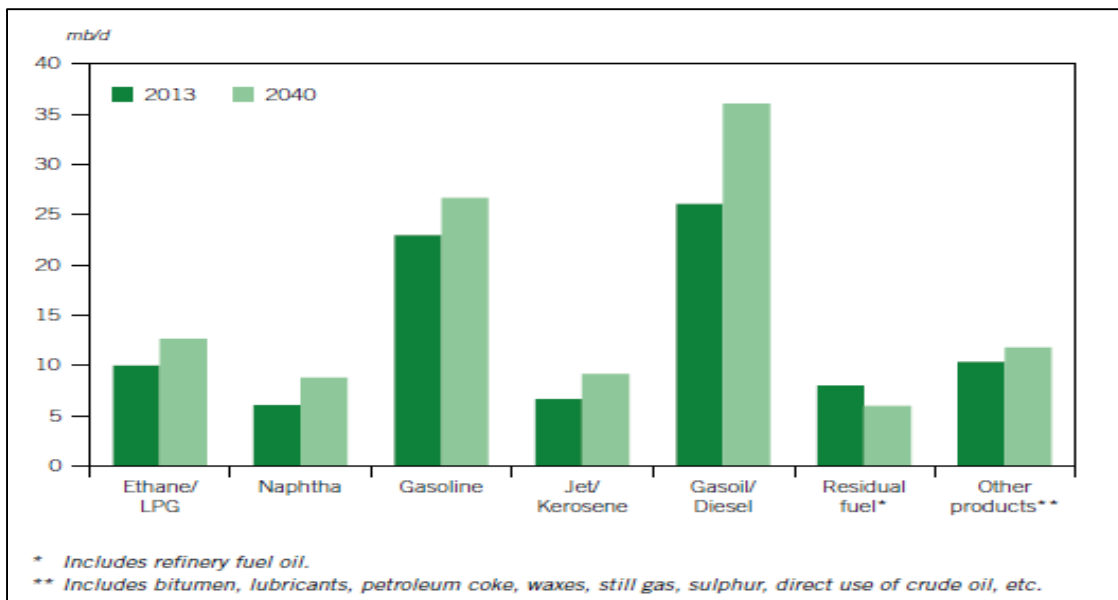


Figure 1.3 Global product demands, 2013 and 2040 [4]

GTL fuels' share in the fuel markets is growing between 2013 and 2040 as well; as shown in Figure 1.4 [4]. Accordingly, GTL Diesel production is expected to increase for the coming 25 years. Therefore, GTL Diesel fuel properties' prediction formulas based on their boiling ranges and carbon contents should be clearly identified, in order to assist boosting GTL Diesel fuel's market value based on solid information similar to those established for conventional diesel.

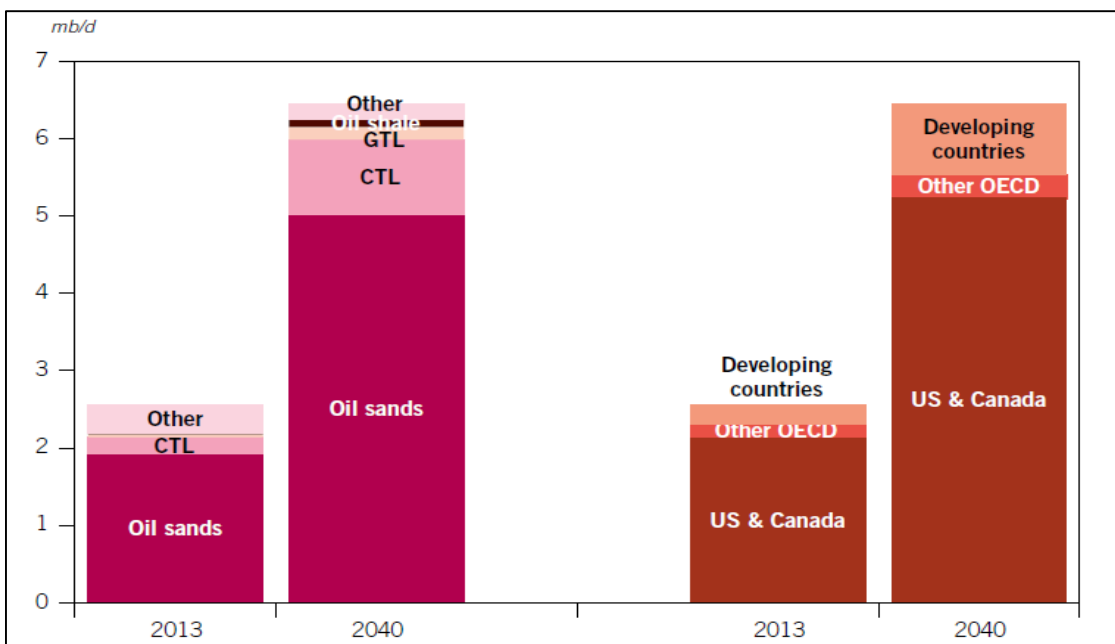


Figure 1.4 Non-OPEC other liquids supply by type and region, 2013 and 2040 [4]

Conventional Diesel is a complex combination of hydrocarbons produced by the distillation (physical separation) of crude oil and conversion process units such as Hydrocracker and Coker units in typical crude oil refineries. Conventional diesel carbon number distribution ranges from C₉ to C₂₀ (boiling points are in the range of approximately 163- 357 °C). For European markets, carbon numbers and final boiling-points values could reach up to C₂₈ and 390°C, respectively.

Conventional diesel contains normal and branched-chain alkanes (paraffins), cycloalkanes (naphthenes), aromatics and mixed aromatic cycloalkanes. Normal alkanes usually predominate [5]. On the other hand, GTL Diesel is a much simpler hydrocarbon combination, which is mainly normal and *iso* paraffinic compounds.

Table 1.2 represents typical carbon content for GTL Diesel compared to typical Ultra Low Sulfur Diesel (ULSD) [6]. ULSD diesel fuel meant to be with low sulfur content. Diesel fuel available in Europe and North America is of a ULSD type since almost 2006.

Table 1.2 GTL Diesel typical carbon content compared to ULSD [6]

	CHEMICAL STRUCTURE	GTL DIESEL	ULSD
General Carbon Type		Carbon Content (Mole% C)	Carbon Content (Mole% C)
- Aromatic Carbon		0.5	12.9
- Aliphatic Carbon		99.5	87.1
- CH Carbon		0.8	7.0
- CH ₂ Carbon		78.5	61.1
- CH ₃ Carbon		20.1	18.9
Aromatic Carbon Breakdown	C_nH_{2n-6}	0.5	17.0
- Peripheral Un-substituted Aromatic Carbon		0.3	
- Heteroaromatic Carbon		0.2	
Total (n + iso) Paraffinic Carbon	C_nH_{2n+2}	93.0	43.7
Total Cycloparaffinic Carbon	C_nH_{2n}	6.7	39.3
- Cycloparaffinic CH		0.2	9.1
- Cycloparaffinic CH ₂		6.1	26.9
- Cycloparaffinic CH ₃		0.4	3.3

1.1.1 Diesel Fuel Grades

Diesel fuel keeps the world economy moving, from consumer goods moved around the world, to the generation of electric power, to increased efficiency on farms. Diesel fuels play a vital role in strengthening the global economy and the standard of living [7]. For Diesel fuel markets, it is important to identify different grades for diesel based on different characteristics, such as sulfur content, density and origin as a strait run diesel or a blended diesel. Data below indicates different Diesel grades.

- Grade No. 1-D S15/S500/S5000: A special-purpose, light middle distillate fuel for use in diesel engine with 15/500/5000 ppm sulfur (maximum) respectively.
- Grade No. 2-D S15/500/5000: A general purpose, middle distillate fuel for use in diesel engine with 15/500/5000 ppm sulfur (maximum) respectively.
- Grade No. 4-D: A heavy distillate fuel, or a blend of distillate and residual oil, for use in low- and medium-speed diesel engines in applications involving predominantly constant speed and load.

ASTM Standard D975 identified the conventional diesel properties with respect to each grade as shown in Table 1.3 [7].

Table 1.3 ASTM D 975 requirements for diesel fuels

Property	Test Method	S15, S500, S5000* No. 1-D	S15, S500, S5000* No. 2-D	S15, S500, S5000* No. 4-D
Flash Point, °C (°F), min	D 93	38 (100)	52 (125)	55 (130)
Water and Sediment, % volume, max	D 2709 D 1796	0.05	0.05	0.05
Distillation Temperature, °C (°F), 90% Volume Recovered: Min. Max. or Simulated Distillation, °C (°F) 90% Volume Recovered: Min. Max.	D 86 D 2887	288 (550)	282 (540) 338 (640)	
Kinematic Viscosity, mm ² /sec at 40°C (104°F): Min. Max.	D 445	1.3 2.4	1.9 4.1	5.5 24
Ash, % mass, max	D 482	0.01	0.01	0.1
Sulfur, ppm ($\mu\text{g/g}$), max	D 5453	15.0	15.0	-
% Mass, max	D 2622	0.05	0.05	-
% Mass, max	D129	0.50	0.50	2.0

Table 1.3 Continued

Property	Test Method	S15, S500, S5000* No. 1-D	S15, S500, S5000* No. 2-D	S15, S500, S5000* No. 4-D
Copper Strip Corrosion Rating, max After 3 hours at 50°C (122°F)	D 130	No. 3	No. 3	-
Cetane Number, min One of the following must be met: (1) Cetane Index, min (2) Aromaticity, % volume, max	D 613 D4737-10 D 1319	40 40 35	40 40 35	30 - -
Cloud Point, °C (°F), max or LTFT/CFPP, °C (°F), max	D 2500 D 4539/ D 6371	Varies	Varies	-
Ramsbottom Carbon Residue, max (% mass on 10% Distillation Residue)	D 524	0.15	0.35	-
Lubricity, 60°C, WSD, microns, max	D 6079	520	520	-

1.1.2 GTL Diesel Grades

GTL fuel is virtually free of aromatics, polycyclic aromatics, olefins, sulfur, nitrogen and metals. The fuel is colorless and almost odorless and has a higher Cetane number than conventional diesel [36]. Compared to conventional diesel, there are no ASTM specifications for GTL Diesel; however, manufacturing and consuming companies for GTL Diesel have their own specifications based on their targeted distribution markets.

Table 1.4 represents GTL Diesel marketing specifications for ORYX GTL, SHELL, BP and MERCURIA.

Table 1.4 Marketing specifications for GTL Diesel

Parameter	Test Method	Units	ORYX GTL Limits / Standards	SHELL Limits	BP Limits	MERC U-RIA Limits
Appearance at 17 - 23 °C	ASTM D4176	rating	Clear & Bright	Same as std	Same as std	Same as std
Colour	ASTM D1500	rating	1 max	2.5 max	3.0 max	3.0 max
Density @ 15 °C	ASTM D4052	kg/m ³	760 min 780 max	760 min 780 max	760 min 780 max	760 min 780 max
Distillation corrected to 101.3 kPa IBP Recovered at 250 °C Recovered at 350 °C 95% evap (v/v) Final boiling point	ASTM D86	°C % (v/v) % (v/v) °C °C	Report 65 max 85 min 360 max Report	Same as std	Same as std	Same as std
Flash point (closed PM) at 101.3 kPa	ASTM D93	°C	> 55	Same as std	Same as std	Same as std
# Kinematic viscosity at 40°C	ASTM D445	cSt	1.5 min	2.5 - 4.5 min	Same as std	2.0 – 4.1 min
Cetane index	ASTM D4737	Calc	70 min	Same as std	Same as std	Same as std
Cold Filter Plugging Point	ASTM D6371	°C	-6 max	-5 max	-5 max	-5 max
Cloud point	ASTM D5771 and ASTM D2500	°C	-3 max	-2 max	-2 max	Same as std
Ash	ASTM D482	mass %	0.01 max	Same as std	Same as std	Same as std
Sediment by extraction	ASTM D473	mass %	0.01 max	Same as std	Same as std	Same as std
Water content at 20°C	ASTM D6304	mg/kg	150 max	Same as std	Same as std	Same as std

Table 1.4 Continued

Parameter	Test Method	Units	ORYX GTL Limits / Standards	SHELL Limits	BP Limits	MERC U-RIA Limits
Total sulfur	ASTM D5453	mg/kg	5 max	10.0 max	Same as std	Same as std
Copper corrosion (3 hr @ 50°C)	ASTM D130	rating	1 max	Same as std	Same as std	Same as std
Total acid No.	ASTM D974	mg KOH/g	0.1 max	Same as std	Same as std	Same as std
Conductivity @ 20°C	ASTM D2624	pS/m	200 min	100 min	100 min	100 min
Aromatics	IP 391/95	mass %	1 max	Same as std	Same as std	Same as std
Polycyclic aromatic hydrocarbons	IP 391/95	mass %	1 max	11 max	11 max	Same as std
Carbon residue on 10 % distillation residue	ASTM D4530	mass %	0.2 max	Same as std	Same as std	Same as std
Oxidation Stability	ASTM D2274	g/m ³	20 max	25 max	25 max	25 max
Lubricity (HFRR)	ASTM D6079	WSD µm	Report	Same as std	Same as std	Same as std
Particulate matter	EN ISO 12662	mg/kg	24 max	Same as std	Same as std	Same as std

1.2 Literature Review

Composing relationships between conventional diesel hydrocarbon compositions and its physical properties started decades ago. Therefore, in the literature reports; researchers can find strong mathematical correlations that can be applied to explain those relationships. However, for the GTL Diesel that is not the case; similar correlations are still considered under development.

Table 1.5 shows some of the literature reviews conducted for conventional diesel characterization and its relationship between compositions and properties, as well as GTL Diesel specifications.

Table 1.5 Relevant literature in the field of this study

Year of Publication	Name of Publisher	Title of Publication	Authors	Research Major Scope
1985	Energy & Fuels, 1985 Vol 64	Property-composition relationships for diesel and kerosene fuels [8]	David J. Cookson, Jozef L. Latten, Ian M. Shawt and Brian E. Smith	Compositional details of 18 diesel fuels using both H.P.L.C. and ^{13}C N.M.R techniques. Relationships between fuel composition and a range of fuel properties were obtained
1988	Energy & Fuels, 1988 Vol 2	Investigation of the Chemical Basis of Diesel Fuel Properties [9]	David J. Cookson, C. Paul Lloyd, and Brian E. Smith	Relationships to translate fuel quality specifications from constraints on fuel properties to constraints on chemical composition
1990	Energy & Fuels, 1990 Vol 4	Calculation of Jet and Diesel Fuel Properties Using ^{13}C NMR Spectroscopy [10]	David J. Cookson and Brian E. Smith	Composition has been defined with the use of ^{13}C NMR data alone and is expressed in terms of the fraction of aromatic carbon (C_{ar}) and the fraction of n-alkyl carbon (C_n)
1992	Energy & Fuels 1992, Vol. 6	Observed and Predicted Properties of Jet and Diesel Fuels Formulated from Coal Liquefaction and Fischer-Tropsch Feed stocks [11]	David J. Cookson and Brian E. Smith	Utilizing previously derived fuel composition-property relationships for jet and diesel fuels of fixed boiling range, deriving from Fischer-Tropsch synthesis, coal hydro-liquefaction, and petroleum sources and their blends.

Table 1.5 Continued

Year of Publication	Name of Publisher	Title of Publication	Authors	Research Major Scope
2002	ELSIVER	Neural Network Prediction of Cetan Number and Density of Diesel Fuel from its Chemical Composition Determined by LC and GC-MS [12]	Hong Yang, Zbigniew Ring, Yevgenia Briker, Norma McLean, Wally Friesen, Craig Fairbridge.	General Regression Neural Network (GRNN) used for non-linear correlation for Cetane prediction gave better results than multiple regression method, however for simpler correlation problem like density both methods gave similar results.
2004	Presented at the 2004 SAE Powertrain & Fluid Systems Conference & Exhibition	Fuel Property, Emission Test, and Operability Results from a Fleet of Class 6 Vehicles Operating on Gas-To-Liquid Fuel and Catalyzed Diesel Particle Filters [13]	Teresa L. Alleman, Leslie Eudy, Matt Miyasato, Adewale Oshinuga, Scott Allison, Tom Corcoran, Sougato Chatterjee, Todd Jacobs	Comparison study between GTL diesel and conventional diesel for 6 trucks operating in southern California showed the GTL fuel had cold flow properties suitable for year-round. With additives to meet lubricity standards, GTL fuel met or exceeded ASTM D975 fuel properties.
2010	ELSIVER	Inductive Modeling of Physico-Chemical properties: Flash Point of Alkanes [14]	D.Mathieu	Prediction of alkanes flash point from their molecular formula using a new model for quantitative structure-property relationships.
NA	UOP	LAB Industry [20]	UOP	Kerosene required composition to be suitable feedstock to LAB industry

Table 1.5 Continued

Year of Publication	Name of Publisher	Title of Publication	Authors	Research Major Scope
2013	Oxford Institute for Energy Studies	GTL A Viable Alternative to Oil-Derived Transport Fuels [15]	Craig Brown	Clean-burning, high quality characteristics of GTL diesel fuel, seemingly offer a viable substitute to Diesel oil-derived transport sector.
	University of Chemical Technology and Metallurgy – Sofia, Bulgaria	Investigation on Diesel cold flow properties [19]	R.Dinkov, D. Stratiev D. Penev G. Cholakov	Generating mathematical correlations for Conventional diesel properties.
	National technical University of Athens	Use of Mathematical Expression for the estimation of selected diesel fuel properties [30]	D. Karonis, E. Lois, S. Stournas	To predict some diesel properties using experimental data and related mathematical expressions.
2014	The 3rd International Conference on Design Engineering and Science	Effect of Combustion Design for Diesel Dual Fuel Engine [16]	Osamu SAOTOME, Fumiya SATO, and Katsuhiko TAKEDA	A feasibility study to reduce total hydrocarbon (THC) emission for diesel dual fuel (DDF) engine by using GTL Diesel fuel from combustion design perspective.

As indicated in the above literature, excessive studies have been conducted for conventional diesel; however, there is still vast room for research for GTL Diesel characterization to have robust correlation for GTL Diesel fuel specifications based on its composition.

1.3 Industry and Academic Research Consortium Activities in GTL Diesel Fuels

As illustrated in Figure 1.5, a research consortium was established between DaimlerChrysler AG in Stuttgart, Sasol-Chevron Consulting Ltd in London and Sasol Oil (Pty) Ltd in Johannesburg to study the effect of pure GTL Diesel Fuels and its blends with EU Diesel on emissions and engine performance. The consortium summarized their important findings below [22]:

- 1- Use of GTL Diesel fuel in unmodified vehicles engines led to large reductions of CO, HC and PM emissions without compromising NOx emissions even if compared to a sulfur free European diesel fuel.
- 2- The high Cetane number of the GTL fuel was advantageous during cold-start and low temperature operation.
- 3- There is a large potential for further reductions in soot and NOx emissions of existing engines if the engine is recalibrated for optimum use of the GTL Diesel.
- 4- Very promising results were achieved also with GTL diesel as a blending component for use with conventional diesel fuel. The emission benefits scale up over-linear fashion with the GTL fraction.



Figure 1.5 Research consortium to study GTL Diesel effect on emissions and engine performance [17]

To study the effect of GTL Diesel usage as a pure fuel on engines in Qatar, a recent research was launched between ORYX GTL Company, Supreme Education Council (SEC), Texas A&M University at Qatar (Chemical and Mechanical Engineering Programs), Qatar University, Mowasalat (KARWA) and Qatar Fuel (WOQOD) [18] as shown in Figure 1.6. Twenty school buses have been used for the study; ten of the buses ran with GTL Diesel as pure fuel without any engine modification and the remaining ten buses ran with conventional diesel. The study has been carried on for a period of 3-months. Texas A&M University at Qatar has used its world-class fuel characterization laboratory to analyze the properties of both Diesel fuels and the lubricants. Meanwhile, the Mechanical Engineering Engine Laboratory measured the emissions of the combusting GTL Diesel and compared it with the conventional diesel emissions. There

was a dramatic drop in the emissions in the case of GTL Diesel fuel compared to conventional diesel, because of the superiority in the properties as summarized earlier.



Figure 1.6 ORYX GTL consortium to study the effect of GTL Diesel on schools buses

[18]

CHAPTER II

RESEARCH PROBLEM AND OBJECTIVES

2.1 Research Problem

As shown previously in Table 1.5 in the literature review chapter; extensive studies were conducted over the past decades to understand the role of hydrocarbon composition change of the conventional diesel fuels on their properties and combustion behavior; however, similar research activities on the GTL Diesel are quite limited to industry and few academic groups.

GTL Diesel specifications can be improved by changing their hydrocarbon structure, i.e. carbon content and boiling range. Nevertheless, certain specifications could be poorly affected as well. Investigating the relations between GTL Diesel fuel carbon content together with its boiling range and their specifications is essential for predicting GTL Diesel properties at different compositions. This in turn will enhance the design of the distillation columns to improve the separation process of diesel fuel cuts at different boiling ranges, based on the targeted fuel distribution market. The prediction of these relationships could be established through mathematical correlations between the fuel composition and its properties. Several reports in literature showed the capability of modeling and predicting the properties for the conventional diesel fuel from its composition as in Cookson and co-workers' study [9]. They investigated the quality of conventional diesel fuels based on composition and related these properties to the fuel

carbon cut. Elbashir's research team has conducted similar extensive investigations but for the GTL Jet fuel [33].

Another literature report by Cookson and Smith addressed the prediction of GTL Diesel specifications. They tried to utilize previously derived fuel composition-property relationships for jet and diesel fuels of fixed boiling ranges; these fuels were derived from Fischer-Tropsch synthesis, coal hydro-liquefaction, and petroleum sources plus their blends [11]. The main difference between the Cookson and Smith study and the research conducted for this thesis is that the latter predicted the composition-property relationships for different boiling ranges of GTL Diesel cuts rather than fixed boiling ranges.

2.2 Research Objectives

The major driver for this research was to compare the GTL Diesel cuts at different boiling ranges and carbon number content against their respective market specifications. Another objective was to develop mathematical correlations that helped in predicting the GTL Diesel properties at various boiling ranges and carbon number contents. The aim is to support the industry in developing new superior generations of GTL Diesel fuels, in terms of specifications and combustion behavior compared to those currently in the market. Building data banks for GTL Diesel properties at different boiling ranges and carbon distributions will boost advanced and future research work in the field of GTL technology in general, and GTL fuels specifically. Moreover, this research investigated the possibility for modifying the existing GTL Diesel manufacturing plants and supports future consideration for changing the design of new GTL plants.

CHAPTER III

RESEARCH METHODOLOGY

The following steps summarize the proposed methodology used to perform this research study:

- 1- The first step covered the preparation of different samples of GTL Diesel at different boiling ranges (these will be referred to as cuts), by using a fractionation column module in Texas A&M Qatar's Fuel Characterization Lab (FCL). The GTL Diesel fuel that was provided by ORYX GTL Company was fractionated into two cuts: light cuts and heavy cuts based on different Initial Boiling Points (IBP), as shown in Table 3.1.

Table 3.1 GTL Diesel cuts IBP

Cut No.	1	2	3	4	5	6	7	8	9	10
IBP, °C	>130	>140	>150	>160	>170	>180	>190	>200	>210	>215

- 2- GTL Diesel heavy cuts in addition to the ORYX GTL's Diesel fuel were analyzed for several physical properties of critical importance for the fuel's certification by the automotive industry. The analyzed properties included carbon distribution, atmospheric distillation, density, viscosity, flash point, Cetane index, pour point and cloud point. Table 3.2 shows the standard testing methods that were used for this purpose.

Table 3.2 Standard testing methods

Analysis	ASTM Method / Other	Test Title	Test device
Fractionation	N/A	Fractionating of Petroleum Products.	SPINNING BAND DISTILLATION SYSTEM, B/R Instrument Corporation
Distillation	D-86	Distillation of Petroleum Products at Atmospheric Pressure	Petrotest ADU4+
Carbon Distribution	D-3238 – 95	Calculation of Carbon Distribution and Structural Group Analysis of Petroleum Oils by the n-d-M Method	Agilent 5975 Series MSD
Density	D 4052	Density, Relative Density, and API Gravity of Liquids by Digital Density Meter	Anton Paar DMA 4100
Viscosity	D-7042	Standard Test Method for Dynamic Viscosity and Density of Liquids by Stabinger Viscometer. (and the Calculation of Kinematic Viscosity)	Anton Paar SVM 3000
Flash point	D-93 Procedure A	Flash Point by Pensky-Martens Closed Cup Tester	Automated Pensky-Martens Flash Point, Seta PM-93
Cetane Index	D 4737	Calculated Cetane Index by Four Variable Equation	Calculation
Cloud Point / Pour Point	D-5773	Cloud Point	Phase Technology 70Xi series LAB analyzer

- 3- The results obtained for GTL Diesel heavy cuts were compared to the market specification to identify possible improvements.
- 4- The applicability of the conventional diesel fuel composition-property prediction correlations to the GTL Diesel composition was verified. A typical example of prediction correlation is the one used to determine the Cold Flow properties of conventional diesel [19], where cloud point (CP) is related to the boiling range and specific gravity as shown below.

$$CP = a + bT_{50} + cT_{90} + dT_{90-20} + eT_{50} * T_{90} + fSG + gSG * T_{90} \quad (3.1)$$

where:

T_{50} = temperature at which boils 50 % (v/v) according to ASTM D 86, °C;

T_{90} = temperature at which boils 90 % (v/v) according to ASTM D 86, °C;

T_{90-20} = difference in temperatures of 90 % (v/v) and 20 % (v/v) boiling from the fraction;

SG = specific gravity

a, b, c, d, e, f, and g = regression coefficients with the following values [19]:

$$a = 40.5188082034628 \qquad \qquad b = 0.352055808730715$$

$$c = 0.0213385486437754 \qquad \qquad d = -0.11817892070543$$

$$e = -0.00116227648075031 \qquad \qquad f = -345.341766942041$$

$$g = 0.91964970145254$$

- 5- New mathematical correlations were developed to predict the properties of the GTL Diesel heavy cuts using simple modeling software such as LINGO.
- 6- The carbon number distribution of the GTL Diesel light cuts were identified. Data were recorded as reference for future work to investigate the suitability of the light GTL Diesel cuts for feedstock to Linear Alkyl Benzene (LAB) industry. GTL Diesel Light cuts may become attractive because their carbon number distribution between C₉-C₁₄ is the most suitable feedstock for LAB industry [20].

CHAPTER IV

EXPERIMENTAL SETUP

In order to achieve the targeted objectives of this study, a sophisticated experimental campaign utilizing the advanced analytical equipment at Texas A&M at Qatar's Fuel Characterization Lab (FCL) was developed. The FCL is operated utilizing high standards in Data Quality Management System for the testing procedures, data collection and verification. In addition, the lab follows strict safety regulations and procedures.

The FCL quality manual described elsewhere [22], which applies to all laboratory personnel work in the lab. The lab is currently an ISO 9001-2008 certified lab for several standard fuels' characterization tests. The quality manual is maintained current and up-to-date by the assigned laboratory personnel who is responsible for ensuring the follow up of Quality Management System.

The Quality manual of FCL for a research work covers the following sections:

- Quality policy
- List of equipment and test methods
- Quality system
- Job description of laboratory personnel
- Document Control
- Traceability of Measurements
- Review of All Customer Requests and Contracts

- Calibration/ Verification of Test Procedures 11
- Sample Handling
- Laboratory Environment
- Procedures for Calibration, Verification, and Maintenance of Equipment
- Internal Quality Control Procedures
- Control of Nonconforming Products
- Corrective Action Procedure
- Preventive Active Procedure
- Complaints and Feedback.
- Reporting Analytical Results

Work instructions were maintained according to analytical methods and made available for the lab personnel. They specify the required equipment and fixtures, the resources and skills, and test verifications to be performed to measure process and product quality. Work instructions are approved by the Project Manager and are maintained in the document control system. All data collected in this research project is based on this data Quality Management System.

As mentioned earlier in Table 3.2, seven main laboratory devices were used for the experimental activities in addition to a set of chemicals, materials, glass wares and utilities that were needed to complete the required analysis for this study as shown in Tables 4.1, 4.2 and 4.3.

Table 4.1 List of chemical used for the experimental activities

Chemicals	Source / CAS number
Ethanol of assay \geq 99.99%, (2,000 ml)	64-17-5
Acetone of assay \geq 99.99%, (2,000 ml)	67-64-1
GTL Diesel	ORYX GTL Co.

Table 4.2 List of glass wares

Glass Wares	Number of Units
Flasks 500 mm	2
Flasks 1000 mm	2
Beakers 400 mm	2
Bottles 500 mm	20
Bottles 400 mm	10
Measuring Tube 10 mm	2
Measuring Tube 500 mm	2
Measuring Tube 1000 mm	1
Funnel	2

Table 4.3 List of materials / utilities

Material / Utilities	Number of Units
Plastic Wash Dropper Bottles 500 mm	4
Tissue paper rolls	2
Pack of rubber gloves	2
Can Key	1
Cotton Cloth small pieces	10
Bottle of Dishes Soap	1
Air Supply for Drying	-
Potable Water for Washing	-
Electricity for Lighting and Powering equipment	-

Safety standards for personnel and equipment were fully insured; Table 4.4 represents the personal protection equipment (PPE) and safety equipment required for working in the laboratory.

Table 4.4 LAB PPE and safety equipment

PPE / Safety Equipment	Number of units
Safety Goggles	2
Rubber gloves (Packs)	1
LAB Coats	2
Fume Hood	1

For the sensitivity of the results of each experiment, careful cleaning procedures were required. Below is a detailed description about the cleaning procedures for the glassware used for the experiments.

1. The top edge was rinsed with ethanol plastic dropper all around while the glassware was slowly rotated, in order to ensure complete coverage to all side surfaces. Then, it was shaken vigorously to ensure sufficient coverage to the bottom surface. After that, it was dried with an air supply source at the fume-hood.
2. The same procedure was repeated again with the acetone plastic dropper to remove any remaining traces of ethanol on the surfaces.
3. Some glassware required extra washing with a brush wetted with dish soap to remove any dust traces or unknown materials.

4.1 Experiment Design

Experiments required for this research study were designed in advance before starting the lab work to ensure the quality and validity of the data required for the study. FCL Objective is to produce technically supportable laboratory test results that accurately and precisely describe the sample for the purpose of reporting to the internal and external customers. FCL has developed a quality management system that comply with ISO 9001:2008 certification requirements to insure quality of service and results for industry and academia partners. An efficient Quality Management System and Data Management System were followed to maintain both the quality of the results and the integrity of FCL

testing facility, Figures 4.1 and 4.2 illustrate the pillars for both Quality Management System and Data Management System main tasks.

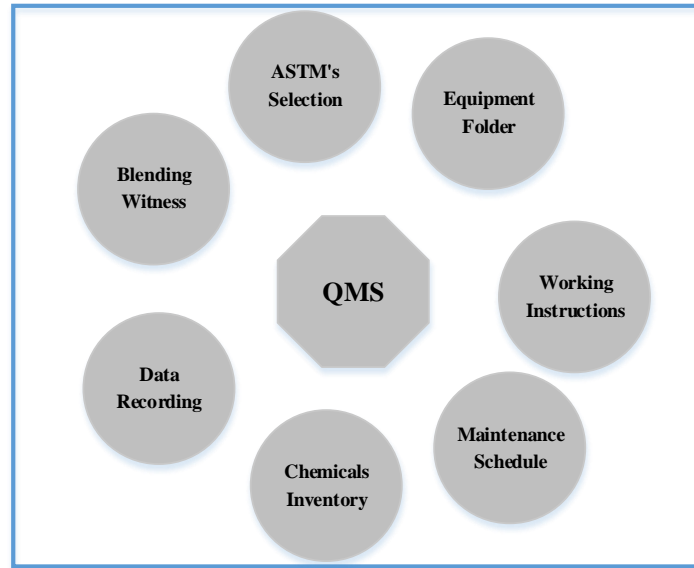


Figure 4.1 Pillars of quality management system



Figure 4.2 Pillars of data management system

High quality control of each test was considered; for the tests that were adopted from ASTM, all ASTM instructions for the precisions of the results were followed. Below Table 4.5 summarize mainly the repeatability of some tests. Except for the fractionation testing, all the analysis were repeated three times for accuracy.

Table 4.5 ASTM tests repeatability and reproducibility values

ASTM Method	Test	Repeatability*	Reproducibility**
D4052 – 11	Density, g/ml	0.00031	0.0005
D93-12	Flash point, °C	0.029 × mean results only in one case in twenty	0.071 × mean results only in one case in twenty
D7042 – 14	Dynamic viscosity, mPa·s Kinematic viscosity, mm ² /s	0.006705 0.00782	0.0122 0.0133
D5773 – 10	Cloud Point, °C	0.7°C only in one case in twenty	2.2°C only in one case in twenty
D4737 – 10	Calculated Cetan Index	Exact	Exact

* The difference between successive test results, obtained by the same operator using the same apparatus under constant operating conditions on identical test material

** The difference between two single and independent results, obtained by different operators working in different laboratories on identical material.

4.1.1 GTL Diesel Fractionation

The first part of the experimental work was to prepare the ten samples of GTL Diesel at different initial boiling points (IBP). This task was performed by a fractionation column that worked under regulated vacuum pressure; below is the detailed description for the column and the procedures for implementation.

The fractionation column as shown in Figures 4.1 and 4.2 consists mainly of unit controller, pot flask in two different sizes 500 or 1000 mm, heating mantle, thermometers, reflux system, vacuum pump, condenser and receivers' flasks.

The GTL Diesel sample was placed in the pot flask and heated according to the program assigned for the required cut point, where the light cut of the sample was separated and condensed in the top receivers while the required heavier GTL Diesel cut remained in the pot flask. Ten different programs were defined for the fractionator controller to have ten different GTL samples at different initial boiling points. All runs were under vacuum atmosphere of 100 milli bar (mbar) to accelerate the fractionation process.

According to ASTM petroleum-analysis distillation procedures, Initial Boiling Point (IBP) is the recorded temperature when the first drop of distilled vapor is liquefied and falls from the end of the condenser [34]. The target fractionated samples should have different IBPs of 130, 140, 150, 160, 170, 180, 190, 200, 210 and 215 °C. The condensed volume of the sample at the top of the fractionation column was marked as the GTL Diesel light cut while the remains in the bottom of the fraction column were marked as the GTL Diesel heavy cuts.

It was noticed that the actual IBP of the ten samples when analyzed with ASTM D86 distillation was different from that entered in the fractionation column program. This has been attributed to different fractionating conditions, mainly applied pressure (i.e. 100 mbar vacuum vs. atmospheric pressure).

Samples Preparation

- 1- Ten samples of 500 ml of GTL Diesel were taken from two five-liter cans provided by ORYX GTL Co.
- 2- Each sample was split in the fractionation column; the heavy GTL Diesel cut remaining in the pot flask was stored in clean half-liter glass bottle and labeled with the higher than programmed cut temperature (e.g. GTL Diesel IBP > 170 °C). Meanwhile, the light GTL Diesel cut received in the top receivers was stored in 100-500 ml clean glass bottles (based on their received volumes) and labeled with the lower than programmed cut temperature (e.g. GTL Diesel FBP < 170 °C).
- 3- All labeled samples were kept in a refrigerator to ensure the safety of the samples and to avoid any vaporization of light components from the samples at elevated temperatures.
- 4- After these steps the main samples were ready for the planned analysis of properties.

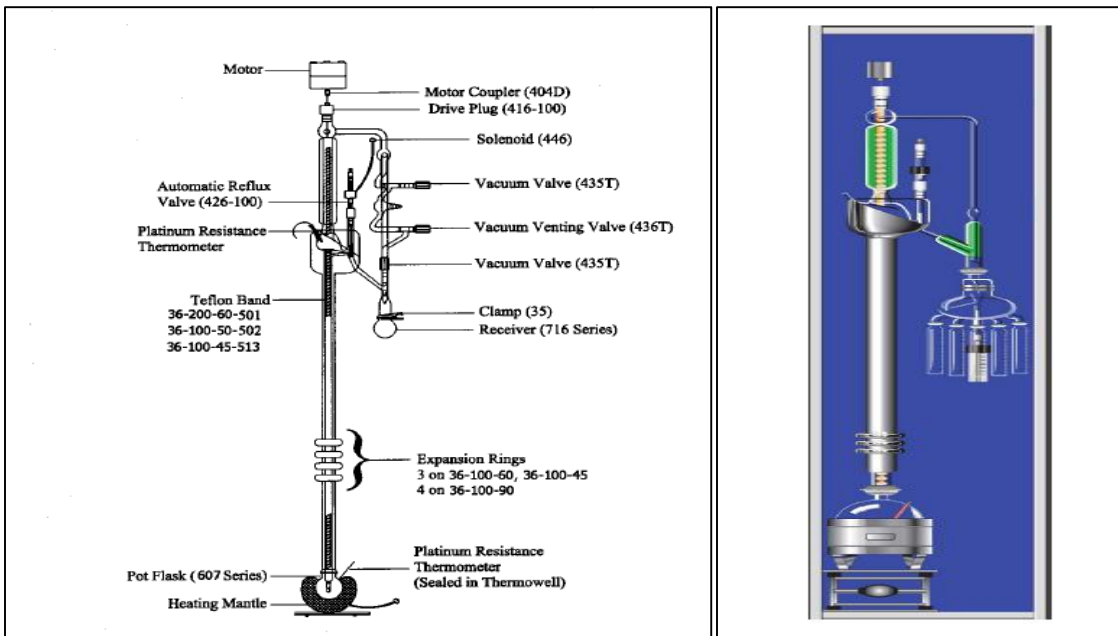


Figure 4.3 FCL LAB fractionation column sketch



Figure 4.4 B/R Instrument corporation fractionation column and control unit

4.1.2 Atmospheric Distillation Analysis

After generating ten different GTL Diesel heavy cuts samples at different IBP, whole boiling range was tested with an approved test method; atmospheric distillation test ASTM D86 [34] was performed using LAB device Petrotest ADU4+ as shown in Figure 4.3. The details of using this equipment are included in Appendix A.



Figure 4.5 ASTM D86 atmospheric distillation Petrotest ADU4+

4.1.3 Carbon Distribution

Similar to the atmospheric distillation analysis ran for the ten GTL Diesel cuts together with the whole cut of the GTL Diesel, this time Agilent GC with mass selective detector as shown in Figure 4.4 was used to determine the carbon distribution and content for each sample. The Agilent GC/MS system fitted with a Mass Selective Detector performed quantitative and qualitative analyses of petroleum products [29]. The column involved has the following specifications: HP5 column, MS grade, 30m long, 250 μ m

diameter and 0.25 μm thickness (usually expressed like: 30mx250 μm x0.25 μm). No calibration method was used; only area normalization method for quantification of results was used. Methods of verification used was the NIST built-in library and MS Data software.



Figure 4.6 Agilent GC/MS with mass selective detector

4.1.4 Density Analysis

Density was the first property of interest in comparing the ten different GTL Diesel heavy cut samples. Normally GTL Diesel density is lower than conventional Diesel. Density unit of measurement used in this study was kg/m³.

The principle of density test can be described as follows. The tested sample was injected into the testing tube that has a shape of U passage. The U-shaped tube oscillates

at specific frequency to excite the electrons. A digital analyzer receives the signal carried by excited electrons and translates it into density [24].

All samples labeled GTL Diesel > IBP's °C obtained from the fractionation test were tested for density using Anton Paar DMA 4100 as shown in Figure 4.4 with ASTM D4052.



Figure 4.7 Density analyzer Anton Paar DMA 4100

4.1.5 Viscosity Analysis

The second GTL Diesel specification of interest was viscosity. Viscosity is the resistance of a fluid to flow and has the units of mPa.S for dynamic viscosity and mm²/s (cSt) for kinematic viscosity. It is an important parameter for any fuel and especially diesel fuel for the design of any internal combustion engine, where the abrasion of the internal

parts of the engines will be dramatically affected by the viscosity of the fuel used. All GTL Diesel heavy cut samples generated from the fractionation test and labeled > IBP °C tested using Anton Paar SVM 3000 by test method of D-7042 as shown in Figure 4.5. Normally GTL Diesel viscosity was measured at 40 °C as per the test method [25].

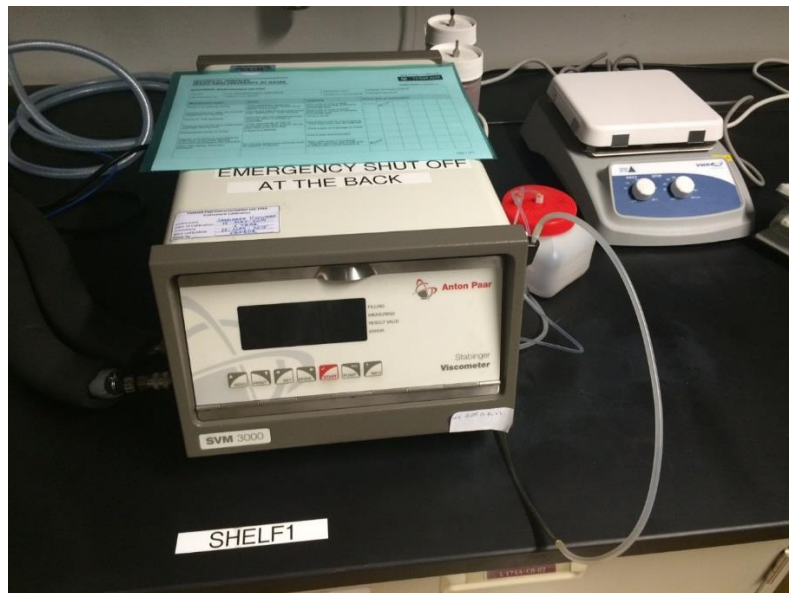


Figure 4.8 Viscosity analyzer Anton Paar SVM 3000

4.1.6 Flash Point Analysis

The third GTL Diesel characteristic specification was the flash point. The flash point of a volatile material is the lowest temperature at which vapors of a fluid will ignite. It is an important parameter for any fuel for the design of internal combustion engines, where the flash point is needed to determine the design of the ignitor and its ignition temperature. Another important reason for the flash point measurement is the storage safety temperature; in hot countries, diesel fuel flash point temperature should be high

enough to avoid any fuel flashing and vaporization leading to hazardous scenarios. All the GTL Diesel heavy cut samples generated from the fractionation test and labeled > IBP °C were tested using Automatic Pensky-Martens Closed Cup Flash Point Tester Model 35000-0, by test method ASTM D-93 Procedure A as shown in Figure 4.6. GTL Diesel flash point is high compared to conventional diesel derived from crude oil [27].



Figure 4.9 Flash point automated Pensky-Martens

4.1.7 Cloud and Pour Points Analysis

The fourth and the fifth GTL Diesel specifications were the cloud and pour points.

Cloud point is the temperature below which waxy material in diesel starts to give a cloudy appearance, while the pour point is the temperature at which the diesel becomes semi-solid and loses its fluidity. Both cloud and pour points are important properties in the design of diesel engines especially in cold countries where the diesel fuel can plug the injection nozzles if it has high cloud and pour points. All GTL Diesel heavy cuts samples were analyzed following the test method of ASTM D-5773 using the apparatus Phase Technology 70Xi series LAB analyzer.

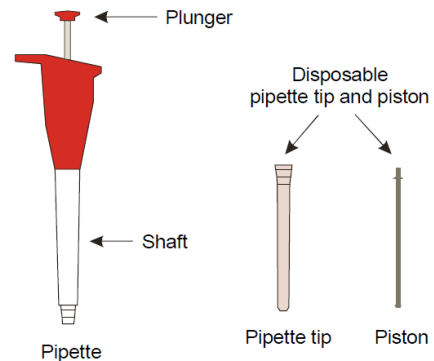
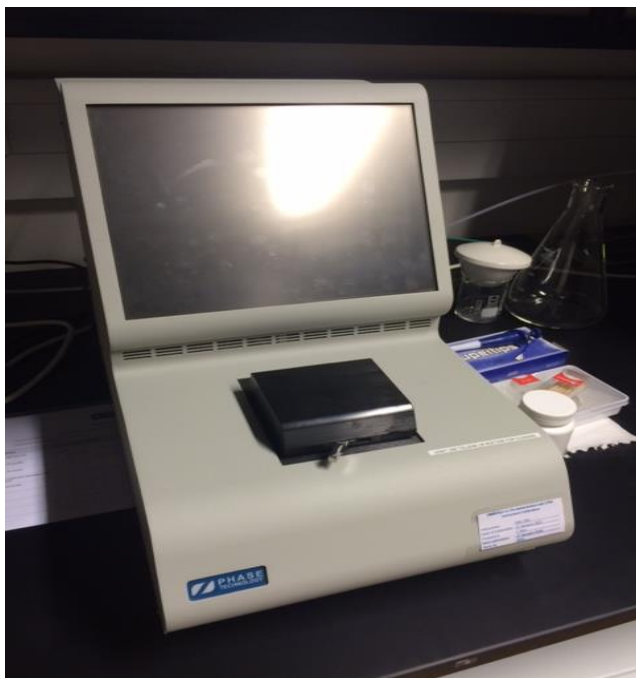


Figure 4.10 Cloud and pour points analyzing device

CHAPTER V

RESULTS AND DISCUSSION

Upon completion of the tests, all the results were tabulated as shown in Appendix B; several trends were generated in order to present the results obtained together with proper explanations of the data. Those trends indicate the change of GTL Diesel specifications with respect to the change of both carbon number distribution and boiling range.

5.1 GTL Diesel Fractionation

As indicated earlier in research methodology CHAPTER III, ten samples were fractionated into two parts: light and heavy cuts. Table 5.1 and Figure 5.1 show that the percentage of light cuts volume increased by increasing the initial boiling point of the cut.

Table 5.1 Light and heavy cuts percentage volume at different IBP's and 100 mbar

Cut #	1	2	3	4	5	6	7	8	9	10
Test Set Temp.	130	140	150	160	170	180	190	200	210	215
Actual IBP at 1 atm.	164	170	179	190	198	210	218	227	237	240
% light cut	0.8%	2.2%	5.2%	8.8%	12.0%	16.0%	19.6%	23.6%	26.8%	28.6%
% Heavy Cut	99.2%	97.8%	94.8%	91.2%	88.0%	84.0%	80.4%	76.4%	73.2%	71.4%

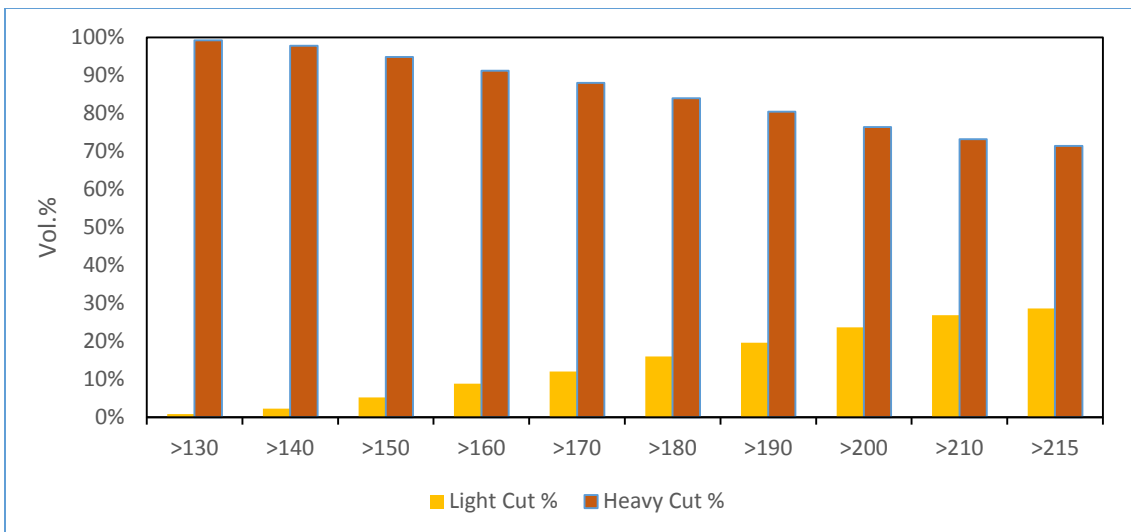


Figure 5.1 Light to heavy GTL Diesel cuts volume percentage

5.2 Carbon Distribution for GTL Diesel Heavy Cuts

After splitting the samples into light and heavy cuts, heavy cuts were analyzed using GC for the carbon number distribution; that was the first test conducted for the heavy cuts. All GC graphs are shown in Appendix B.

Figure 5.2 represents the overall carbon number distribution for the heavy cuts. Lighter carbon numbers (C_6-C_8) decreased, while middle carbon numbers (C_9-C_{13}) increased by increasing the IBP of the cut; this is due to the separation process of light cuts where light carbon numbers were removed and the middle and heavy carbon numbers remained in the heavy cuts.

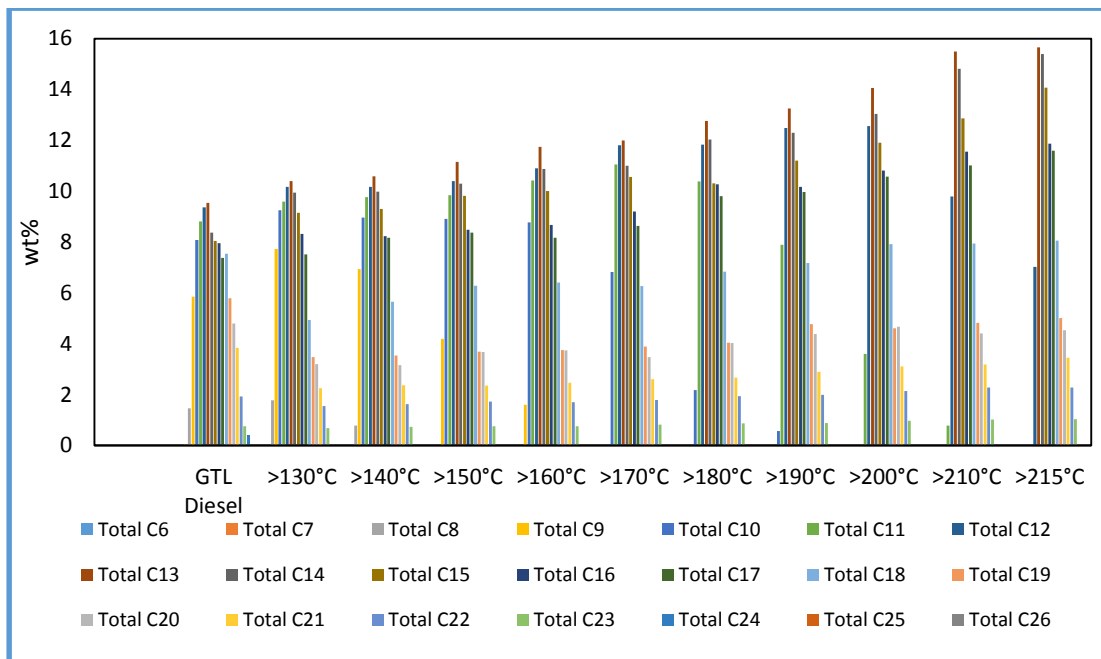


Figure 5.2 Overall carbon distribution for heavy cuts

In order to have more indicative presentation, it was decided to represent the carbon number distribution data using carbon number grouping rather than the individual carbon number represented in Figure 5.2. The classification below is also related to specific fuel cuts which are better known to industry:

- (C₈+C₉+C₁₀+C₁₁) as Light Kerosene
- (C₁₂+C₁₃+C₁₄+C₁₅) as Heavy Kerosene.
- (C₁₆+C₁₇+C₁₈+C₁₉) as Light Diesel.
- (C₂₀+C₂₁+C₂₂+C₂₃) as Heavy Diesel.

Figure 5.3 represents the overall carbon number distribution considering the carbon number grouping. The trend of the figure shows that the Light Kerosene wt% reduced as the IBP increased while the Heavy Kerosene and Light Diesel wt% increased; in all cases Heavy Diesel wt% was found to be less affected. Again as mentioned earlier, this is due to the separation process of light cuts where light carbon numbers were removed and the middle and heavy carbon numbers remained in the heavy cuts.

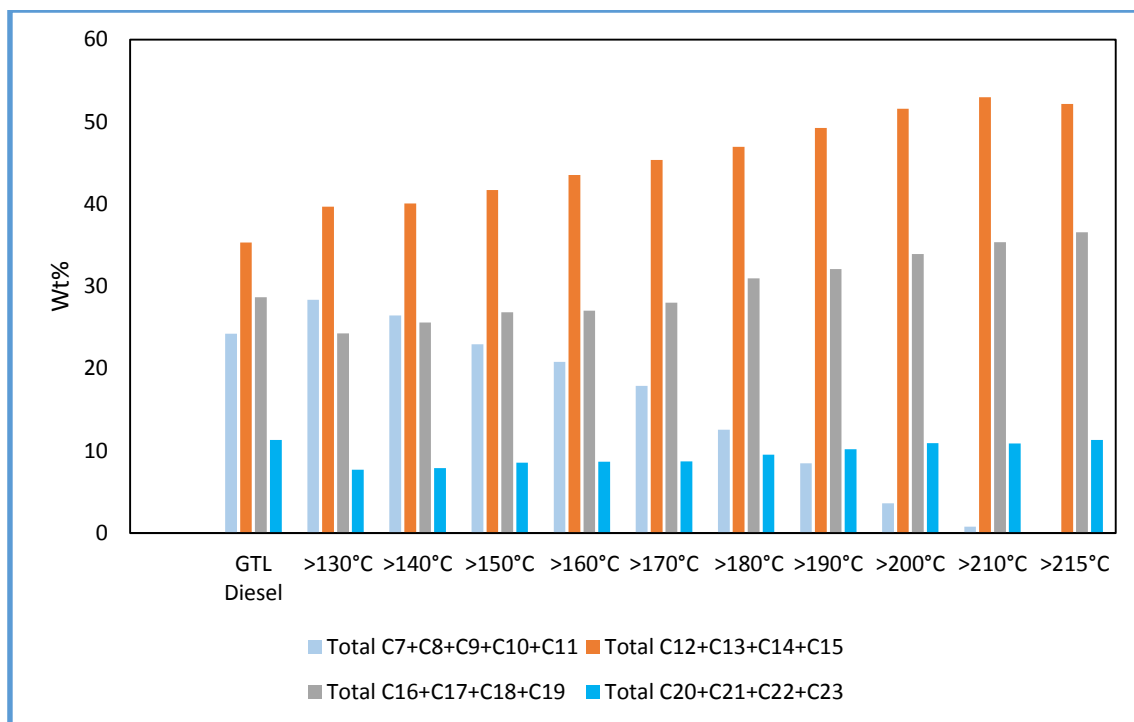


Figure 5.3 The effect of IBP on GTL Diesel carbon number grouping for heavy cuts

5.3 Carbon Distribution for GTL Diesel Light Cuts

GTL Diesel Lights cuts were analyzed for carbon distribution by GC; light carbon numbers (C_7-C_9) reduced, while the heavier carbon numbers ($C_{10}-C_{13}$) increased by increasing the IBP. Figure 5.4 represents the overall carbon number distribution for the light cuts.

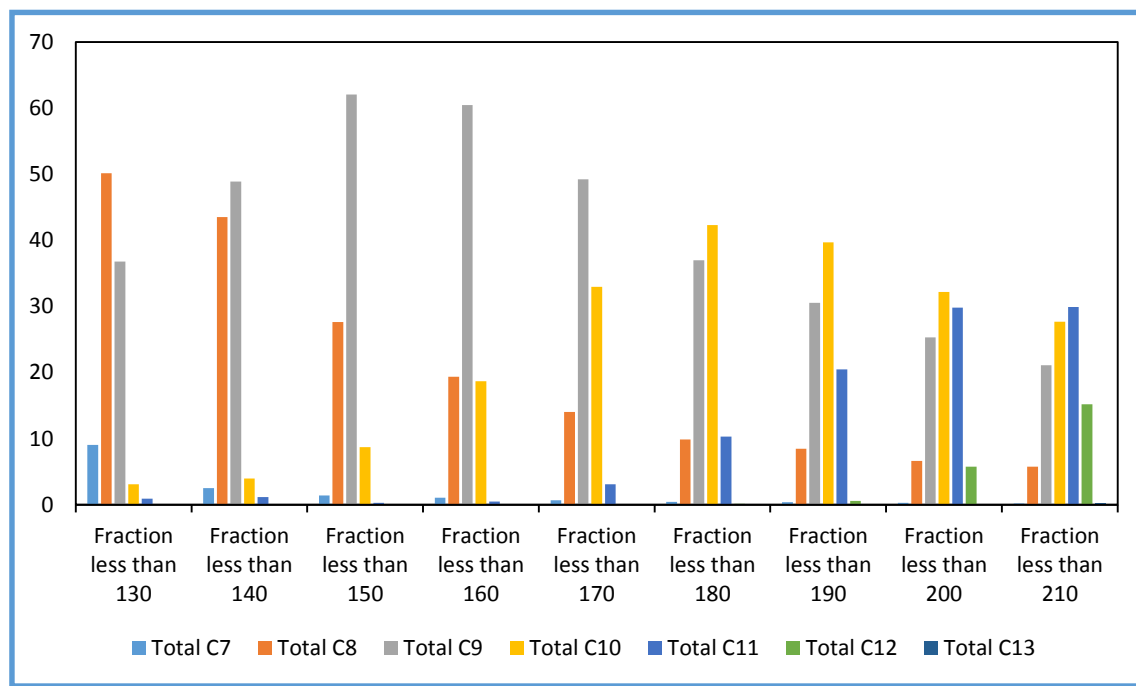


Figure 5.4 The effect of IBP on carbon number distribution for light cuts

5.4 Atmospheric Distillation

The second test for the GTL Diesel heavy cuts determined the atmospheric distillation profiles using ASTM D-86 analysis. Figure 5.5 represents the distillation data for each cut. Since it was difficult to extract a general trend from the figure, it was decided to select some critical points and represent them as shown in Figure 5.6. The figure shows

that distillation data of T₁₀ and T₂₀ values increased by increasing the IBP while the T₅₀ values slightly increased; T₉₀ values was almost constant for all the cuts. These increases were due to separation of the light ends by the fractionation process, where heavier hydrocarbon content was generated.

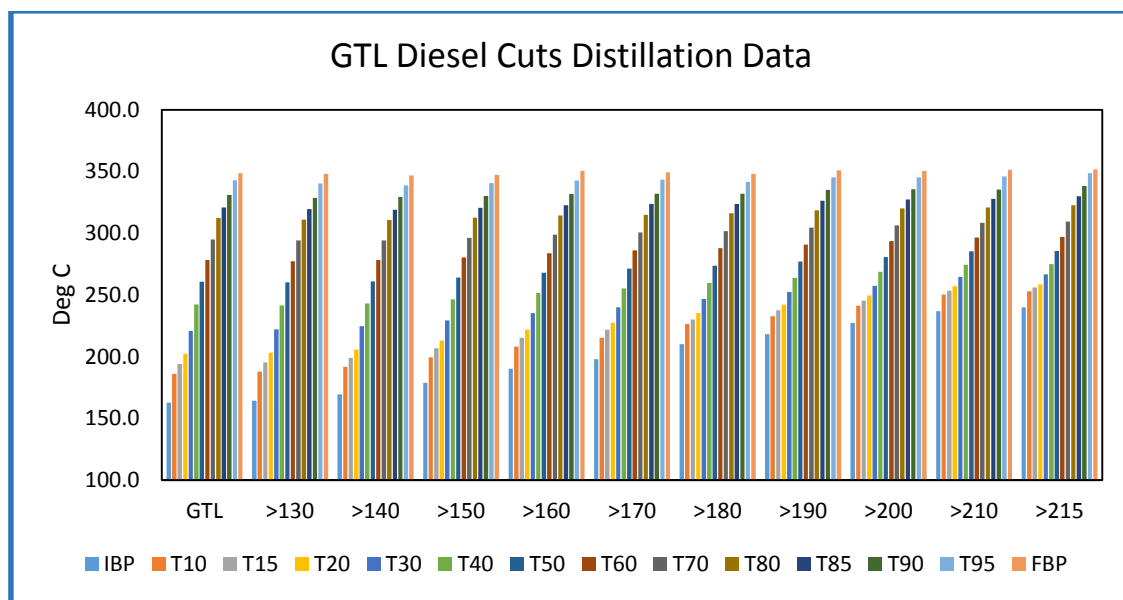


Figure 5.5 The effect of IBP on D86 distillation data for GTL Diesel cuts

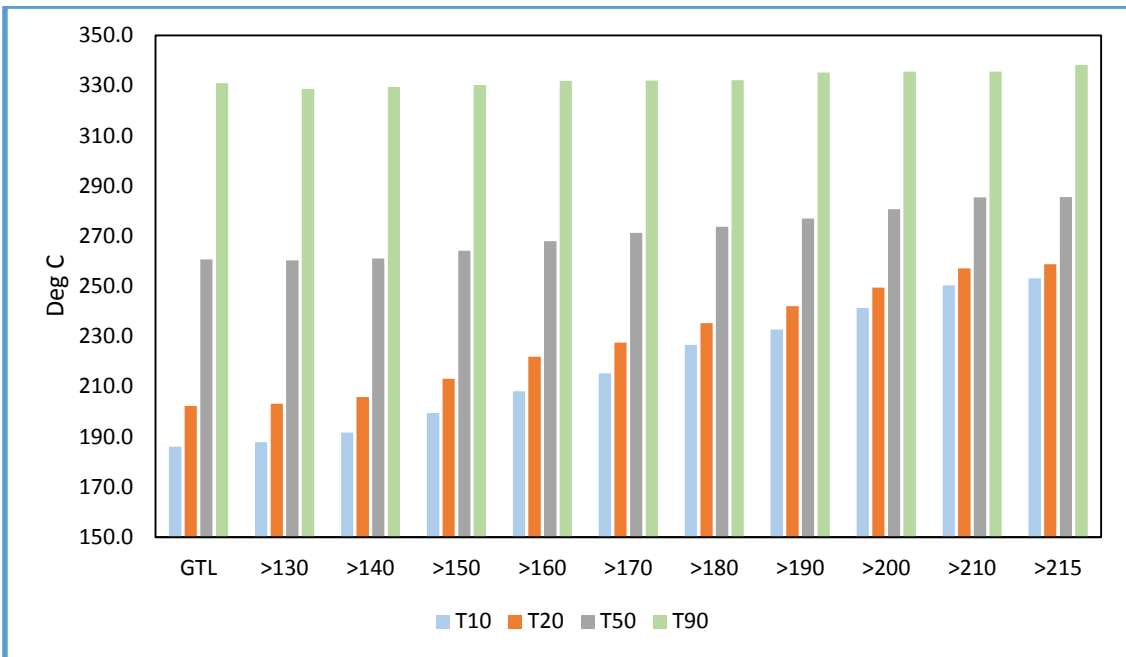


Figure 5.6 Change of T₁₀, T₂₀, T₅₀ and T₉₀ distillation data with IBP of the cut.

Certain distillation data (T₁₀, T₂₀, T₅₀ and T₉₀) were selected to be represented individually in Figure 5.6, since these data were used in many mathematical correlations to calculate different physical properties similar to cloud points as shown below in Equation 5.1. The target behind this formula was predicting the Cloud point property at different boiling range to prevent any problems similar to crystals appear [19].

$$CP = a + bT_{50} + cT_{90} + dT_{90-20} + eT_{50} * T_{90} + fSG + gSG * T_{90} \quad (5.1)$$

where CP is the cloud point and a, b, c, d, e, f, and g are regression coefficients, and SG is the specific gravity.

5.5 Density Analysis

The third test conducted was the density analysis using Anton Paar DMA 4100 based on test method of ASTM D4052. Figure 5.7 represents the measured density of each cut while comparing the minimum and maximum limits as per market specifications earlier mentioned in Table 1.4 of min. 760 to max. 780 kg/m³. The recorded readings for density of GTL Heavy cuts were bounded by lower value of 767.7 kg/m³ and upper value of 781.7 kg/m³.

The density profile is quite representative since it shows that the higher the IBP of the cut, the higher the density; this exactly matched the Diesel Fuels Technical Review by CHEVRON [7]. All the results fell between the limits of market specifications except the cuts numbered 9 and 10 (IBP>210 and >215 °C) respectively, where their densities exceeded the maximum limit of 780 kg/m³.

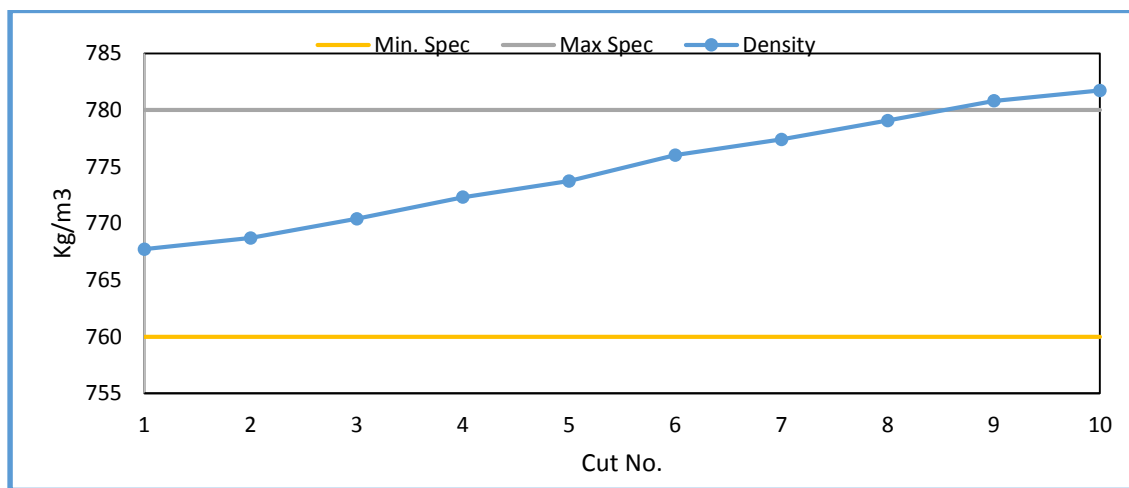


Figure 5.7 Density of GTL Diesel heavy cuts compared with market specification (min. 760 kg/m³ and max. 780 kg/m³)

Furthermore as shown in Figure 5.8, the density change is almost linear with the change of the average boiling range. Average boiling range is the average of distillation temperatures of IBP, T₁₀, T₂₀.... to FBP.

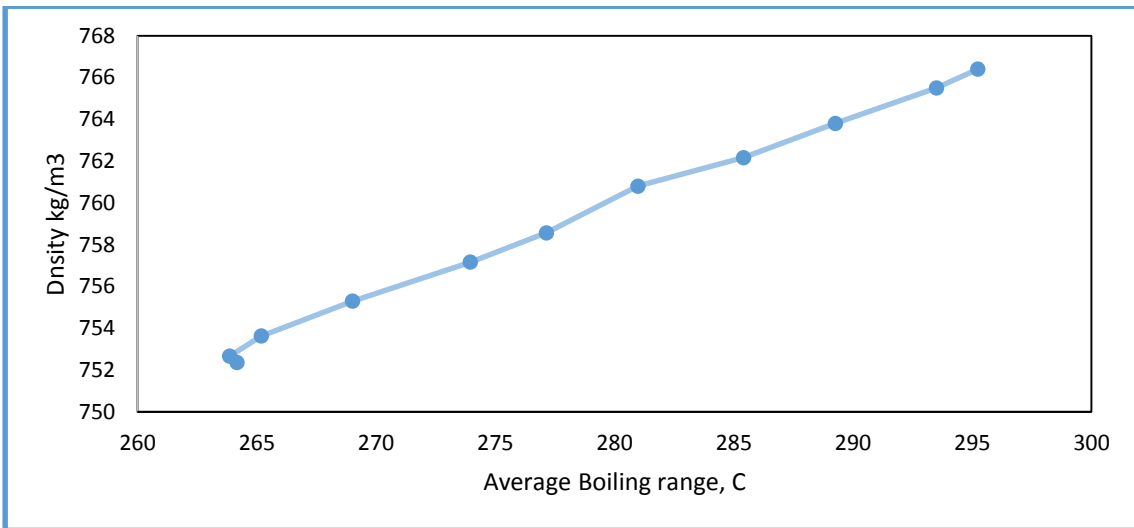


Figure 5.8 Change of GTL Diesel heavy cuts with the change of average boiling range

5.6 Viscosity Analysis

The fourth test conducted for the GTL Diesel heavy cuts was the viscosity analysis using Anton Paar SVM 3000 based on ASTM D-7042. As shown in Figure 5.8, all the results for the heavy cuts, kinematic viscosity are fallen between the marketing specifications limits of 1.5 to 4.5 cSt as mentioned in Table 1.4. Figure 5.9 shows the dynamic viscosity results for the heavy GTL Diesel cuts as well. The recorded readings for kinematic viscosity were bounded by lower value of 2.24 cSt. and upper value of 3.36

cSt, while the recorded readings for dynamic viscosity were bounded by lower value of 1.67 mpa.s. and upper value of 2.58 mpa.s.

Both kinematic and dynamic viscosity results showed increase in their values as the IBP increased, i.e. the heavier the fuel cut is higher the viscosity. That was expected since the close relation between density and viscosity of diesel fuels at same temperatures as mentioned in the report by Goodheart-Willcox about Diesel fuels [35].

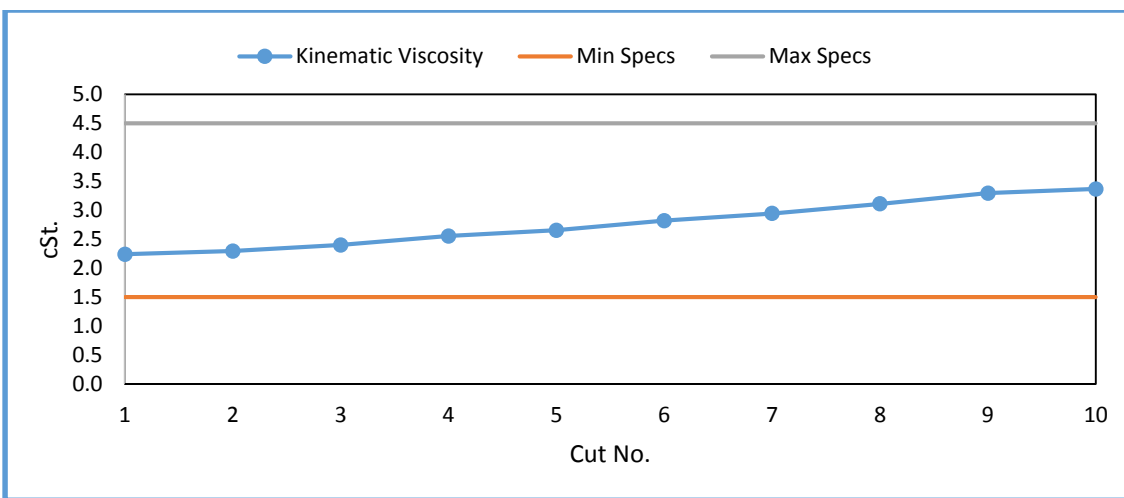


Figure 5.9 Kinematic viscosity of heavy GTL Diesel cuts compared with market specification (1.5 to 4.5 cSt)

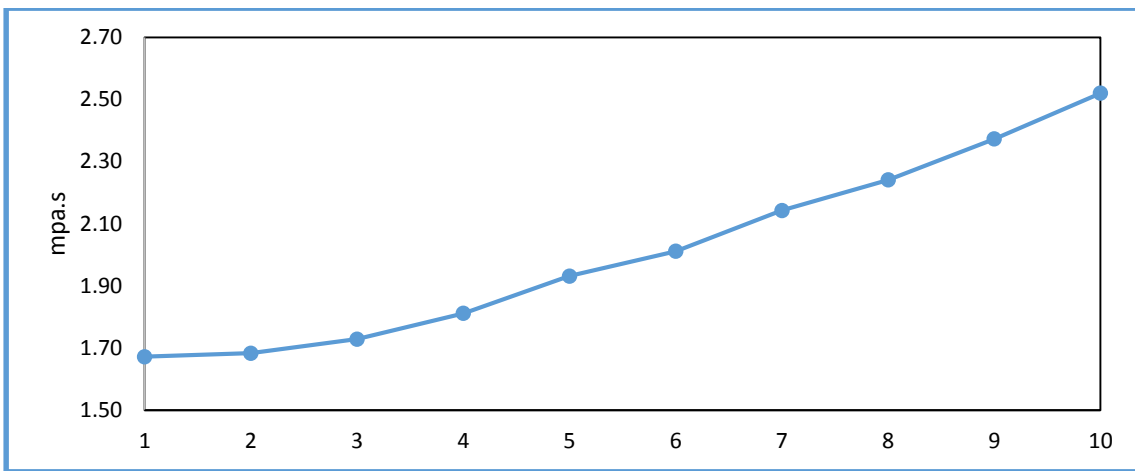


Figure 5.10 Change of dynamic viscosity of GTL Diesel heavy cuts with the change of IBP.

5.7 Flash Point Analysis

The fifth test conducted for the GTL Diesel heavy cuts was the flash point analysis using Automatic Pensky-Martens Closed Cup Flash Point Tester Model 35000-0, based on ASTM D-93 Procedure A. Figure 5.10 shows that the flash points of all fuel cuts are above the minimum marketing specifications limit of 55 °C. The recorded readings for flash point were bounded by lower value of 59 °C and upper value of 113 °C. Higher GTL Diesel Flash Point is better in terms of product safety storage temperature especially in hot countries similar to the Gulf Countries, as it allow safe storage in tanks at severe climatic conditions in the summer while ambient temperature may exceed 50 °C. Similarly, in this part of the world it is important to ensure safer storage of these fuels in trucks/cars tanks without vaporizing the volatile hydrocarbon, which may lead to fire in case these vapors subjected to ignition source or excessive heat.

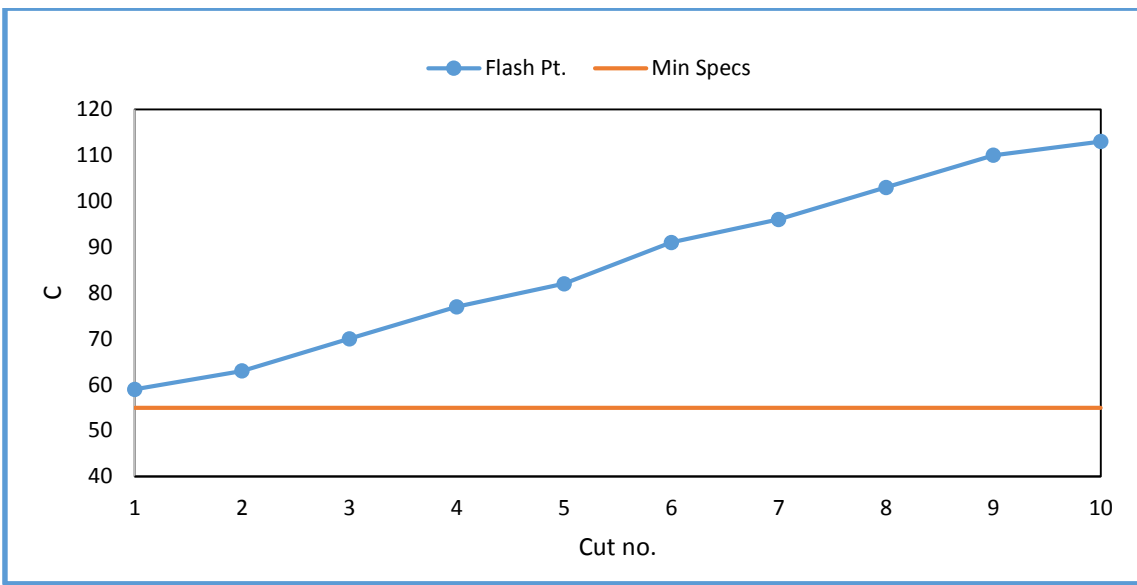


Figure 5.11 Flash point of GTL Diesel heavy cuts compared with market specification

5.8 Cloud and Pour Point Analysis

The sixth test conducted for the GTL Diesel heavy cuts was the cloud point and the pour point analysis using the LAB apparatus Phase Technology 70Xi series equipment, the LAB analyzer is based on test M D-5773.

Figure 5.11 shows that the measured cloud point for the GTL Diesel heavy cuts and the marketing specifications; where the results fallen below the maximum limits of -3.0 °C for the cuts of IBP > 130 to > 170 °C, while the rest of the cuts results showed higher than the market specification that is considered as off specification results, This specification is important specifically for the European and North American market since the ambient temperature in the winter may easily reach to -10 °C. The recorded readings for cloud point were bounded by lower value of -5.7 °C and upper value of -0.2 °C.

Again if considered that heavier GTL Diesel with higher cloud point will be consumed in Gulf Council Countries area, in this case the cloud point measures will be on specification as the lowest ambient temperature in the winter in most of the region could be 0 °C. So cloud point and Pour point specification may change based on the target market.

Both cloud and pour points behavior with respect to IBP was expected where higher the IBP was the higher their values, as the close relation between diesels fuels cloud point and density [35].

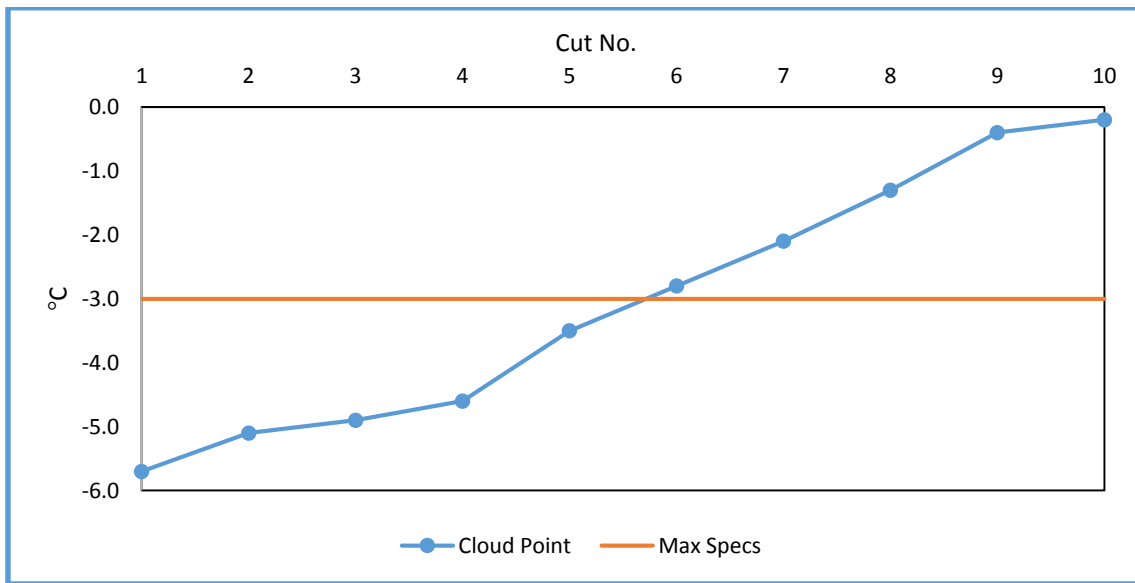


Figure 5.12 Cloud point of GTL Diesel heavy cuts compared with market specification

The results for the pour points were not properly representing the expected changes with respect to the IBP as shown in Figure 5.12. Pour points results were the same for the first six cuts, in the cut number seven there was a response in results; that was mainly due

to the accuracy of measuring that can be in the range of three degrees. So the results of the first six cuts could be fallen between -9 and -6 °C. The test was repeated three times but the results were not showing insignificant change in pour points values for the first six cuts. The recorded readings were bounded by lower value of -9 °C and upper value of -3 °C.

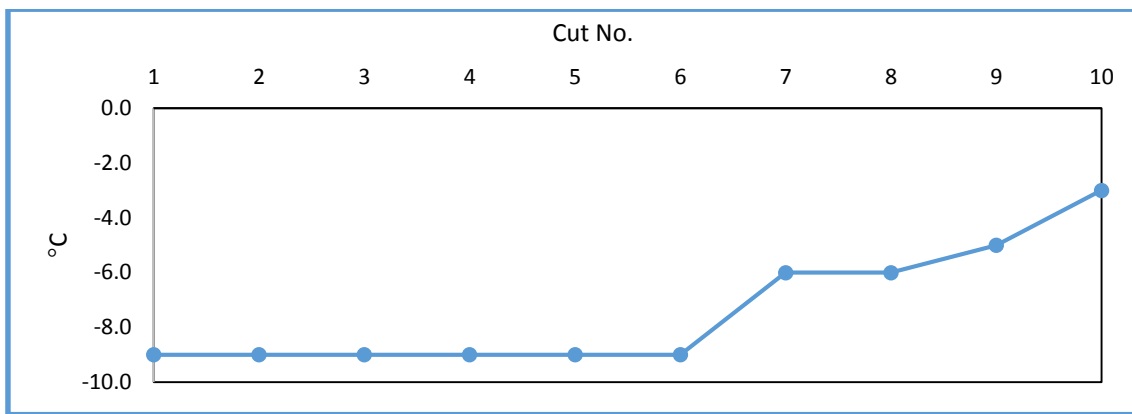


Figure 5.13 Pour point of GTL Diesel heavy cuts

5.9 Cetane Index Calculation

The ease of diesel fuel oil ignition and the manner in which it burns determine the ignition quality of the fuel oil. The fuel must then be able to vaporize quickly and ignite without a flame or spark. The ignition quality of a diesel fuel is determined by its Cetane number rating, or Cetane Index [35]. Cetane index has been calculated for the GTL Diesel heavy cuts as per the ASTM Standard Procedure A (D4737-10) as shown in Equation 5.2 below, which is specified for conventional diesel grades as shown earlier in Table 1.3,

same time it is also specified by ORYX GTL Co. as approved equation for calculating Cetane Index for GTL Diesel.

$$\begin{aligned}
 CCI = & 45.2 + (0.0892)(T_{10N}) + [0.131 + (0.901)(B)][T_{50N}] + \\
 & [0.0523 - (0.420)(B)][T_{90N}] + [0.00049][(T_{10N})^2 - (T_{90N})^2] + (107)(B) \\
 & + (60)(B)^2 \quad (5.2)
 \end{aligned}$$

where:

CCI: Calculated Cetane Index by Four Variable Equation

D = Density at 15°C, g/mL determined by Test Methods D1298 or D4052,

DN = D - 0.85,

B = [e^(-3.5)(DN)] - 1,

T₁₀ = 10% recovery temperature, °C, determined by Test Method D86.

T_{10N} = T₁₀ - 215,

T₅₀ = 50% recovery temperature, °C, determined by Test Method D86.

T_{50N} = T₅₀ - 260,

T₉₀ = 90% recovery temperature, °C, determined by Test Method D86 and

T_{90N} = T₉₀ - 310.

Figure 5.13 shows the results for the Cetane Index calculation for each fuel cut. The calculated results were bounded by lower value of 83.9 °C and upper value of 90.9 °C. The Cetane Index was found increasing by increase of the IBP of GTL Diesel cut that was expected since Cetane Index calculation is a function of GTL Diesel density as well as the boiling points data.

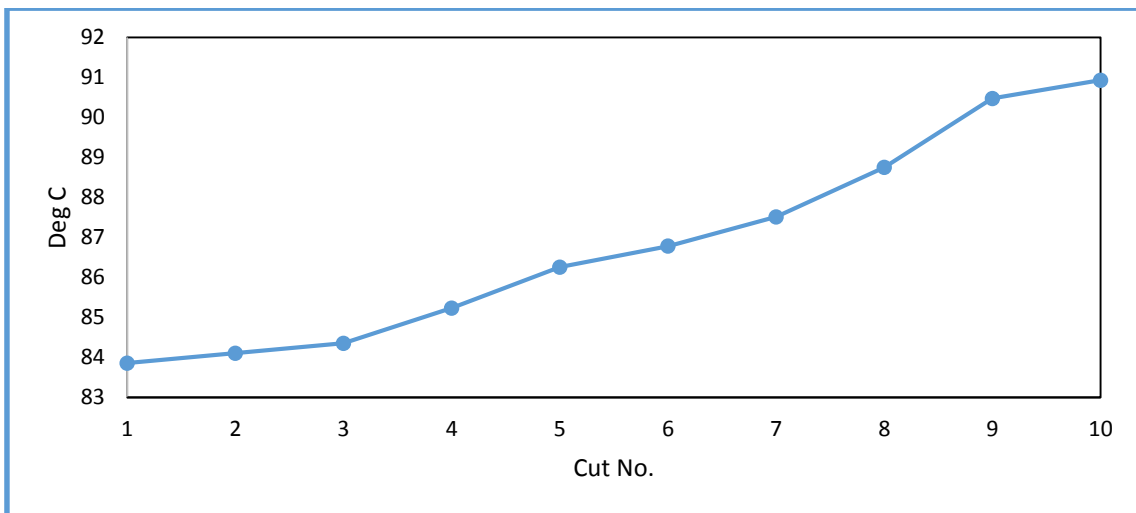


Figure 5.14 The impact of IBP change on GTL Diesel heavy cuts calculated Cetane Index

CHAPTER VI

MODELING

One of the objectives of this research work as listed in Chapter II, is to develop a mathematical correlations for GTL Diesel properties at different boiling ranges and their carbon distribution. According to the literature review mentioned in Chapter (Table 1.5), most of the developed correlations were specific to conventional diesel obtained from crude oil while very limited studies addressed similar correlations for GTL Diesel.

GTL Diesel properties similar to density, flash Point, viscosity and cloud point have been measured in TAMUQ FCL at different boiling range and carbon number distribution as shown and discussed in Chapter V. These data have been used to verify existing models and correlations in literatures that developed for conventional diesel fuels. For the properties that failed to fit literature correlations, new correlations and regressions investigated that can lead to better predictability of the GTL Diesel fuels' properties based on their hydrocarbon composition.

Regression analysis is a statistical process for estimating the relationships among variables, it is used for modeling and analyzing of numerical data that can be used to discover the relationship between two or more variables; Regression attempts to determine the strength of the relationship between one dependent variable and a series of other changing variables (known as independent variables). Regression can assist in prediction, estimation, and verification of empirical and calibrating models [32].

Interactions between Lab results data obtained from the analysis and models were implemented as the following methods [37]:

1. Data were needed to test a model.
2. Data were needed to estimate the values of the parameters appearing in a model.

This is called calibrating a model.

3. Data were needed to suggest a right model. The models called empirical model that is based entirely on data.

LINGO is a comprehensive powerful software designed to build and solve linear, nonlinear, quadratic, quadratically constrained, second order cone, stochastic, and integer optimization models faster, easier and more efficient. LINGO provides a completely integrated package that includes a powerful language for expressing optimization models [32].

As mentioned earlier in the literature review in CHAPTER I, and the research methodology in CHAPTER III, conventional diesel fuel has many existing composition-property prediction models, these models will be tested for GTL Diesel using the obtained actual data from the Lab analysis. As mention above in the first modeling method, if we have a model that we need to test the values of the parameters appearing in the model this is called model testing, as per the below example; where Equation 6.1 was generated for conventional diesel and the below coefficients have been calculated for conventional diesel as well

$$CP = a + bT_{50} + cT_{90} + dT_{90-20} + eT_{50} * T_{90} + fSG + gSG * T_{90} \quad (6.1)$$

where regression coefficients are,

$$\begin{aligned} a &= 40.5188082034628 & b &= 0.352055808730715 & c &= 0.0213385486437754 \\ d &= -0.11817892070543 & e &= -0.00116227648075031 & f &= -345.341766942041 \\ g &= 0.91964970145254 \end{aligned}$$

For the second modeling method (calibrating model), in case the existing model for composition-property prediction for conventional diesel has failed to be applied to GTL Diesel, as there was no reasonable fit between the actual Lab results and model results. Then it was required to calculate new coefficients and test them, in order to obtain best fit between the actual data and the model data. For calculating the correlation/parameters of any GTL Diesel property; LINGO was used where, half of the lab results (for cuts number 1,3,5,7 and 9) were used to estimate the regression coefficients, the rest of Lab results (for cuts 2,4,6,8, and 10) were used to test the accuracy of these coefficients. As an example, for Equation 6.1, new coefficients have been estimated by LINGO as below.

$$\begin{aligned} a &= 1195.917 & b &= -5.382029 & c &= -2.632678 \\ d &= 0.1358335 & e &= 0.1992243E-01 & f &= 759.4667 \\ g &= -4.907416 \end{aligned}$$

For the third modeling method (empirical model), in case that one of the GTL Diesel properties completely failed to follow an existing model made for conventional diesel, even after estimation of new coefficients. New model was generated using similar

models for conventional diesel but with some change of the independent variables; new coefficients for that model were calculated using LINGO as well. Example for the new model and its coefficients is below.

$$P = a_0[\text{Light Kerosene}] + a_1[\text{Heavy Kerosene}] + a_2[\text{Light Diesel}] \\ + a_3[\text{Heavy Diesel}] \quad (6.2)$$

where regression coefficients are,

$$a_0 = 12.6769 \quad a_1 = -0.3166 \quad a_2 = -0.1909 \\ a_3 = 0.1302 \quad a_4 = -0.6788$$

From the three examples above, some of the regression coefficients are negative values; this is due to that regressions solutions are numerical and not physical and the negative parameters are needed to fit the Lab data. For cloud point as an example; since at lower temperature readings, some crystallization for the heavier hydrocarbon content may occur that can affect model output; this could be one of the reasons behind the negative values in the model.

Below is detailed discussion for each GTL Diesel property where the above mentioned three modeling methods were utilized. The figures below represent validation of the models. The 45-degree line in the figures below represents the perfect match (Ideal Model) between the actual Lab measured properties for each cut and the calculated values obtained from our correlation.

6.1 Cloud Point Model, using Distillation Data

6.1.1 Using Literature Regression Coefficients (Model Testing)

In 2011, Dinkov, et al. investigated diesel cold flow properties at the University of Chemical Technology and Metallurgy – Sofia, Bulgaria [19]. He tested cloud point (CP) and cold filter plugging point (CFPP) of 20 diesel range boiling fractions from different origin (both straight run and conversion effluents i.e. from Hydrocracker and Coker units). Equation 6.1 was developed to estimate the cloud point property for conventional diesel.

$$CP = a + bT_{50} + cT_{90} + dT_{90-20} + eT_{50} * T_{90} + fSG + gSG * T_{90} \quad (6.1)$$

where regression coefficients are,

$$\begin{aligned} a &= 40.5188082034628 & b &= 0.352055808730715 & c &= 0.0213385486437754 \\ d &= -0.11817892070543 & e &= -0.00116227648075031 & f &= -345.341766942041 \\ g &= 0.91964970145254 \end{aligned}$$

Table 6.1 shows the calculated cloud point (dependent variable) for GTL Diesel heavy cuts by knowing the distillation data (independent variables). Table 6.1 also indicates the measured CP values from the lab experiments.

Table 6.1 Calculation of cloud point (CP) from distillation data

cut	>130	>140	>150	>160	>170	>180	>190	>200	>210	>215
T50	260.3	261.1	264.1	268.0	271.3	273.7	277.0	280.7	285.4	285.6
T90	328.6	329.4	330.2	331.9	332.0	332.1	335.1	335.6	335.5	338.2
T90-20	125.4	123.6	117.1	110.0	104.5	96.8	93.1	86.1	78.4	79.4
SG	0.767	0.768	0.770	0.772	0.773	0.776	0.777	0.779	0.780	0.781
Calc. CP	-8.19	-7.70	-6.76	-5.41	-4.89	-4.11	-2.59	-1.76	-1.13	-0.19
Meas CP	-5.7	-5.1	-4.9	-4.6	-3.5	-2.8	-2.1	-1.3	-0.4	-0.2

Figure 6.1 shows the plot of the model calculated and measured CP values for different GTL Diesel heavy cuts. The calculated CP data from Equation 6.1 failed to predict the experimentally measured values as can be seen in Figure 6.1. This poor predictability of the literature equation could be attributed to the failure of the literature regression coefficients for conventional diesel fuel to fit the data for the heavy cuts of the GTL Diesel fuel.

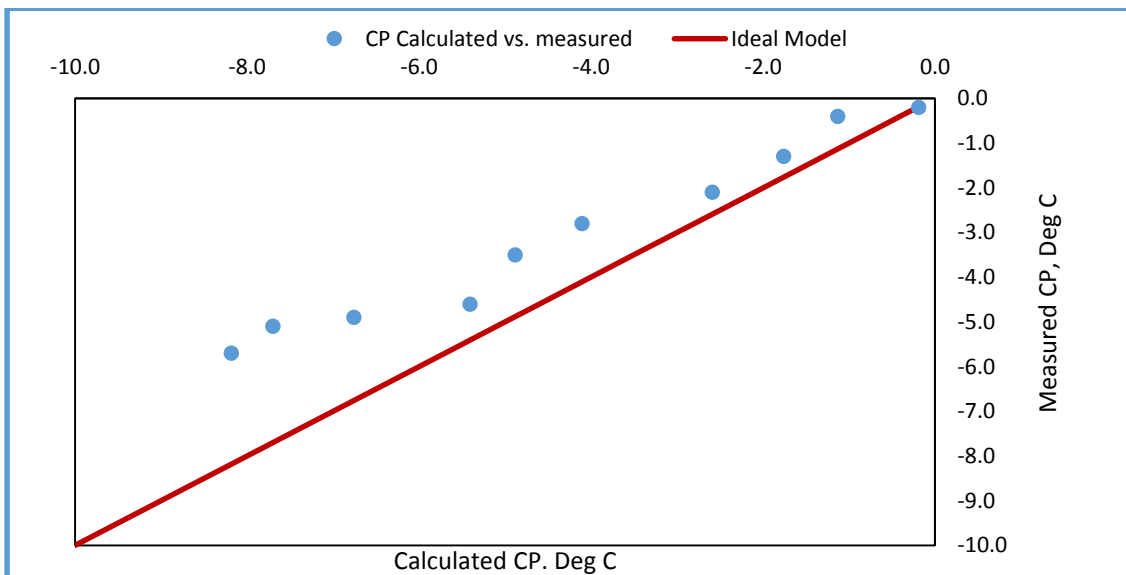


Figure 6.1 Cloud point calculated using literature regressions [19] and Eq. 6.1 vs. Lab measured values at different IBP

6.1.2 Using Estimated LINGO Regression Coefficients (Calibrating Model)

In this study we have utilized LINGO software to develop a better correlation for the Cloud point of GTL diesel fuels by obtaining new regression coefficients for this purpose. The detailed program is shown in APPENDIX C while Figure 6.2 shows the relationship between the CP values obtained from the new regression coefficients listed below and the experimental data. The figure shows significant improvement in the predictability of the CP for the GTL diesel fuel.

The new coefficients calculated by LINGO are:

$$a = 1195.917$$

$$b = -5.382029$$

$$c = -2.632678$$

$$d = 0.1358335$$

$$e = 0.1992243E-01$$

$$f = 759.4667$$

$$g = -4.907416$$

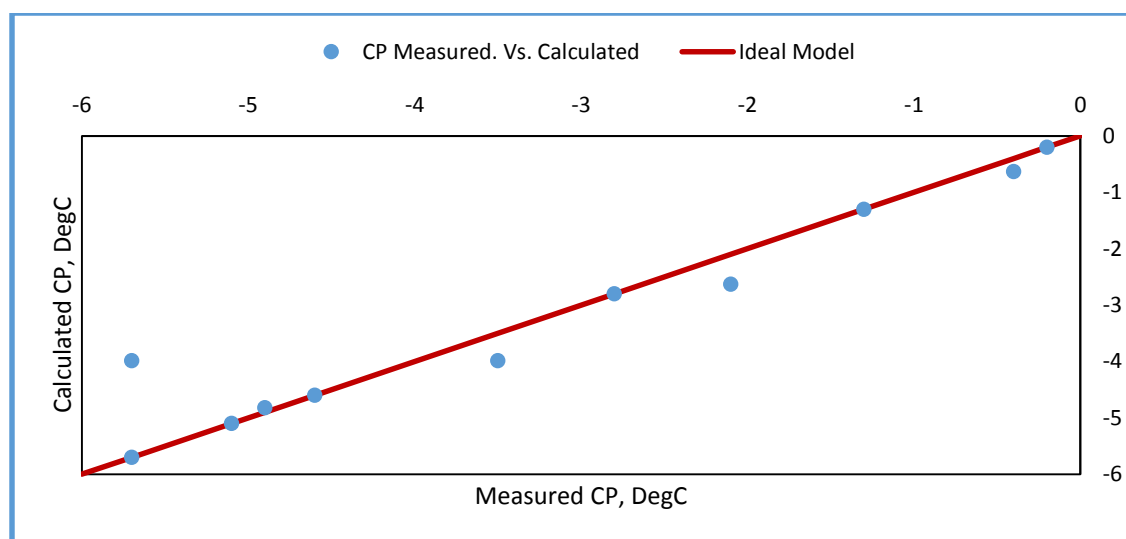


Figure 6.2 Cloud point calculated vs. measured at different IBP using LINGO regression.

The calculated cloud point values became aligned with the measured values in a much better fit, accordingly the formula used from the literature [19] still valid however new regression coefficients were estimated.

6.2 Modeling the Kinematic Viscosity using Distillation Data

6.2.1 Using Literature Regression Coefficients (Model Testing)

Karonis, et al. from the National Technical University of Athens, Greece [30] developed mathematical expression for the estimation of the properties of selected diesel fuel properties. Experiments were performed using 128 gas oil samples from different conventional refineries, the majority of predictions were based on distillation data and densities of the samples.

Below Equation 6.3 developed to estimate the Kinematic Viscosity for conventional diesel at 40°

$$V_{40} = a \cdot DENS + b \cdot DENS^2 + c \cdot D_{10}^2 + \frac{d}{D_{10}} + e \cdot D_{50}^2 + \frac{f}{D_{50}^2} + g \cdot D_{90}^2 + \frac{h}{D_{90}} + i \quad (6.3)$$

where:

V₄₀: Kinematic Viscosity, cSt at 40°

DENS: Fuel Density g/ml at 15°.

D₁₀: Distillation Temperature for the 10% volume.

D₅₀: Distillation Temperature for the 50% volume.

D₉₀: Distillation Temperature for the 90% volume.

Table 6.2 Calculation of kinematic viscosity from distillation data, literature regressions coefficients

Cut	>130	>140	>150	>160	>170	>180	>190	>200	>210	>215
Dens	0.76772	0.768706	0.770406	0.77231	0.773738	0.776016	0.77741	0.779076	0.78081	0.781728
Dens2	0.58939	0.590908	0.593525	0.59646	0.598670	0.602200	0.60436	0.606959	0.60966	0.611098
D10	187.9	191.7	199.5	208.1	215.3	226.6	232.7	241.3	250.4	253.1
D10^2	35306.41	36748.89	39800.25	43305.61	46354.09	51347.56	54149.29	58225.69	62700.16	64059.61
D50	260.3	261.1	264.1	268.0	271.3	273.7	277.0	280.7	285.4	285.6
D50^2	67756.09	68173.21	69748.81	71824.00	73603.69	74911.69	76729.00	78792.49	81453.16	81567.36
D90	328.6	329.4	330.2	331.9	332.0	332.1	335.1	335.6	335.5	338.2
D90^2	107978.0	108504.4	109032.0	110157.6	110224.0	110290.4	112292.0	112627.4	112560.3	114379.2
Kin Visc Calculated	2.385	2.275	2.127	2.077	2.096	2.195	2.369	2.628	2.991	3.114
Kin Visc Measured	2.2362	2.2938	2.3981	2.5513	2.6517	2.8165	2.9405	3.1065	3.2919	3.3636

a, b, c, d, e, f, g, h, i Regression coefficients

$$a = 124.08$$

$$b = -69.74$$

$$c = 1.82E-04$$

$$d = 3.86E+03$$

$$e = 6.26E-05$$

$$f = 1.52E+05$$

$$g = 2.58E-05$$

$$h = 1.06E+03$$

$$i = -9.13E+01$$

Figure 6.3 indicates the plot between the calculated kinematic viscosity and measured values for different GTL Diesel heavy cuts; it is clear that the correlation from literature did not succeed to match the calculated values with the measured ones; this is due to the failure of the literature regression coefficients for conventional diesel fuel to fit the data for the heavy cuts of the GTL Diesel fuel.

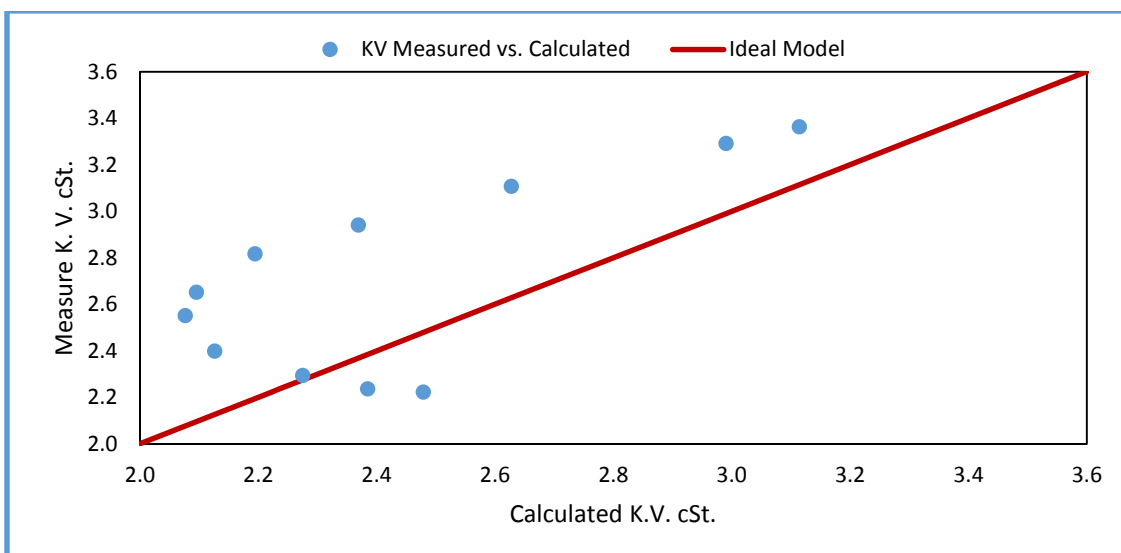


Figure 6.3 Kinematic viscosity (KV) measured values vs. calculated using literature regression coefficients [30]

6.2.2 Using Estimated LINGO Regression Coefficients (Calibrating Model)

Since the existing regression coefficients from the literature [30] failed to give good fitting between the actual measured values in Lab and the literature model results; LINGO software estimated better regressions coefficients for the cloud point of GTL Diesel fuels. The detailed program is shown in APPENDIX C, Figure 6.4 shows the improvement of the model by calculating new regression coefficients. The new calibrating model data was found to be in excellent agreement with the experimental data based on the new regression coefficient obtained using LINGO.

The new coefficients calculated by LINGO are:

$$\begin{array}{llll} a = 69.6489 & b = 107.1539 & c = -5.88E-05 & d = 1.38E+03 \\ e = 1.35E-04 & f = 1.26E+00 & g = -7.79E-05 & h = 1.51E+00 \\ i = -1.20E+02 \end{array}$$

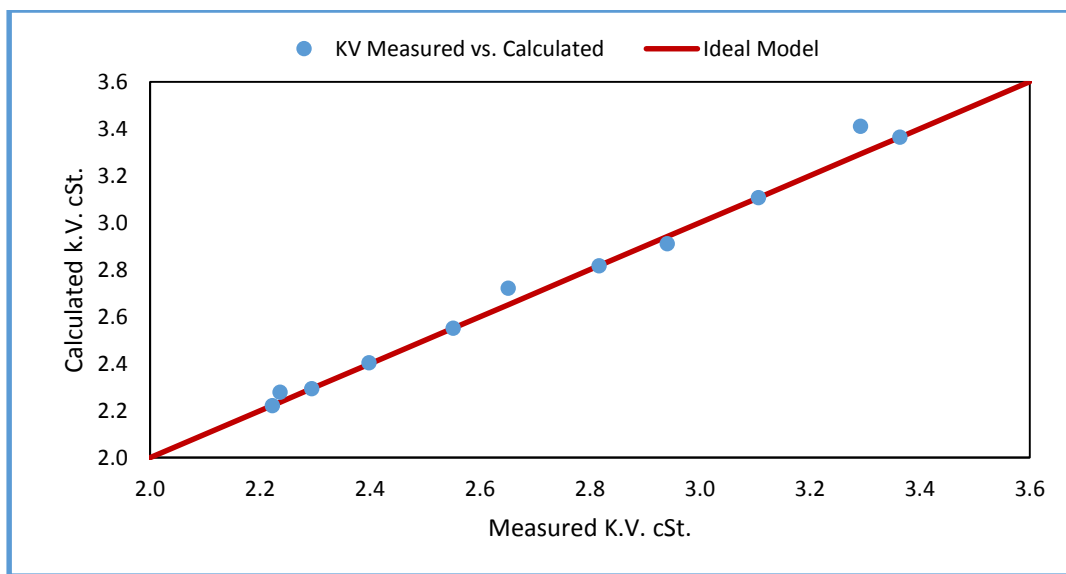


Figure 6.4 Kinematic viscosity measure vs. calculated using LINGO new regression coefficients

Table 6.3 Calculation of kinematic viscosity using distillation data, and new regressions coefficients

Cut	>130	>140	>150	>160	>170	>180	>190	>200	>210	>215
Dens	0.76772	0.768706	0.770406	0.77231	0.773738	0.776016	0.77741	0.779076	0.78081	0.781728
Dens2	0.58939	0.590908	0.593525	0.59646	0.598670	0.602200	0.60436	0.606959	0.60966	0.611098
D10	187.9	191.7	199.5	208.1	215.3	226.6	232.7	241.3	250.4	253.1
D10^2	35306.41	36748.89	39800.25	43305.61	46354.09	51347.56	54149.29	58225.69	62700.16	64059.61
D50	260.3	261.1	264.1	268.0	271.3	273.7	277.0	280.7	285.4	285.6
D50^2	67756.09	68173.21	69748.81	71824.00	73603.69	74911.69	76729.00	78792.49	81453.16	81567.36
D90	328.6	329.4	330.2	331.9	332.0	332.1	335.1	335.6	335.5	338.2
D90^2	107978.0	108504.4	109032.0	110157.6	110224.0	110290.4	112292.0	112627.4	112560.3	114379.2
Kin Visc Calculated	2.2780	2.2938	2.4033	2.5513	2.7215	2.8165	2.9109	3.1065	3.4110	3.3636
Kin Visc Measured	2.2362	2.2938	2.3981	2.5513	2.6517	2.8165	2.9405	3.1065	3.2919	3.3636

6.3 Various Properties Model, using Normal and *iso* Paraffin Data

6.3.1 Using Literature Regression Coefficients (Model Testing)

In 1992, Cookson and Smith from Melbourne Australia developed a common formula for different conventional Diesel fuels using different regression coefficient for each property [11]. In their model they simple used the paraffin's and aromatic content, i.e. total normal paraffin [n], total *iso*-paraffin (branched) [BC] and total Aromatics [Ar] [11]. Equation 6.4 used below different conventional diesel properties.

$$P = a_1[n] + a_2[BC] + a_3[Ar] \quad (6.4)$$

where P is the property and a_1 , a_2 and a_3 are regression coefficients as shown in Table 6.4

Table 6.4 Literature regression coefficients for various properties

	a_1	a_2
Cloud point	28	-43
Density	1.3579	1.143
Cetan Index AP	98.4	48.4

Table 6.5 and Figures 6.5, 6.6 and 6.7 represent the calculation of the specs using the literature data [11].

Table 6.5 Calculation of various properties using n, iso paraffin, literatures regressions

Cut No.	>130°C	>140°C	>150°C	>160°C	>170°C	>180°C	>190°C	>200°C	>210°C	>215°C
n-Paraffin	0.7035	0.6912	0.691	0.685	0.6812	0.6797	0.6846	0.6815	0.6952	0.6953
i-Paraffin	0.297	0.309	0.309	0.315	0.318	0.320	0.315	0.319	0.305	0.305
Cloud point calc	6.949	6.067	6.057	5.618	5.382	5.263	5.615	5.382	6.359	6.358
Cloud point meas.	-5.7	-5.1	-4.9	-4.6	-3.5	-2.8	-2.1	-1.3	-0.4	-0.2
Inverse Sp. Gr.	1.294	1.292	1.292	1.291	1.289	1.289	1.290	1.290	1.292	1.293
Density calc	772.689	774.133	774.227	774.795	775.836	775.823	775.259	775.453	773.755	773.605
Density Meas.	767.72	768.706	770.406	772.31	773.738	776.016	777.41	779.076	780.81	781.728
diesel index calc	83.575	82.970	82.955	82.669	82.441	82.380	82.620	82.480	83.160	83.175
diesel index ASTM	82.081	82.265	82.882	83.674	84.323	84.986	85.708	86.493	87.391	87.526

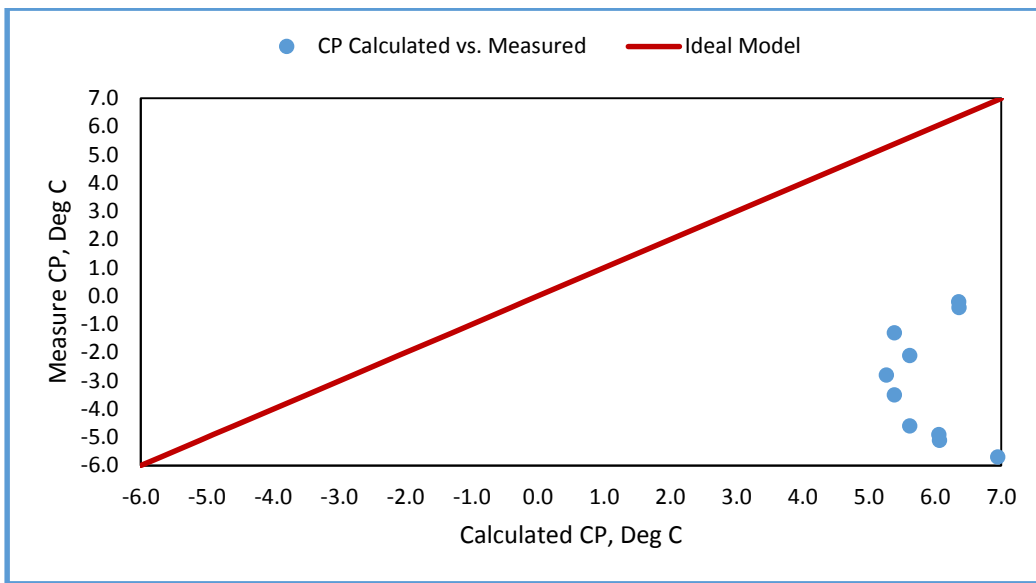


Figure 6.5 GTL Diesel calculated vs. measured CP using paraffin's content and literature regressions [11]

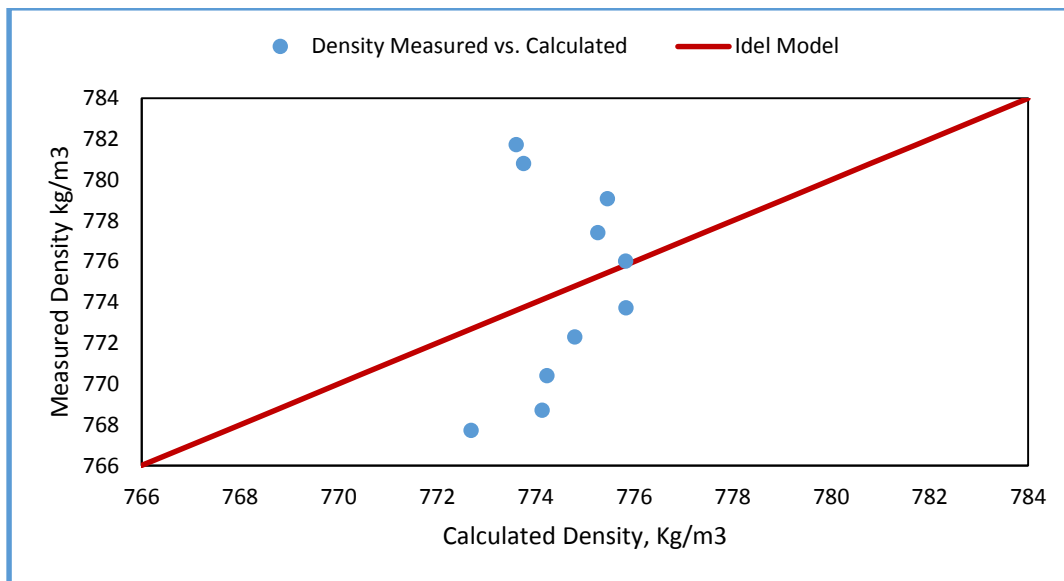


Figure 6.6 GTL Diesel calculated vs. measured density using paraffin's content and literature regressions [11]

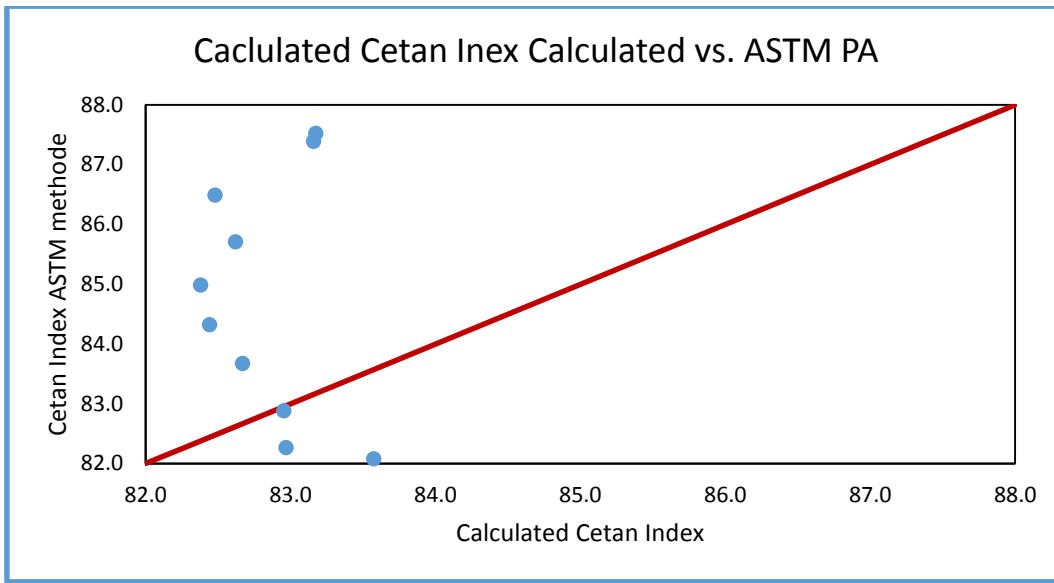


Figure 6.7 GTL Diesel calculated vs. ASTM Cetane Index using paraffin's content and literature regressions [11]

From the figures above it is clear that Cookson and Smith model completely failed to predict the experimental measured GTL diesel fuel properties for the cloud point, density, and Cetane Index.

6.3.2 Using Estimated LINGO Regression Coefficients (Calibration Model)

LINGO was used to calculate new regression coefficients for the GTL Diesel fuel samples. The LINGO Program for this model can be found in Appendix C, below Equation 6.5 was used for the GTL Diesel for various properties.

$$P = a_0 + a_1[nP] + a_2[iP] \quad (6.5)$$

where nP is normal paraffin content in wt. basis and iP are *iso* paraffin in wt. basis. The new regression coefficients are listed in Table 6.6.

Table 6.6 New estimated regressions coefficients using LINGO for n, iso paraffin

	a_0	a_1	a_2
Cloud point	18.990	-0.1217	-0.4146
Density	806.106	-0.212	-0.9713
Dynamic Viscosity	2.485	-0.0145	0.0007278
Flash Point	267.953	-0.8230	-3.8020

Figures 6.8, 6.9, 6.10 and 6.11 represent the calculation of the GTL Diesel various properties using the LINGO obtained new regression coefficients. Still there was failure of the model to fit the measured data for the heavy cuts of the GTL Diesel fuel. For GTL Diesel by knowing only its paraffin's content, it is difficult to predict its properties by the simple model provided in Equation 6.5.

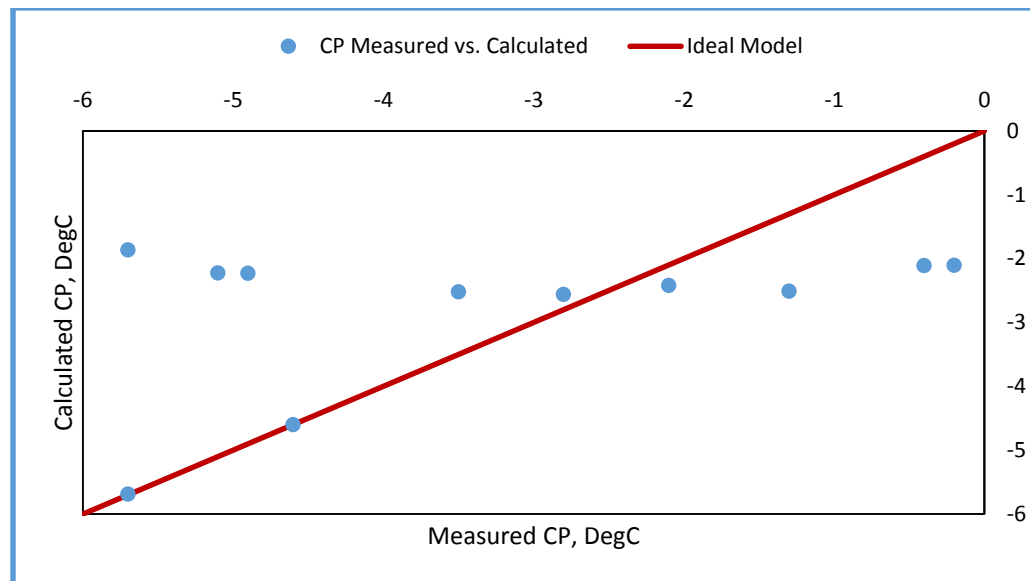


Figure 6.8 Calculated vs. measured cloud point using paraffin's content and LINGO new coefficients

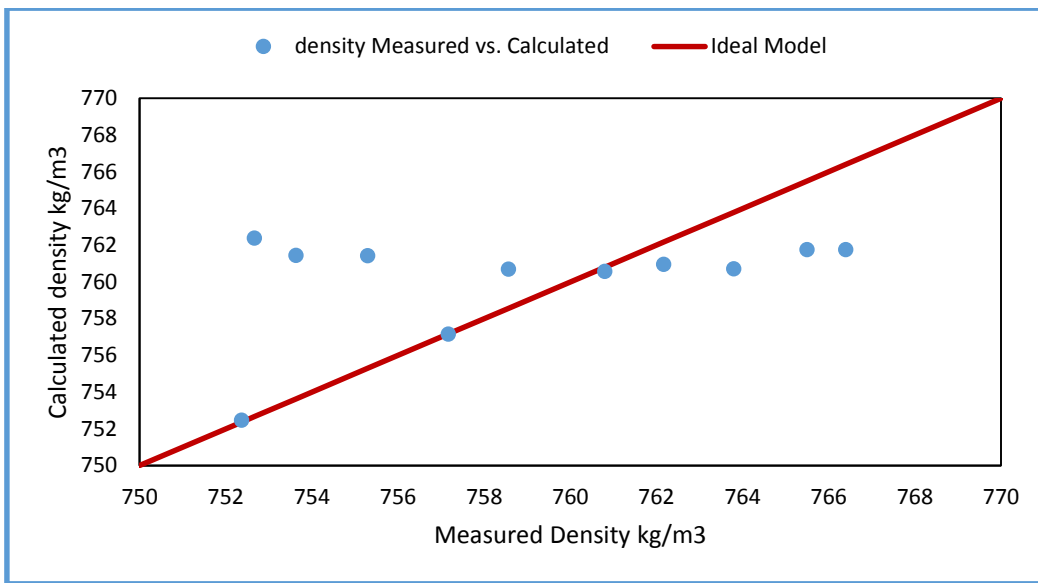


Figure 6.9 Calculated vs. measured density using paraffin's content and LINGO new coefficients

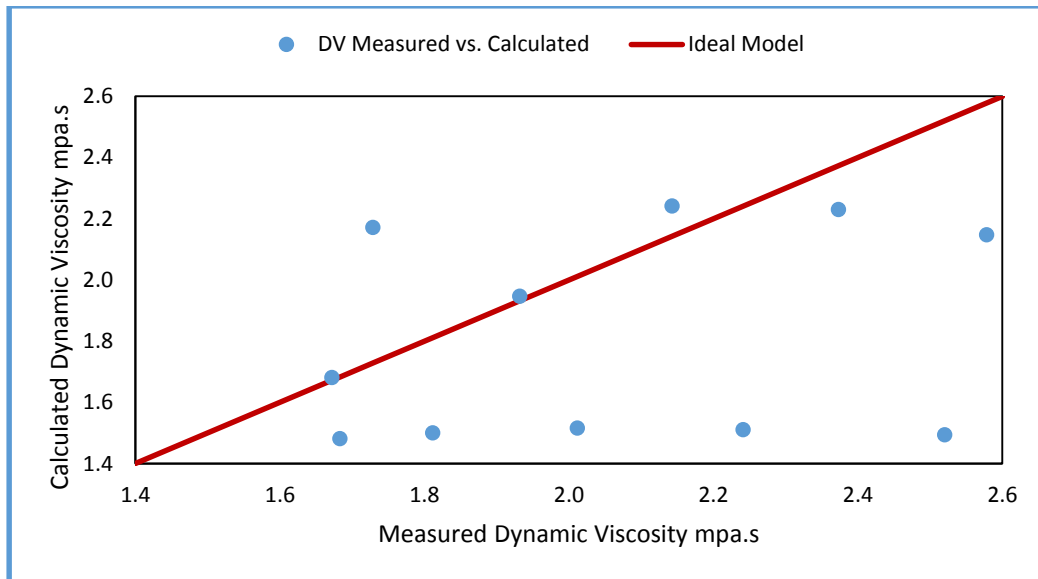


Figure 6.10 Calculated vs. measured dynamic viscosity using paraffin's content and LINGO new coefficients

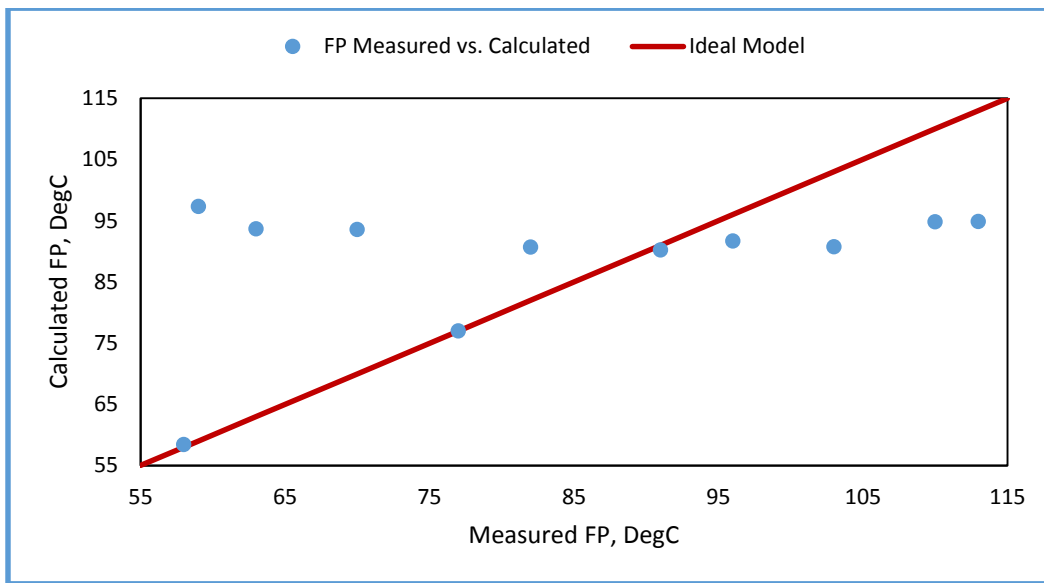


Figure 6.11 Calculated vs. measured flash point using paraffin's content and LINGO new coefficients

The calculated various properties values are not matching with the measured values even after estimating new regression coefficients by LINGO, accordingly the formula used by the literature is not valid for GTL Diesel.

6.4 Various Properties Model, using Individual Carbon Number Distribution Data (Empirical Model)

Since the simple model from literature for predicting the GTL Diesel properties by knowing the normal and *iso* paraffin's content failed, it was investigated further to design a new model using the individual carbon number distribution for each sample, Equation 6.5 below used for the prediction.

$$\begin{aligned}
P = & a_0 + a_1[C_9] + a_2[C_{10}] + a_3[C_{11}] + a_4[C_{12}] + a_5[C_{13}] + a_6[C_{14}] + a_7[C_{15}] \\
& + a_8[C_{16}] + a_9[C_{17}] + a_{10}[C_{18}]
\end{aligned} \tag{6.5}$$

where P is the GTL Diesel property, C is the weight percentage of carbon content and a_0 to a_{10} are regression coefficients, LINGO was used to determine these coefficients. Below Table 6.7 shows the calculated coefficients for each property.

Table 6.7 Estimated regressions coefficients using LINGO for individual CN

	Cloud Point	Density	Dynamic Viscosity	Flash Point
a_0	1.235	1.235	1.235	-116.880
a_1	1.235	1.235	1.235	1.235
a_2	0.744	19.344	1.199	1.235
a_3	1.235	1.235	1.235	1.235
a_4	1.235	1.235	1.235	0.029
a_5	-19.157	28.969	-18.648	1.235
a_6	163.776	22.975	160.796	-0.983
a_7	-110.865	-63.201	-109.730	31.517
a_8	-211.280	-61.838	-207.387	-15.657
a_9	107.592	107.592	106.491	-3.409
a_{10}	72.880	40.224	71.955	2.723

Figures 6.12, 6.13, 6.14 and 6.15 represent the calculation of the properties using the empirical model (Equation 6.5). Again the model failed to predict the properties for the heavy cuts of the GTL Diesel fuel. Except for flash point property where the fitting was perfect, this means the formula can be used successfully to predict the flash point for GTL Diesel fuels by knowing individual CN contents but not for the rest of the properties.

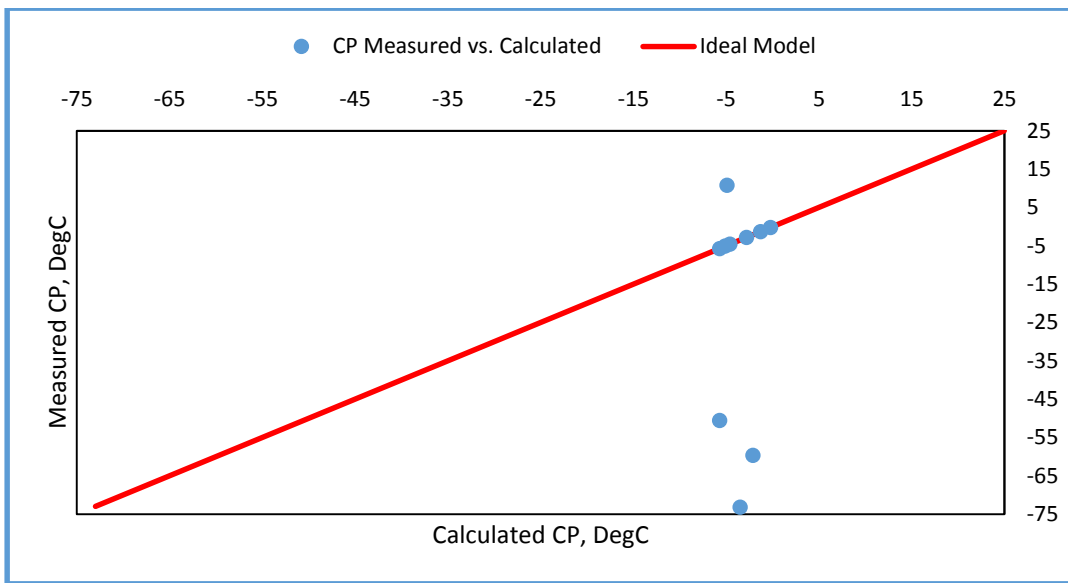


Figure 6.12 Measured vs. calculated cloud point using individual CN at different IBP

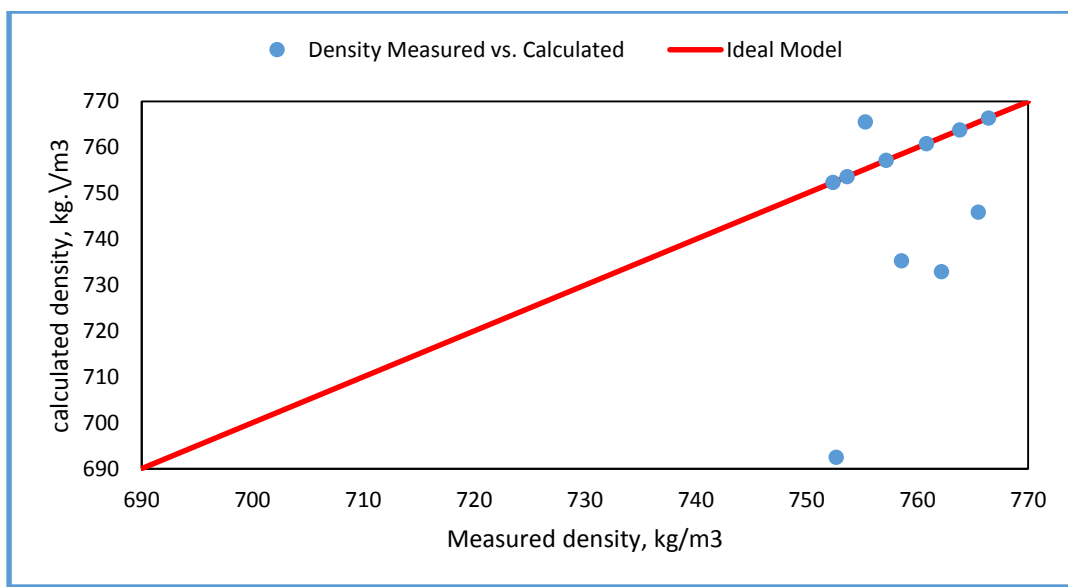


Figure 6.13 Measured vs. calculated density using individual CN at different IBP

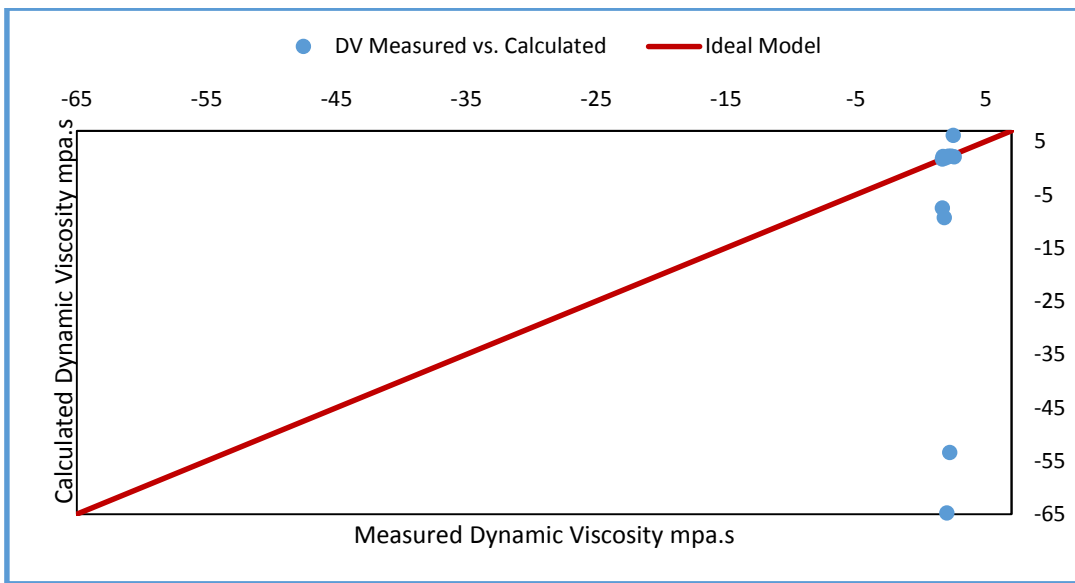


Figure 6.14 Measured vs. calculated dynamic viscosity using individual CN at different IBP

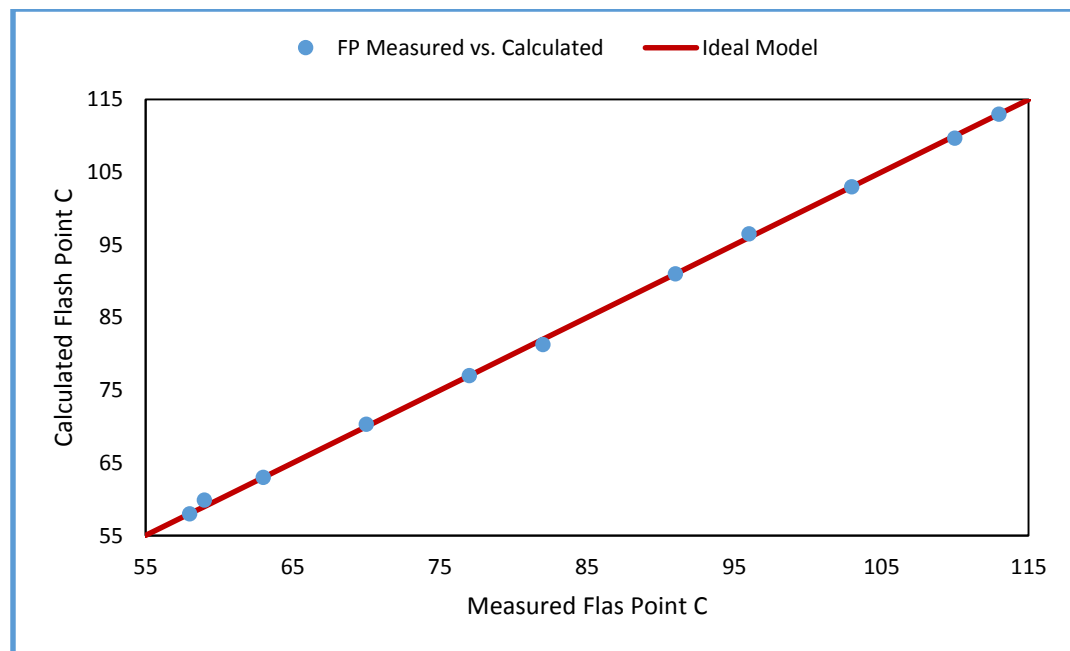


Figure 6.15 Measured vs. calculated flash point using individual CN at different IBP

6.5 Various Properties Model, using Total Carbon Number Grouping Data (Empirical Model)

Utilizing both ideas of the linear equation for normal and *iso* paraffin (calibration model) and the individual carbon number model (empirical model) into new correlation (empirical model), i.e. grouping some carbon numbers into a known hydrocarbon compound/product could be a successful path to formulate good equations to predict the GTL Diesel properties.

Some modern refineries are producing several cuts for kerosene and diesel that could be light and heavy cuts, below are the carbon content groups used for these products [31].

Light Kerosene: C₈, C₉, C₁₀ and C₁₁.

Heavy Kerosene: C₁₂, C₁₃, C₁₄ and C₁₅.

Light Diesel: C₁₆, C₁₇, C₁₈, C₁₉.

Heavy Diesel: C₂₀, C₂₁, C₂₂ and C₂₃

Accordingly, the Equation 6.6 for the properties prediction is as below.

$$P = a_0 + a_1[\text{Light Kerosene}] + a_1[\text{Heavy Kerosene}] + a_2[\text{Light Diesel}] + a_3[\text{Heavy Diesel}] \quad (6.2)$$

where a₀, a₁, a₂ and a₃ are regression coefficients were calculated using LINGO programing. The below Table 6.8 indicates the coefficients.

Table 6.8 Estimated regressions coefficients using LINGO for CN grouping.

	Cloud Point	Density	Dynamic Viscosity	Flash Point
a_0	12.6769	477.8303	-15.0464	-985.1677
a_1	-0.3166	2.5030	0.1515	9.4694
a_2	-0.1909	2.7367	0.1578	10.4530
a_3	0.1302	3.6386	0.2443	13.8121
a_4	-0.6788	1.1346	0.0409	4.2537

Figures 6.16, 6.17, 6.18 and 6.19 represent the calculation of the properties using the new model. It is clearly showing that the new model totally succeeded to fulfill the prediction of physical properties of GTL Diesel by knowing its carbon content and grouping them into main four groups. Accordingly, GTL Diesel Properties similar to density, viscosity, flash point and cloud point can be predicted by knowing the carbon content of GTL Diesel and the new empirical model (Equation 6.2).

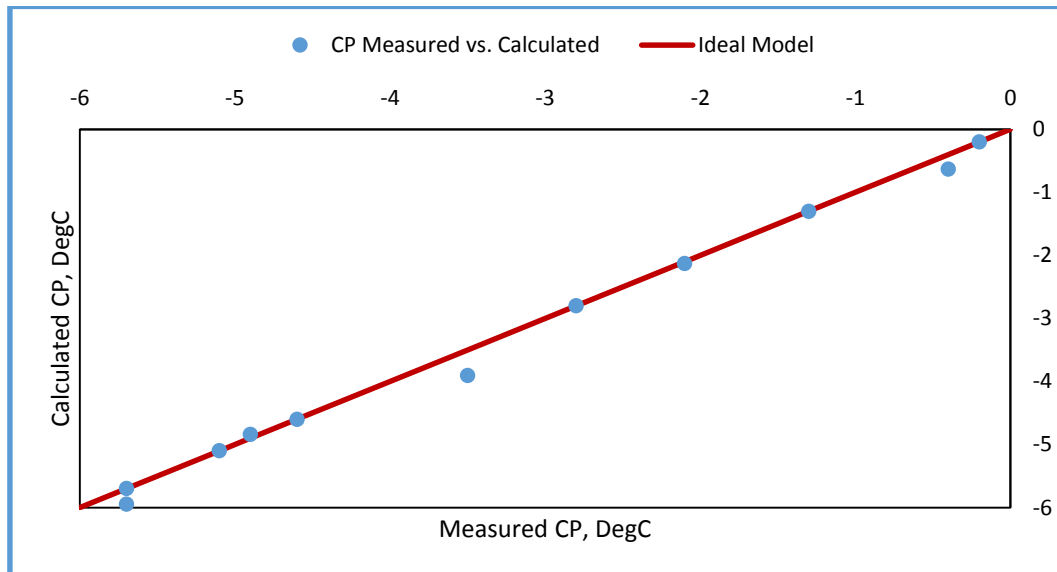


Figure 6.16 Measured vs. calculated cloud point using CN grouping at different IBP

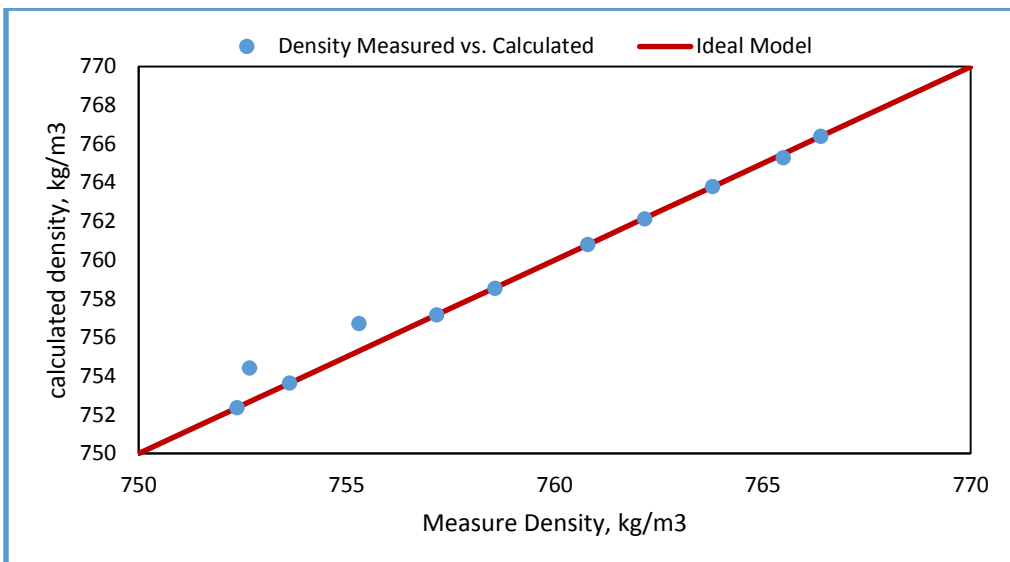


Figure 6.17 Measured vs. calculated density using CN grouping at different IBP

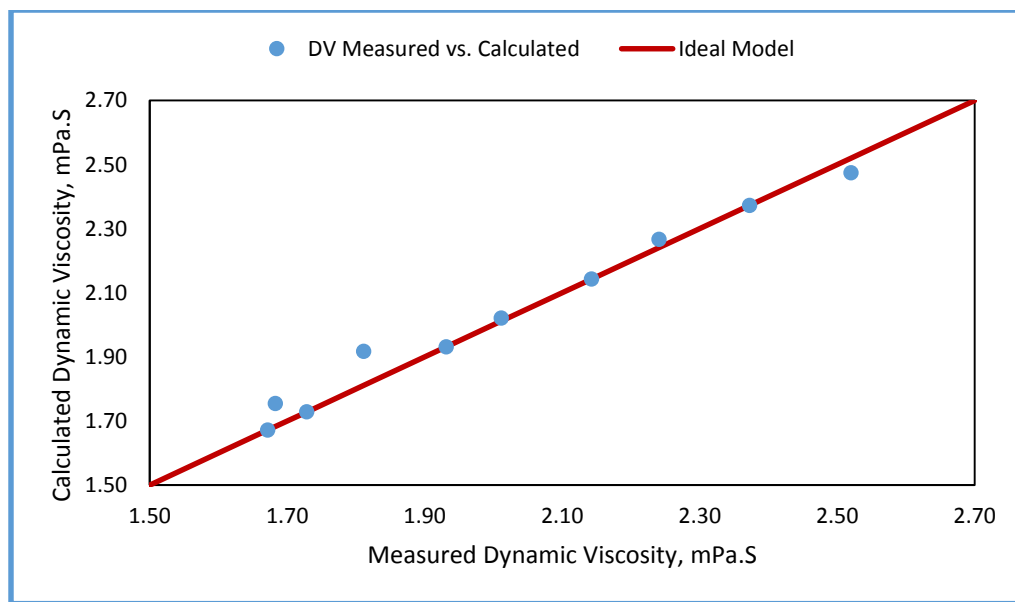


Figure 6.18 Measured vs. calculated dynamic viscosity using CN grouping at different IBP

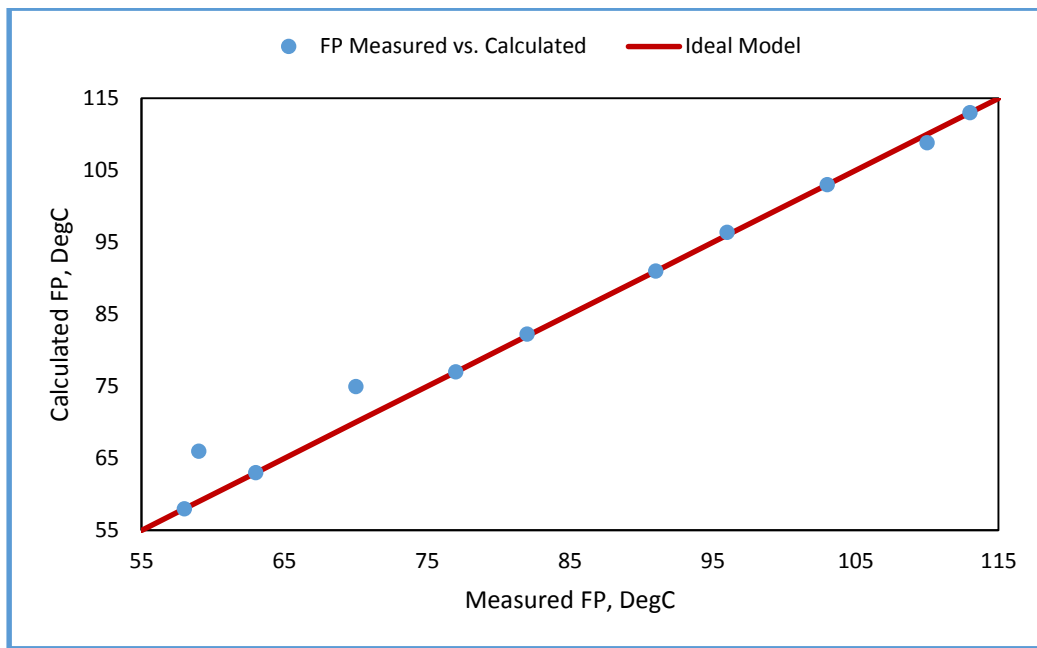


Figure 6.19 Measured vs. calculated flash point using CN grouping at different IBP

CHAPTER VII

CONCLUSIONS AND RECOMMENDATIONS

In conclusion, the research presented reasonable information for the GTL Diesel specifications at different boiling ranges and carbon number distributions, these data were utilized to formulate predication equations that can be used to estimate some GTL Diesel properties by knowing either its distillation data or carbon content. Separating the light components from the GTL Diesel cuts at different IBP then measuring the properties of the heavier cuts, gave a great opportunity to discover the behavior of each property at different boiling range and how far that affect the property with respect to its marketing specification.

The research expressed the improvement of GTL Diesel quality by changing its composition, where the higher carbon numbers GTL Diesel the better were the properties; this can be utilized in real GTL Diesel manufacturing facility where the GTL Diesel composition can be changed to meet certain specifications. GTL Diesel manufacturing is always challenging, where the market demand is always changing. One day, GTL Diesel prices could be higher than GTL Naphtha prices and in the other day the prices change again, the same for the kerosene (Jet Fuel) prices. Accordingly, the GTL Diesel facility should be designed in a way to be as much fixable as possible to be able to produce the highest profitable products as per the market demand.

For an old design GTL plant similar to ORYX GTL where it is only producing three products of LPG, Naphtha and Diesel; there is a good chance for them to modify

their facility to be able to produce an intermediate product between Naphtha and Diesel i.e. Kerosene. Accordingly, they will have good flexibility to change their products slates based on the distribution market requirements.

While in case of new GTL manufacturing facility that is under design phase, it should be considered to have multi GTL products; the implementation will be much easier and cheaper rather than modifying the existing plants. Below summarizes the findings and conclusion for the study.

GTL Diesel specifications were improved with reducing the amount of light hydrocarbon content. Higher GTL Diesel density and viscosity will support GTL Diesel as an independent fuel for Diesel Engines rather than being used as a blend stock with conventional diesel. Higher flash point will support for more sever storage conditions especially in hot climates similar to GCC countries. Higher Cetane Index is improving the performance of the diesel engines. Except for the cloud point and pour point (cold properties), both were increasing, that is considered a drawback in GTL Diesel quality especially in cold countries. It is important to compromise between the GTL Diesel specifications and the target markets; either hot or cold countries, summer or winter climates based on each requirement. As mentioned in CHAPTER I, there is no current ASTM standard for GTL Diesel similar to conventional Diesel; however the manufacturing and distributing companies have formulated set of specifications for GTL Diesel in order to control its trading. The study investigated new areas for GTL Diesel specifications where another formulation can be considered. Table 7.1 proposes new specifications formulation for GTL Diesel; similar to conventional diesel grades in EN-

590 European diesel standards, where it specifies six Temperature Climate Grades of diesel fuel (Grade A...F) which differ in the CFPP values (+5 to -20°C). In addition, there are five Arctic Classes of diesel fuel (Class 0...4) characterized by different properties.

Table 7.1 Proposed GTL Diesel new specification formulation

Property	Unit	GTL Diesel Grades		
		Grade A	Grade B	Grade D
Cloud Point	°C, max	0	-3	-6

This study managed to prove the applicability for GTL Diesel to certain composition-properties related prediction models that were estimated earlier for conventional diesel. The study was able to exclude other models made for conventional diesel as well, where the relation between the models calculated properties and the measured laboratory results were not matching.

Successfully, the study prospered to generate new formulas that are able to predict the GTL Diesel properties at different boiling ranges and carbon number distributions, rather than the formulas of conventional diesel that failed to be applied to GTL Diesel.

In order to test the applicability of each formula, standard error was calculated for each correlation between the composition and the property; standard error was calculated as per the below Equation 7.1.

$$\text{Standard Error} = \sqrt{\frac{\sum (Actual\ Measure - Model\ Result)^2}{(Number\ of\ points - 2)}} \quad (7.1)$$

Table 7.2 below represents the standard error calculated for each GTL Diesel Property where the lower standard error (gray highlighted) is the best model for the GTL Diesel specification. For cloud point property, total carbon number grouping with the regression coefficients calculated by LINGO was the best model. For kinematic viscosity, literature equation utilizing the distillation data and new regression coefficients calculated by LINGO was the best model. For density property, total carbon number grouping with the regression coefficients calculated by LINGO was the best model. For dynamic viscosity property, total carbon number grouping with the regression coefficients calculated by LINGO was the best model. For Flash Point, individual carbon number with the regression coefficients calculated by LINGO was the best model. In general carbon number grouping model was the best successful model to predict GTL Diesel properties by knowing its carbon number distribution.

Table 7.2 GTL Diesel properties prediction equations, standard error

	Distillation Data		Paraffins Content		Individual carbon number	Total Carbon Number Grouping
Equation Source	Literature		Literature		New	New
Regression Source	Literat.	LINGO	Literat.	LINGO	LINGO	LINGO
Cloud Point	1.67	0.66	10.28	2.09	37.3	0.19
Kinematic Viscosity	0.44	0.05	-	-	-	-
Density	-	-	5.16	5.28	26.23	0.05
Dynamic Viscosity	-	-	-	-	31.19	3.06
Flash Point	-	-	-	-	0.47	0.80

For existing GTL Diesel producing facility, similar to ORYX GTL simple modifications can be implemented, by adding additional draw off trays for the existing fractionation column, or adding Diesel splitter downstream the fractionation column as shown in Figure 7.1 below. This modification was already catered in the original design of Shell Pearl GTL, where the fractionation column is designed to produce more products.

The cost of new draw off trays compared to additional new column should be investigated further based on products flow rates and target specification.

For new GTL Diesel production facility, it is much easier to consider the required diesel cuts and the number of products slates in the design phase, where it will be minimal cost compared to the modification of existing GTL facilities.

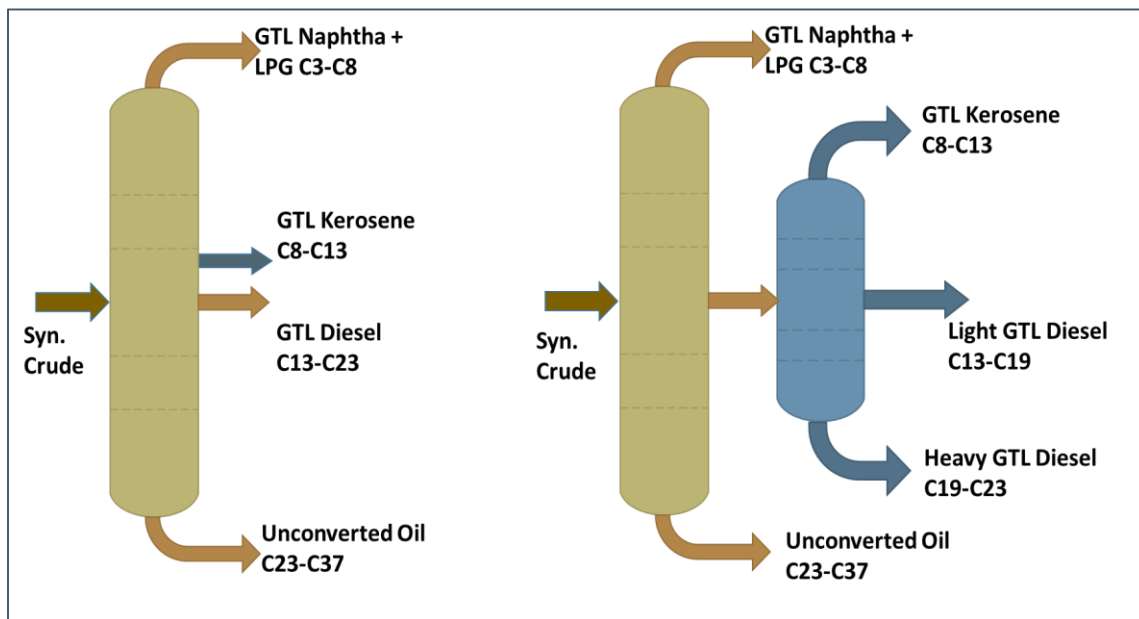


Figure 7.1 Two possible modifications to existing GTL facility to produce additional products

As indicated in Table 5.1 CHAPTER V, the percentage of light fraction of GTL Diesel was increased with the increase of IBP of the cut; it was almost about 30% of the whole sample in case of “< 215°C IBP” sample. So if it is targeted to improve the GTL Diesel specification by removing the light ends and increasing the IBP, this should not mean to lose the light cut products without any profit.

This light hydrocarbon fraction as shown in Figure 5.4 consists of C7 to C13. This carbon distribution is almost kerosene slate, where similar to SHELL Pearl GTL; this slate is extracted as GTL Jet Fuel (SPK) and exported as final product for aviation industry with great profit, Elbashir’s research team have conducted extensive investigations for the GTL Jet fuels [33].

However it could be more profitable to go for further processing where C10 to C13 cut can be extracted, this cut is the most suitable feedstock for the Linear Alkyl Benzene production, however this cut should be normal paraffin [20] and not to be mixed between *iso* and normal paraffins as the current case of SPK. All *iso* component should be saturated to be normal paraffin as well. This could be a new area for research and future work to discover how to extract the specified C10-C13 cut from GTL products, then to saturate this cut with Hydrogen. Feasibility study can be also conducted to investigate the profitability of this new product versus the existing GTL Jet fuel.

The research experiments generated different grades of GTL Diesel, blending study for these different GTL Diesel grades with conventional diesel will investigate

different diesel blends in terms of specification; this research work plan could be similar to Elbashir's research team previous work for GTL kerosene.

REFERENCES

- [1] Franz Fischer and Hans Tropsch at the "Kaiser-Wilhelm-Institut für Kohlenforschung" in Mülheim Van der Ruhr (Germany), United Sates Patent Office, 1930.
- [2] Alternative Fuels and Their Potential Impact on Aviation, D. Daggett and O. Hadaller; Boeing Commercial Airplanes; Seattle, Washington 98124, R. Hendricks; National Aeronautics and Space Administration; Glenn Research Center; Cleveland, Ohio 4135 R. Walther, MTU Aero Engines GmbH, 80995 Munich, Germany..
- [3] David A Wood, "Gas-To-Liquid (GTL) a Review of an Industry Offering Several Routes for Monitizing Natural Gas" *Journal of Natural Gas Scince and Engineering* , vol. 09, November. 2012, Pages 196-208.
- [4] 2014 World Oil Outlook, OPEC, © OPEC Secretariat, 2014, ISBN 978-3-9502722-8-4.
- [5] International Agency for Research on cancer (IARC) MONOGRAPHS VOLUME 45. Diesel Fuels, Chemical and Physical Data, Page 220-221.
- [6] A NMR-Based Carbon-Type Analysis of Diesel Fuel Blends from Various Sources. JT Bays and DL King, Prepared for the U.S. Department of Energy under Contract DE-AC05-76RL01830, Pacific Northwest National Laboratory, May 2013.
- [7] Diesel Fuels Technical Review, CHEVRON, 2007.
- [8] David J. Cookson, Jozef L. Latten*, Ian M. Shawt and Brian E. Smith, Property-composition relationships for diesel and kerosene fuels, Fuel & Energy Journal vol. 64, 1985.
- [9] David J. Cookson, C. Paul Lloyd, and Brian E. Smith, Investigation of the Chemical Basis of Diesel Fuel Properties, Fuel & Energy Journal vol. 2, 1988.
- [10] David J. Cookson and Brian E. Smith, Calculation of Jet and Diesel Fuel Properties Using ^{13}C NMR Spectroscopy, Fuel & Energy Journal vol. 4, 1990.
- [11] David J. Cookson and Brian E. Smith, Observed and Predicted Properties of Jet and Diesel Fuels Formulated from Coal Liquefaction and Fischer-Tropsch Feedstocks, Fuel & Energy Journal vol. 6, 1992.
- [12] Neural Network Prediction of Cetan Number and Density of Diesel Fuel from its

Chemical Composition Determined by LC and GC-MS, .

- [13] Fuel Property, Emission Test, and Operability Results from a Fleet of Class 6 Vehicles Operating on Gas-To-Liquid Fuel and Catalyzed Diesel Particle Filters, Presented at the 2004 SAE Powertrain & Fluid Systems Conference & Exhibition, October 2004, Tampa, Florida. Teresa L. Alleman, Leslie Eudy, Matt Miyasato, Adewale Oshinuga, Scott Allison, Tom Corcoran, Sougato Chatterjee, Todd Jacobs, Ralph A. Cherrillo, Richard Clark, Ian Virrels, Ralph Nine, Scott Wayne, Ron Lansing, 2004.
- [14] Inductive Modeling of Physico-Chemical properties: Flash Point of Alkanes, D.Mathieu, ELSEVER, 2010.
- [15] GTL A Viable Alternative to Oil-Derived Transport Fuels, Craig Brown, Oxford Institute for Energy Studies, 2013
- [16] Effect of Combustion Design for Diesel Dual Fuel Engine, Osamu SAOTOME, Fumiya SATO, and Katsuhiko TAKEDA, The 3rd International Conference on Design Engineering and Science, ICDES 2014, Pilsen, Czech Republic, September 1-3, 2014
- [17] Effect of GTL Diesel Fuels on Emissions and Engine Performance, Rudolf R. Maly Research and Technology, Stuttgart, 10th Diesel Engine Emissions Reduction Conference, August 29 - September 2, 2004, Coronado, California
- [18] ORYX GTL powers school buses with GTL diesel, <http://www.gulf-times.com/qatar/178/details/410092/oryx-gtl-powers-school-buses-with-gtl-diesel>.28 Septemper 2014
- [19] INVESTIGATION ON DIESEL COLD FLOW PROPERTIES, R.Dinkov, D. Stratiev, D. Penev, G. Cholakov, University of Chemical Technology and Metallurgy – Sofia, Bulgaria
- [20] UOP Linear Alkylbenzene (LAB) Complex, Des Plaines sales office, info@uop.com.
- [21] The Fischer-Tropsch Process and Its Influence, Jeremy May, Sept. 26, 2002
- [22] Operating Manual TAMUQ Fuel Characterization Laboratory 174A, PO Box 23874 Engineering Building. Education city, Doha, Qatar
- [23] Work Instructions-Automatic distillation, TAMUQ, January 6, 2014, Doha, Qatar.
- [24] ASTM International. ASTM D4052, “Standard Test Method for Meter Density,

elative Density, and API Gravity of Liquids by Digital Density Meter”. Published November 2011

[25] ASTM International. ASTM D7042. “Standard Test Method for Dynamic Viscosity and density of Liquids by Stabinger Viscometer (and the Calculation of Kinematic viscosity)”. Published October 2012

[26] Standard Practice for measuring Viscosity, Doc. No. WI-L174A-VM-017, Fuel Characterization Lab-174A, TAMUQ, PO Box 23874, Engineering Building. Education city, Doha, Qatar

[27] ASTM International. ASTM D93 “Standard Test Methods for An American National Standard Flash Point by Pensky-Martens Closed Cup Tester”. Published November 2002

[28] Standard Practice for measuring Flash point tester PM-93, Fuel Characterization Lab-174A, TAMUQ, PO Box 23874, Engineering Building. Education city, Doha, Qatar

[29] Standard Practice for measuring Cloud and pour points, Fuel Characterization Lab-174A, TAMUQ, PO Box 23874, Engineering Building. Education city, Doha, Qatar

[30] Use of Mathematical Expression for the estimation of selected diesel fuel properties, D.Karonis, E.Lois, S.Stournas, F.Zannicos, National Technical university of Athens, Greece .

[31] TOTAL PETROLEUM HYDROCARONS, Agency for Toxic Substances and Disease Registry, USA

[32] <http://www.lindo.com/>, LINGO 15.0 - Optimization Modeling Software for Linear, Nonlinear, and Integer Programming.

[33] Elmalik, E.; Raza, B.; Warrag, S.; Ramadhan, H.; Alborzi, E.; Elbashir, N. O. (2014) "Role of Hydrocarbon Building Blocks on GTL Derived Synthetic Jet Fuel Characteristics" Industrial & Engineering Chemistry Research .53 (5), 1856–1865.

[34] ASTM International. ASTM D86, “Standard Test Method for Distillation of Petroleum Products at Atmospheric Pressure”, Published November 2014.

[35] Goodheart-Willcox, Chapter 14, Diesel fuels.

[36] Shell GTL Fuel & Shell GTL Fuel Marine, Product Information Version 2.0 (English) – December 2014

[37] Empirical Models, Mathematical Modeling, Lia Vas, www.usciences.edu/Empirical_models.pdf

APPENDIX A – EXPERIMENTS GUIDELINES

A.1 Atmospheric Distillation

As a principle for automatic distillation, based on its composition, vapor pressure, expected IBP or expected EP, or combination thereof, the sample required was placed in one of four groups. Apparatus arrangement, condenser temperature, and other operational variables were defined by the group in which the sample falls.

Below is the general guidelines for implementing the distillation test [23]:

Sample Preparation:

- 1- Each sample has been stored in the right conditions of 5 °C in the fridge.
- 2- About 100 ml of the test sample was placed into the 125 ml flask. The collecting cylinder was used for this purpose.
- 3- A stopper was fitted at the neck of the cooling tube.
- 4- The flask was inserted in the right position. We made sure that the correct heating plate has been used since the plat diameter can affect the heating rate.
- 5- 3 to 4 boiling stones were placed into the sample before inserting the thermometer (Pt100).
- 6- The collecting 100 ml cylinder was inserted in the recovery chamber.

Running the test

- 1- From start go to AUDCon.
- 2- From file choose “New Sample”, or you choose from previously stored method by clicking on “Open Method”. Save the file as “adx” extension to display the results later.

- 3- There are four groups, each with different parameters (heating rate, condenser temperature..., etc). The parameters can be altered depending on sample being tested. The altered methods can be saved and exported for later use. For GTL Diesel samples group 4 will be used.
- 4- After the correct method or group was chosen, go to the connect bottom on the task bar. Whence the connection with device has been established and the condenser temperature reaches the set value, you can start the distillation.
- 5- After the distillation was done wait for the system to cool down (usually takes about 15 min.) then remove the flask and measure the residue.
- 6- Enter the residue value and then you can display the results (heating curve, data table...etc) from the task bar.

All the results for the eleven samples including the complete cut GTL diesel are recorded in the log book of the test.

A.2 Density Analysis

Below are the general guidelines for implementing the density test for the GTL Diesel samples:

1. Clean the density meter by first injecting acetone and then if calibration is needed inject the ultra pure water. After this has been done inject the sample being tested. The density of the sample should be tested at least three times for accuracy. After testing the sample, the machine needs to be cleaned with acetone.

2. Turn the Density Meter on and wait 15min to stabilize. After the stabilization has taken place check that the reading shows 0.0012 gm/cc for the density and the temperature is roughly 20°C. If the reading is not 0.0012 gm/cc or the machine has not been used for 1 month or more then calibration needs to be done. If the temperature is not 20 then wait another 15min for stabilization.
3. First clean the machine by injecting ~ 2ml of acetone using the green syringe stored with the apparatus. The syringe should be connected to the sample injection port (left side when looking at the ports), and the sample should be injected until it is visible in the exit pipe (connected to storage container).
4. Keep the sample in this position and start the analysis by going to Menu → Adjustment → Density Check → Check Density, when OK appears on the screen select it to confirm the check. Wait for 3 -4 min until the machine beeps indicating the analysis is done.
5. Empty the acetone from the syringe into the machine then remove the syringe. In place of the syringe connect the free pipe coming from the machine (located below the inlet port) and then turn the pump on for 5 min to evacuate the system.
6. Calibration: If calibration is required follow this step, otherwise skip to 9.6. To calibrate use the available ultra pure water (remove using a long tipped medical syringe) and inject into the machine using the labeled green syringe following the sample procedure as in steps 9.2 – 9.4.

7. Test the sample by injecting it into the machine using the same syringe used for injecting acetone, but first wash the syringe thoroughly 2 or 3 times with the sample which is going to be tested. The sample should be tested 3 times for accuracy.
8. After testing the sample, the machine needs to be cleaned with acetone again. If the testing has been completed then it is safe to turn off from the switch at the back of the machine and the at the power socket. If another sample needs to be tested then after cleaning the machine with acetone the next set of tests can be done.

All the results for the GTL diesel samples are recorded in the log book for the test.

A.3 Viscosity Analysis

Below are the general guidelines for implementing the viscosity (kinematic and dynamic) test for the GTL Diesel samples [26]:

- 1- Clean the viscometer by first injecting acetone. After this has been done inject the sample being tested. The viscosity of the sample should be tested at least five times for accuracy. After testing the sample, the machine needs to be cleaned with acetone.
- 2- Select an instrument mode by pressing “MODE”, browse through the list of modes appear, then press “ENTER” to confirm the selection. Press “esc” to leave this window. The mode selected should always be (M0-ASTM (PRECISE)).
- 3- Set the desired measuring temperature, by selecting the menu item “various settings – set temperature” and press “ENTER”. Change the measuring temperature and confirm with ENTER. Temperature range: -56 °C to +105 °C. Testing temperature will be 40 °C.
- 4- Ensure that the cells are clean and dry,

- 5- Fill the syringe with 6ml from your sample and then inject about 2 ml.
- 6- Press the "START" key. The motor starts up to filling speed, the state display changes from "FILLING" to "MEASURING" and the first measuring values appear on the display. These are unstable at first, but become more accurate as the averaging period increases. When the values are stable, the state changes to "RESULT VALID", indicated by the arrow. The motor slows down to filling speed. The instrument asks you to "refill and press ENTER".
- 7- Refill 1 mL from the syringe and press again the "START" key. If the results of the first repetition are within the limits for viscosity and density, the state changes to "RESULT VALID", indicated by two diamonds. The motor slows to filling speed and the display is frozen until the START key is pressed again. in addition the "FILLING" state is displayed. The instrument is now ready to be refilled or to be rinsed and dried and then newly filled.
- 8- Rinse and dry the measuring cells immediately after a measurement is completed.
- 9- All the samples will be repeated three times and the results will be averaged.

All the results for the GTL diesel samples are recorded in the log book for the test.

A.4 Flash Point Analysis

Below are the general guidelines for implementing the Flash Point test for the GTL Diesel samples [28]:

- 1- Switch ON at the rear of the instrument.
- 2- Wait until the START OF TEST screen is displayed.
- 3- When ready for use, the START OF TEST screen will show the message “Enter: Operator”. And Raise the Pod.
- 4- Remove the Sample cup. Clean the Sample Cup, inside of the Lid and Shutter Assembly and the Stirrer with a clean dry lint free cloth.
- 5- Measure 50 ± 0.5 ml of sample into the cup. i.e. fill the Sample Cup to the line. Replace the Sample Cup into the Air Bath. And lower the Pod
- 6- There are two methods of entering data into most of the fields:
 1. Pre-Programmed: Data is selected from a pre-programmed List
 2. Direct Entry: Data is manually entered via the KEYBOARD or NUMBERPAD screens
- 7- Test Methods & Test Profiles, There are two methods of setting the test parameters (ramp rate, stirrer speed, dipping interval etc):
 1. Test Method: A set of test parameters (excluding Expected Flash Point) that conform precisely to the Test Method
 2. Test Profile: A set of custom/modified test parameters (including Expected Flash Point), based on an underlying Test Method
- 8- Expected Flash

There are two methods of inputting the expected flash (Exp.Flash):

1. Test Profile: The Expected Flash is automatically entered if it has been saved as part of the Test Profile
 2. Direct Entry: The Expected flash can be entered into the field, or an existing Expected Flash can be edited.
- 9- Press to start the test. The TEST IN PROGRESS screen will open. Temperature progress will be shown on the graph on the TEST IN PROGRESS screen. The yellow bands on the graph indicate where dipping will take place.
- 10- At the end of the test, the TEST FINISHED screen will display the result as shown in Figure A.1.

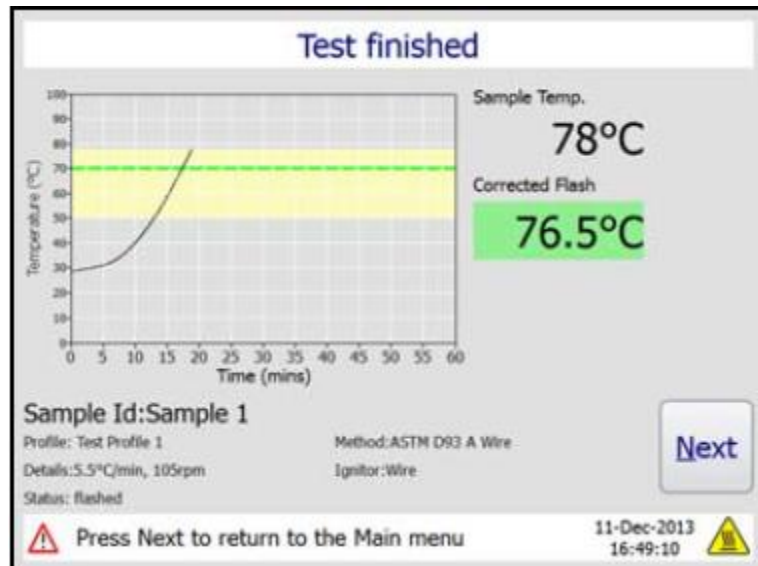


Figure A.1 Flash point test finish screen

11- The Fan will automatically switch on and start to cool the Air Bath. It will continue to run until the bath temperature is below 40°C or the Fan is switched off manually via the INFORMATION screen.

All the results for the GTL diesel samples are recorded in the log book for the test.

A.5 Cloud Point and Pour Point Analysis

Below are the general guidelines for implementing the cloud and pour point test for the GTL Diesel samples [29]

- 1- First prepare the sample by placing the DrySec into a small vial and Filling the vial with about 20ml of the sample. Then clean the sample cup and pipette the sample using a clean pipette tip. Dispense the sample into the sample cup of the analyzer and close the chamber lid.
- 2- The samples should be measured to 1 decimal place and in °C.
- 3- Start the test and wait for the results for cloud points, three results measured, average result will be calculated and presented.
- 4- After results for cloud point, pour points results will come, similarly three results per sample and average result will be presented.
- 5- Pour point results repeatability is +/- 3 for the analysis that is considered high error in the accuracy of the test.
- 6- Pour points results for the samples will not be considered during this study, as the variation of results are not matching the change of the cloud point.

APPENDIX B – EXPERIMENTAL RESULTS

The whole cut GTL Diesel sample received from Industry was analyzed for different analyses, below Table B-1 shows the results obtained.

Table B-1 GTL Diesel whole cut analysis

Carbon Distribution		Distillation D-86	
Component wt%	By GC MS	vol%	C
n-Paraffins	57.3	0	162.7
i-Paraffins	42.73	10	186.1
alfa-Olefins	0	15	194.0
Total alcohol	0	20	202.3
Total C6+	0	30	220.9
Total C7+	0.05	40	242.3
Total C8+	1.47	50	260.7
Total C9+	5.86	60	278.4
Total C10+	8.09	70	295.1
Total C11+	8.82	80	312.3
Total C12+	9.37	85	321.0
Total C13+	9.54	90	331.0
Total C14+	8.37	95	342.9
Total C15+	8.05	100	348.7
Total C16+	7.96	Density Kg/m3	767.41
Total C17+	7.38	Dynamic Vis. Mpa.s	1.672
Total C18+	7.54	Kinematic Vis. Mm ² /s	2.222
Total C19+	5.8	Flash Point, C	58.0
Total C20+	4.8	Cloud Point, C	-5.7
Total C21+	3.84	Pour Point, C	-9.0
Total C22+	1.93	CCI	82.20
Total C23+	0.76		
Total C24+	0.4		
Total C25+	0		
Total C26+	0		

Table B-2 Carbon distribution for heavy GTL Diesel fractions

Composition wt%.	>130° C	>140° C	>150° C	>160° C	>170° C	>180° C	>190° C	>200° C	>210° C	>215° C
n-Paraffins	70.35	69.12	69.1	68.5	68.12	67.97	68.46	68.15	69.52	69.53
i-Paraffins	29.65	30.9	30.91	31.54	31.84	32.02	31.52	31.86	30.48	30.49
Total C6	0	0	0	0	0	0	0	0	0	0
Total C7	0	0	0	0	0	0	0	0	0	0
Total C8	1.78	0.78	0	0	0	0	0	0	0	0
Total C9	7.73	6.94	4.19	1.61	0	0	0	0	0	0
Total C10	9.26	8.97	8.91	8.78	6.83	2.18	0.57	0	0	0
Total C11	9.6	9.77	9.85	10.42	11.05	10.39	7.89	3.6	0.78	0
Total C12	10.17	10.17	10.4	10.9	11.81	11.83	12.49	12.57	9.79	7.03
Total C13	10.4	10.59	11.16	11.75	12	12.76	13.26	14.06	15.5	15.66
Total C14	9.95	9.99	10.3	10.88	11	12.03	12.3	13.04	14.81	15.4
Total C15	9.15	9.31	9.82	10.01	10.56	10.31	11.2	11.91	12.87	14.07
Total C16	8.32	8.23	8.49	8.68	9.21	10.27	10.17	10.81	11.56	11.87
Total C17	7.52	8.17	8.38	8.17	8.64	9.81	9.97	10.58	11.02	11.6
Total C18	4.94	5.66	6.29	6.41	6.27	6.84	7.18	7.92	7.95	8.06
Total C19	3.48	3.54	3.69	3.75	3.89	4.05	4.78	4.61	4.82	5.02
Total C20	3.2	3.17	3.68	3.74	3.48	4.03	4.38	4.68	4.41	4.54
Total C21	2.26	2.37	2.36	2.47	2.61	2.67	2.9	3.11	3.19	3.45
Total C22	1.56	1.63	1.73	1.71	1.79	1.94	2	2.15	2.28	2.28
Total C23	0.68	0.73	0.76	0.76	0.82	0.88	0.89	0.97	1.02	1.04
Total C24	0	0	0	0	0	0	0	0	0	0

Table B-3 Carbon distribution for light GTL Diesel fractions

Composition, wt%	<130°C	<140°C	<150°C	<160°C	<170°C	<180°C	<190°C	<200°C	<210°C
n-Paraffins	57.13	52.9	53.75	55.58	53.84	54.59	55.19	54.38	55.11
i-Paraffins	42.87	47.08	46.3	44.44	46.18	45.44	44.84	45.61	44.88
Total C7	9.06	2.52	1.4	1.07	0.69	0.45	0.36	0.26	0.2
Total C8	50.13	43.51	27.62	19.33	14.03	9.85	8.45	6.62	5.75
Total C9	36.8	48.86	62.02	60.44	49.23	36.99	30.53	25.31	21.09
Total C10	3.1	3.94	8.71	18.69	32.96	42.28	39.67	32.2	27.69
Total C11	0.91	1.15	0.3	0.49	3.11	10.31	20.47	29.83	29.91
Total C12	0	0	0	0	0	0.15	0.55	5.77	15.17
Total C13	0	0	0	0	0	0	0	0	0.18

B.1 Gas Chromatograph Analysis

Every GTL Diesel cuts (heavy and light) have been injected to GC, every cut is represented by a graphical display, each graph contains number of peaks, and each peak represents a component present in the sample. X-axis represents the retention time that is the time interval between sample injection and the maximum of the peak. It is characteristic of the identity of the component under the operating conditions. Each component identity confirmed injecting a reference material under the same operational conditions. The matching of retention time of reference material and the component peak confirms the identity of the unknown sample component.

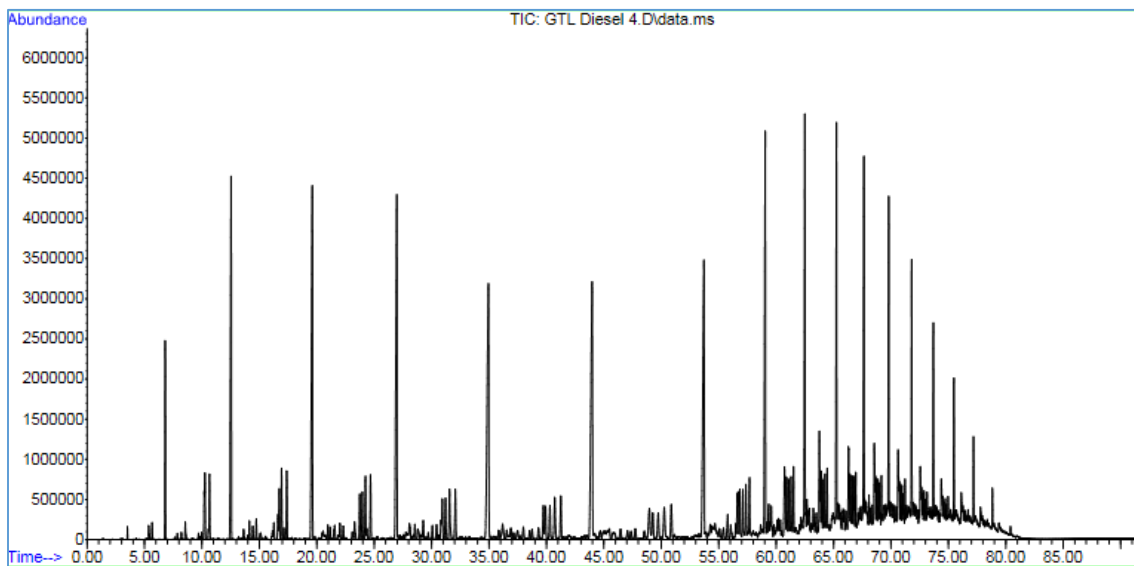


Figure B-1 GTL Diesel whole cut GC carbon distribution analysis

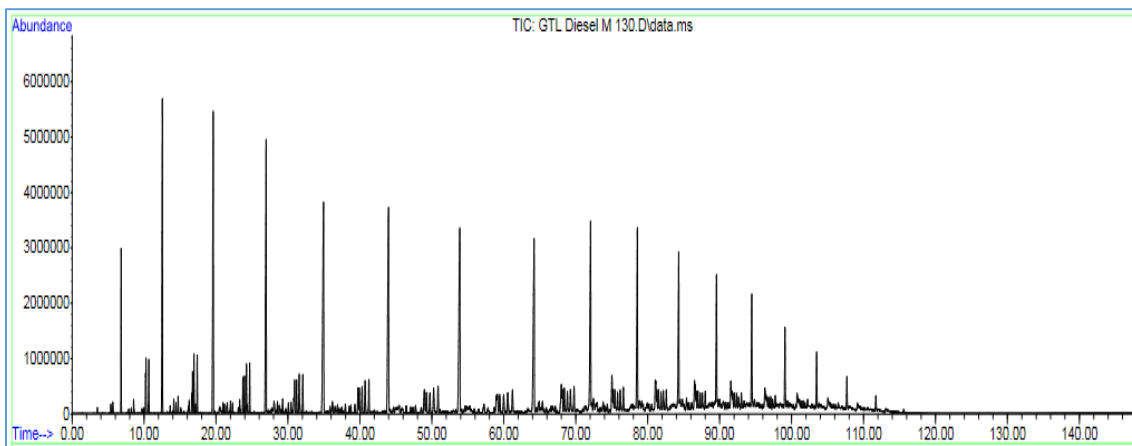


Figure B-2 GTL Diesel cut >130° GC carbon distribution analysis

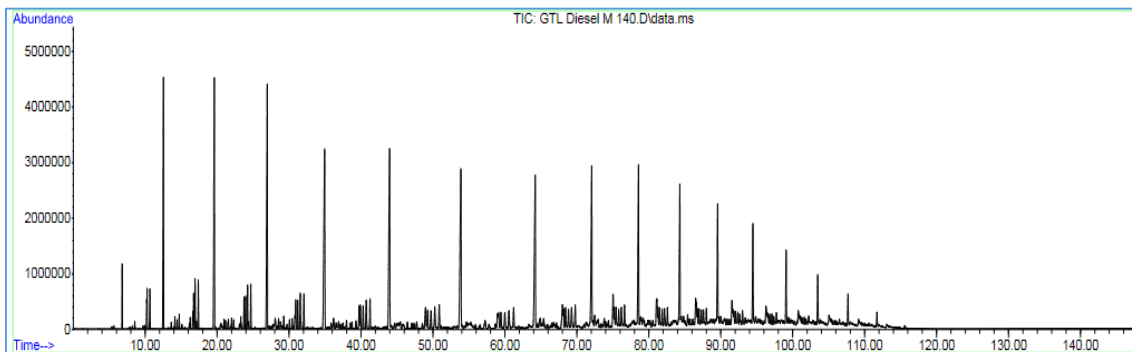


Figure B-3 GTL Diesel cut >140° GC carbon distribution analysis

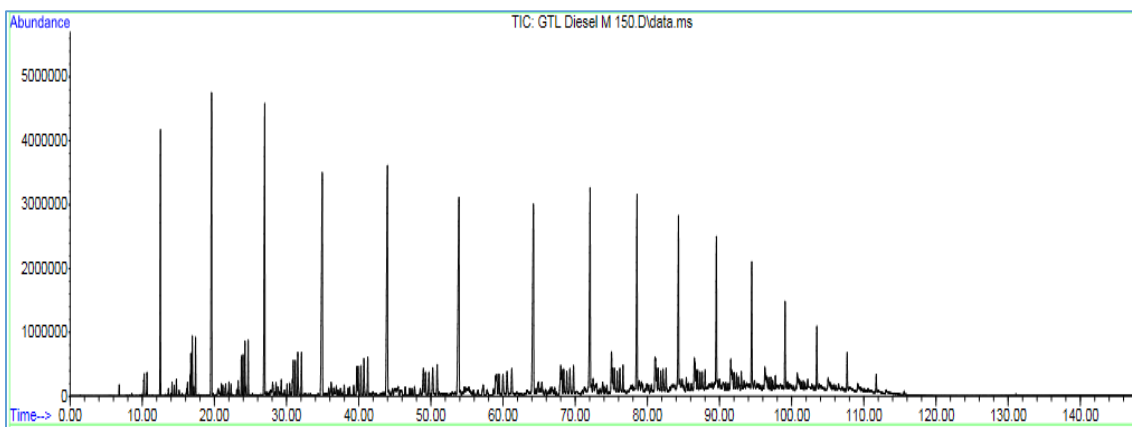


Figure B-4 GTL Diesel cut >150° GC carbon distribution analysis

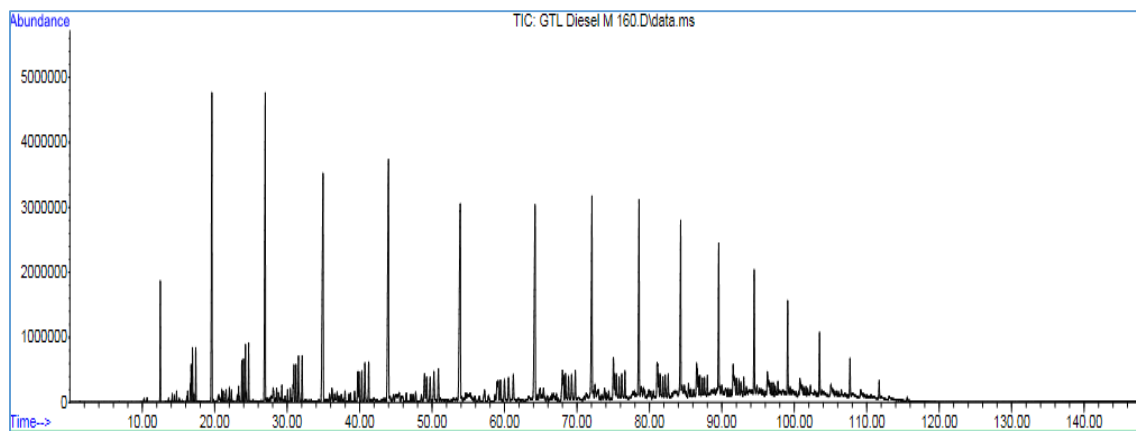


Figure B-5 GTL Diesel cut $>160^\circ$ GC carbon distribution analysis

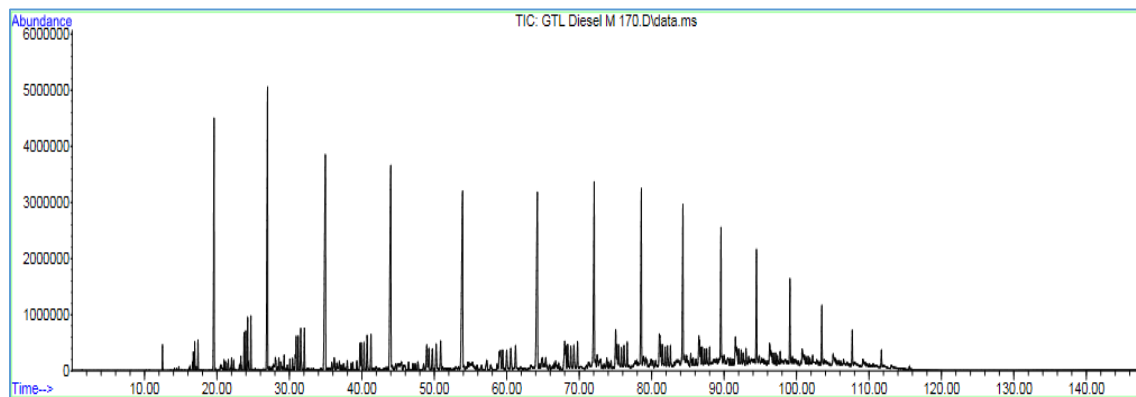


Figure B-6 GTL Diesel cut $>170^\circ$ GC carbon distribution analysis

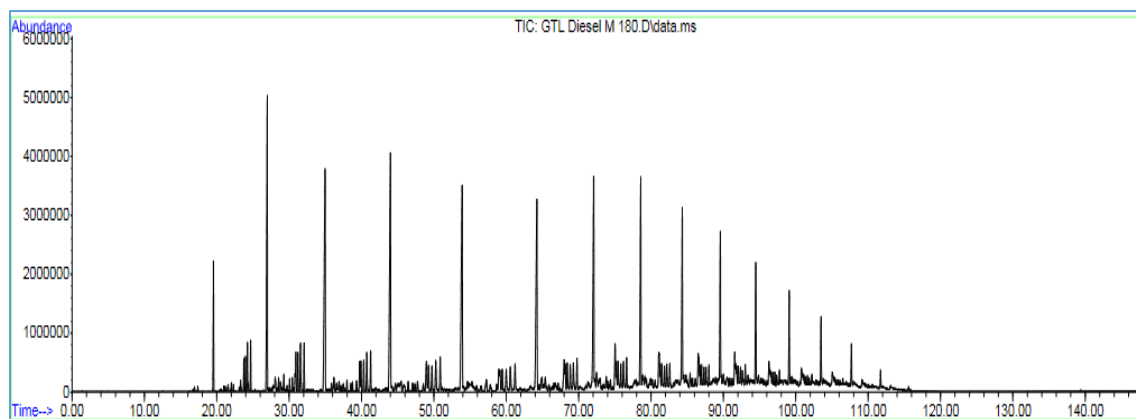


Figure B-7 GTL Diesel cut $>180^\circ$ GC carbon distribution analysis

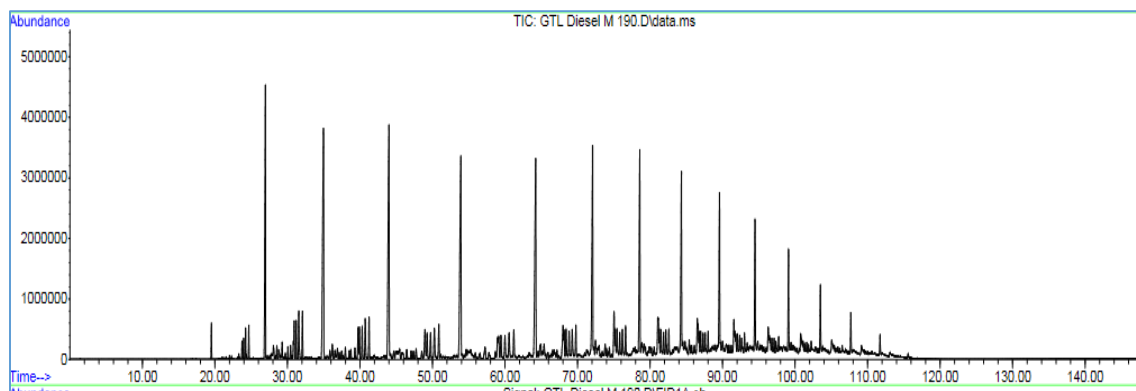


Figure B-8 GTL Diesel cut $>190^\circ$ GC carbon distribution analysis

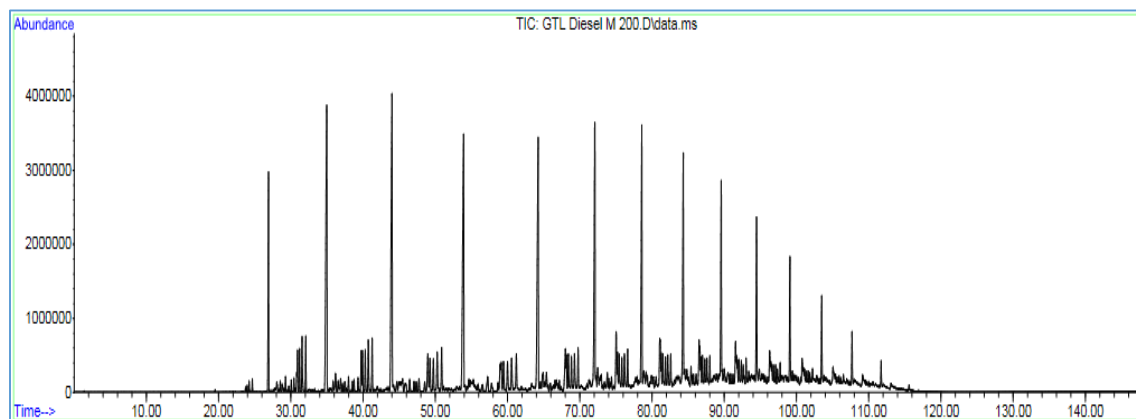


Figure B-9 GTL Diesel cut $>200^\circ$ carbon distribution analysis

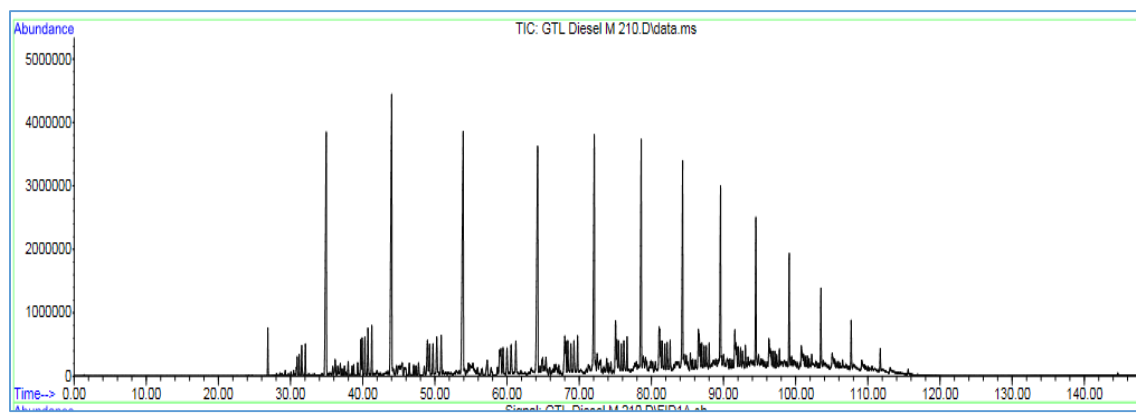


Figure B-10 GTL Diesel cut $>210^\circ$ GC carbon distribution analysis

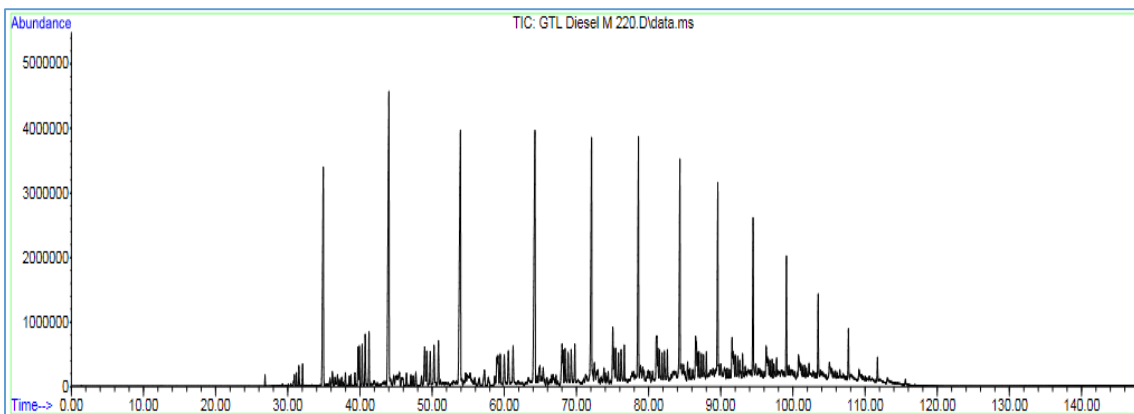


Figure B-11 GTL Diesel cut >215° GC carbon distribution analysis

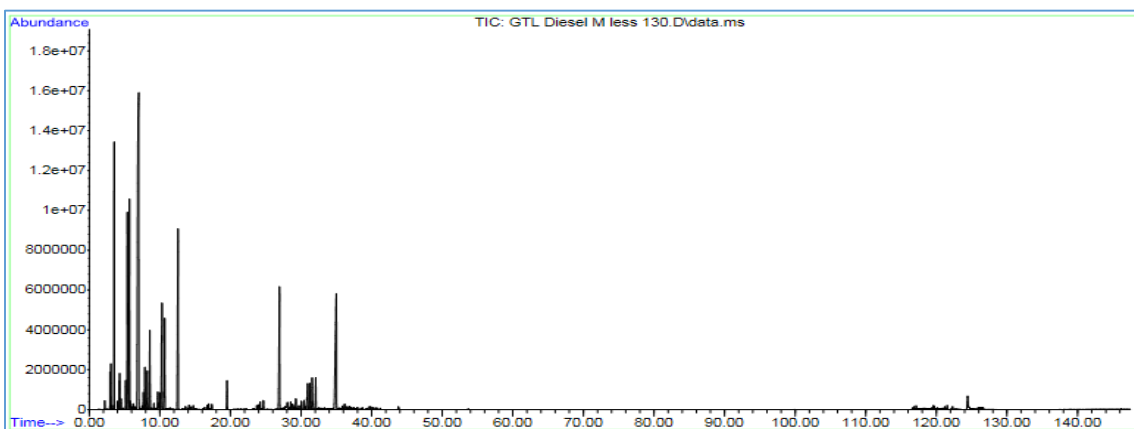


Figure B-12 GTL Diesel cut <130° GC carbon distribution analysis

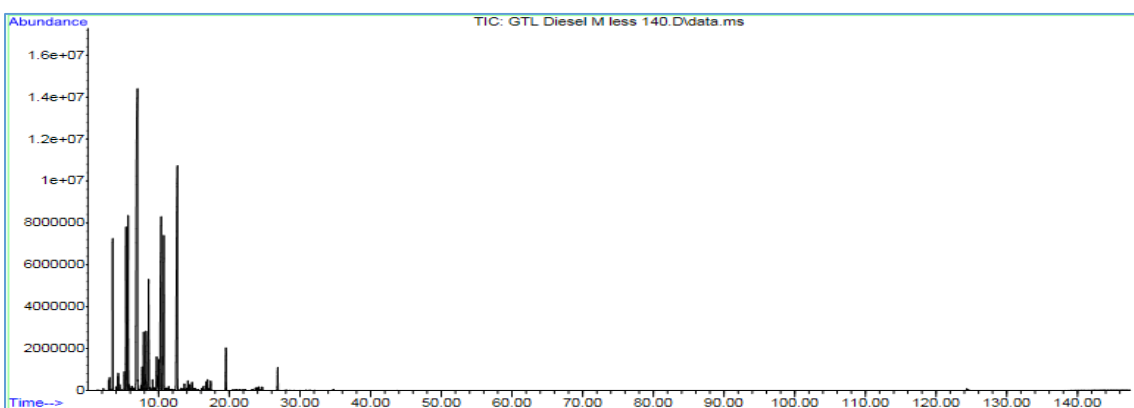


Figure B-13 GTL Diesel cut <140° GC carbon distribution analysis

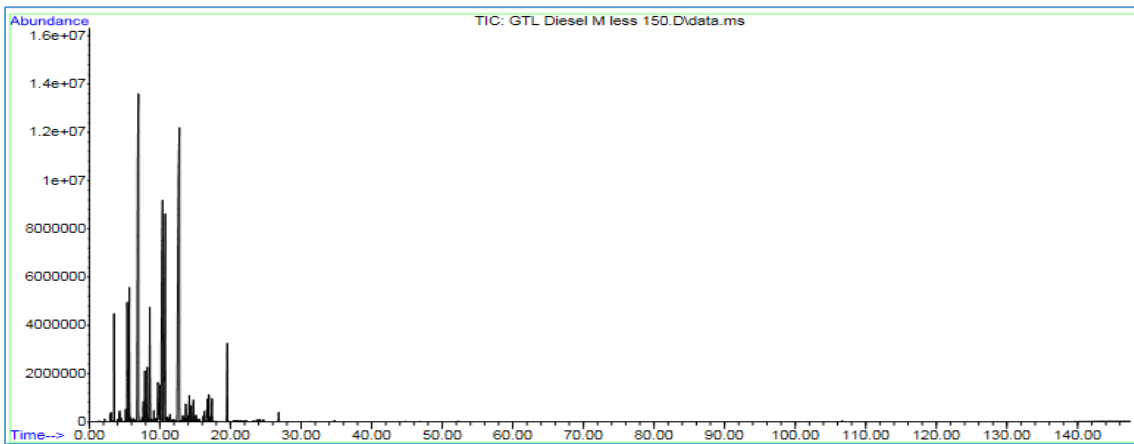


Figure B-14 GTL Diesel cut <150° GC carbon distribution analysis

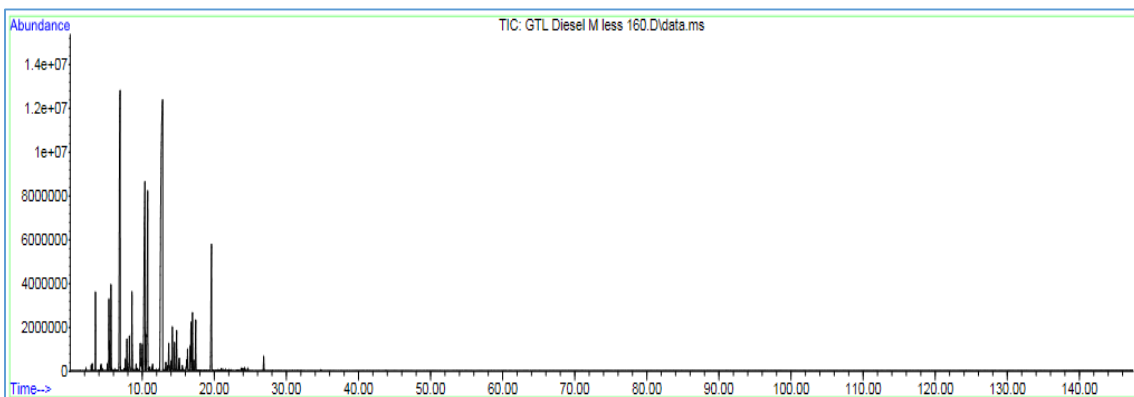


Figure B-15 GTL Diesel cut <160° GC carbon distribution analysis

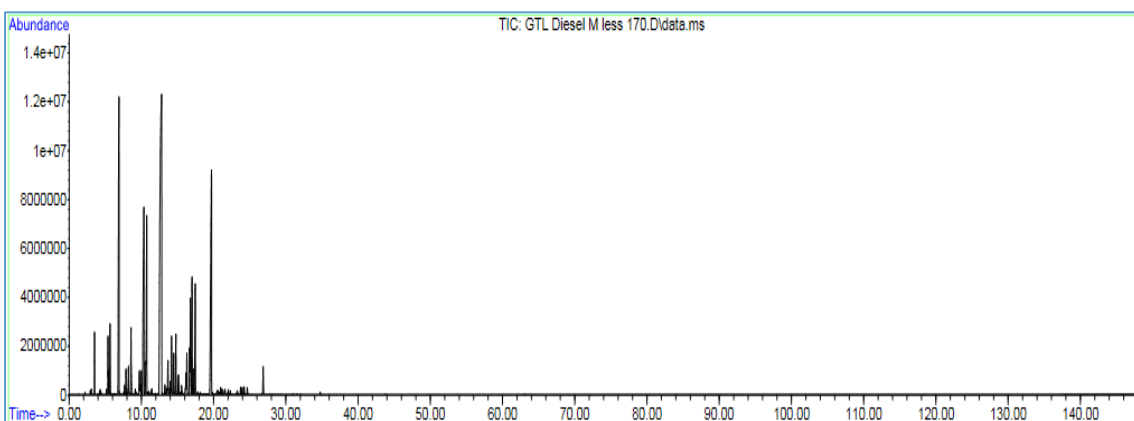


Figure B-16 GTL Diesel cut <170° GC carbon distribution analysis

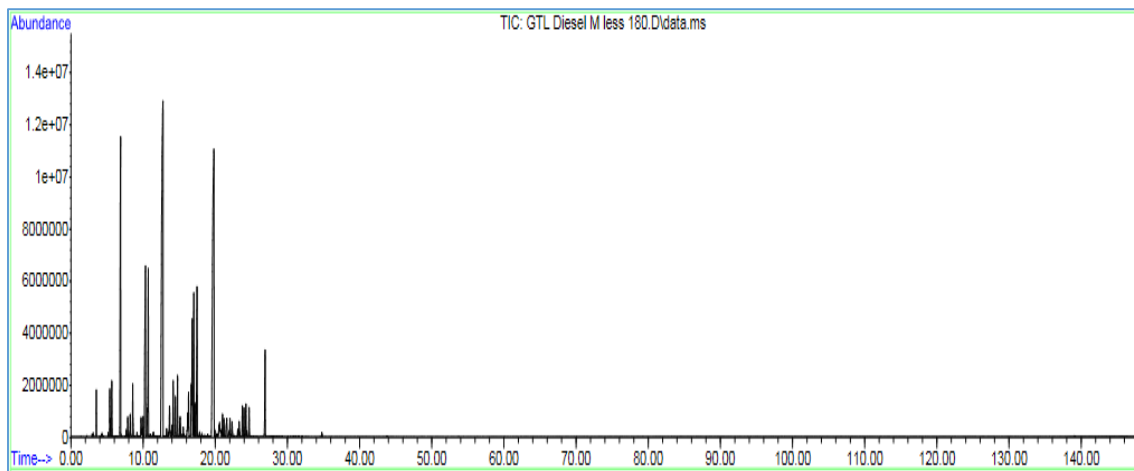


Figure B-17 GTL Diesel cut <180° GC carbon distribution analysis

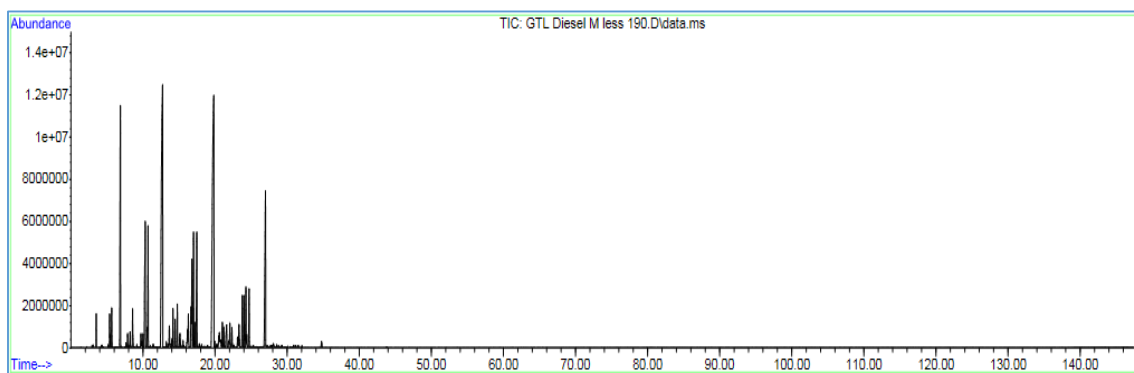


Figure B-18 GTL Diesel cut <190° GC carbon distribution analysis

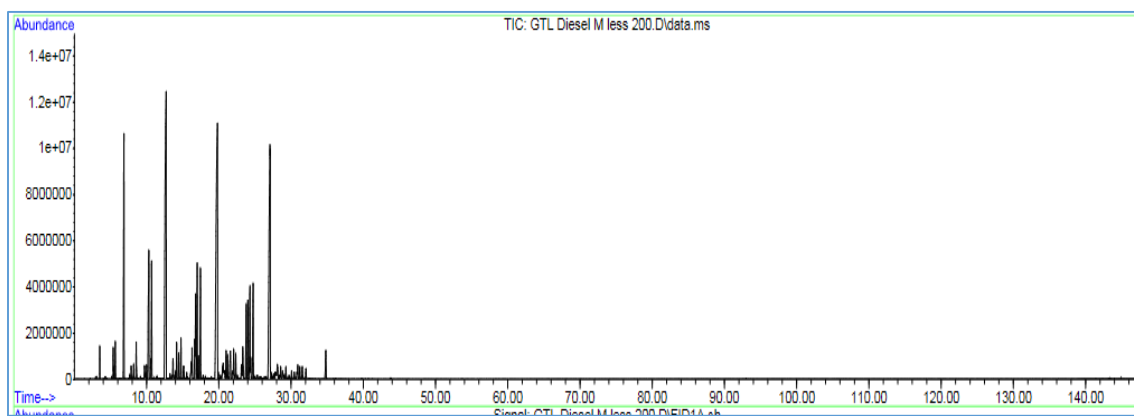


Figure B-19 GTL Diesel cut <200° GC carbon distribution analysis

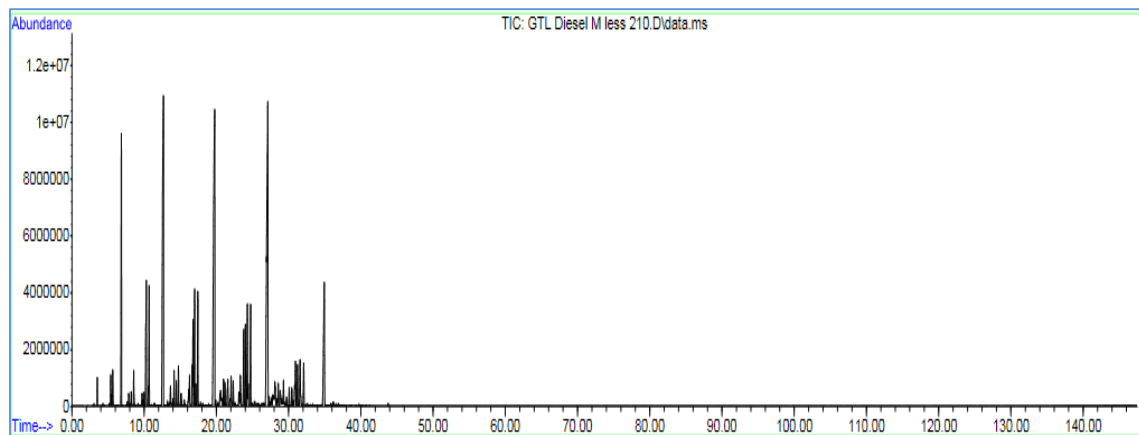


Figure B-20 GTL Diesel cut <210° GC carbon distribution analysis

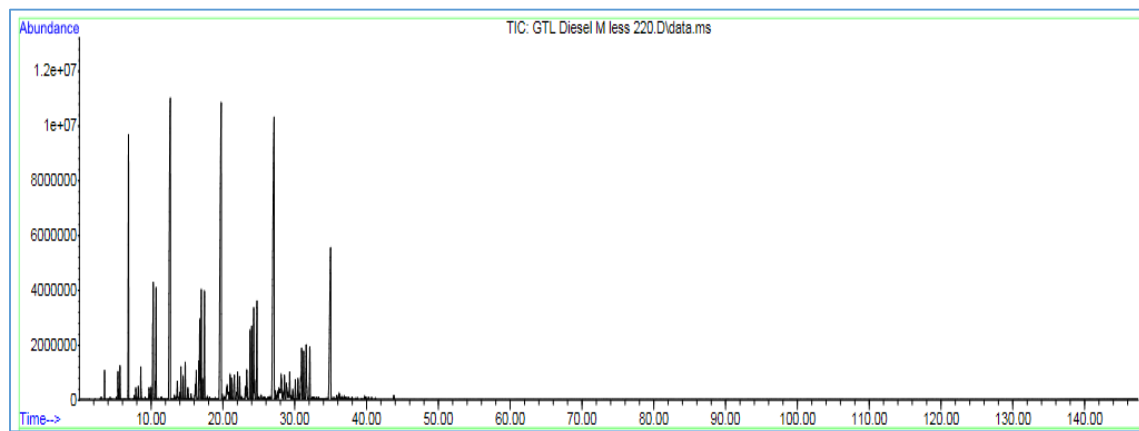


Figure B-21 GTL Diesel cut <215° GC carbon distribution analysis

Table B-4 Distillation results for GTL Diesel heavy cuts

vol%	UOM	>130	>140	>150	>160	>170	>180	>190	>200	>210	>215
IBP	°C	164.2	169.6	178.7	190.1	197.9	210.1	218.2	227.4	236.8	240.0
10%	°C	187.9	191.7	199.5	208.1	215.3	226.6	232.7	241.3	250.4	253.1
15%	°C	195.4	199.0	206.8	215.4	221.9	230.2	237.8	245.4	253.6	256.2
20%	°C	203.2	205.8	213.1	221.9	227.5	235.3	242.0	249.5	257.1	258.8
30%	°C	222.1	224.6	229.3	235.4	240.1	246.8	252.4	257.5	264.7	266.7
40%	°C	241.5	243.1	246.6	251.6	255.4	259.6	263.8	268.8	274.4	275.1
50%	°C	260.3	261.1	264.1	268.0	271.3	273.7	277.0	280.7	285.4	285.6
60%	°C	277.4	278.3	280.5	283.9	286.1	287.9	290.9	293.6	296.6	297.0
70%	°C	294.1	294.3	296.2	298.9	300.7	301.7	304.5	306.5	308.4	309.6
80%	°C	311.1	310.8	312.5	314.3	315.0	316.3	318.7	320.2	320.9	322.6
85%	°C	319.7	319.2	320.7	322.7	323.8	323.7	326.3	327.4	327.8	329.9
90%	°C	328.6	329.4	330.2	331.9	332.0	332.1	335.1	335.6	335.5	338.2
95%	°C	340.4	338.9	340.6	342.8	343.5	341.6	345.4	345.3	346.1	348.6
FBP	°C	348.1	346.8	347.3	350.4	349.5	348.1	350.9	350.4	351.4	351.8

Table B-5 Cloud and pour point results for GTL Diesel heavy cuts

Cut	Spec	UOM	Test1	Test2	Test3	Average
GTL	CP	°C	-5.5	-5.6	-6	-5.7
	PP	°C	-9	-9	-9	-9.0
>130	CP	°C	-5.6	-5.6	-5.8	-5.7
	PP	°C	-9	-9	-9	-9.0
>140	CP	°C	-4.9	-5.2	-5.3	-5.1
	PP	°C	-9	-9	-9	-9.0
>150	CP	°C	-5.0	-5.0	-4.8	-4.9
	PP	°C	-9.0	-9.0	-9.0	-9.0
>160	CP	°C	-4.7	-4.4	-4.6	-4.6
	PP	°C	-9.0	-9.0	-9.0	-9.0
>170	CP	°C	-3.6	-3.3	-3.6	-3.5
	PP	°C	-9.0	-9.0	-9.0	-9.0
>180	CP	°C	-2.9	-2.4	-3.0	-2.8
	PP	°C	-6.0	-6.0	-6.0	-6.0
>190	CP	°C	-2.2	-2.2	-2.0	-2.1
	PP	°C	-6	-6	-6	-6.0

Table B-5 Continued

Cut	Spec	UOM	Test1	Test2	Test3	Average
>200	CP	°C	-1.2	-1.4	-1.3	-1.3
	PP	°C	-6	-6	-3	-5.0
>210	CP	°C	-0.3	-0.5	-0.5	-0.4
	PP	°C	-3	-3	-3	-3.0
>215	CP	°C	-0.4	-0.1	-0.1	-0.2
	PP	°C	-3	-3	-3	-3.0

Table B-6 Dynamic and kinematic viscosity results for GTL Diesel heavy cuts

Cut	Spec	UOM	Test1	Test2	Test3	Average
GTL	Dynamic Vis.	mPa.s	1.6676	1.6696	1.6788	1.6720
	Kinematic Vis.	cSt.	2.2167	2.2192	2.2308	2.2222
>130	Dynamic Vis.	mPa.s	1.6831	1.6828	1.6835	1.6831
	Kinematic Vis.	cSt.	2.2363	2.2357	2.2366	2.2362
>140	Dynamic Vis.	mPa.s	1.7280	1.7282	1.7299	1.7287
	Kinematic Vis.	cSt.	2.2929	2.2932	2.2952	2.2938
>150	Dynamic Vis.	mPa.s	1.8116	1.8110	1.8115	1.8114
	Kinematic Vis.	cSt.	2.3984	2.3977	2.3983	2.3981
>160	Dynamic Vis.	mPa.s	1.9315	1.9308	1.9329	1.9317
	Kinematic Vis.	cSt.	2.5512	2.5500	2.5527	2.5513
>170	Dynamic Vis.	mPa.s	2.0167	2.0180	1.9996	2.0114
	Kinematic Vis.	cSt.	2.6586	2.6603	2.6361	2.6517
>180	Dynamic Vis.	mPa.s	2.1435	2.1424	2.1424	2.1428
	Kinematic Vis.	cSt.	2.8176	2.8160	2.8160	2.8165
>190	Dynamic Vis.	mPa.s	2.2412	2.2411	2.2412	2.2412
	Kinematic Vis.	cSt.	2.9406	2.9405	2.9404	2.9405
>200	Dynamic Vis.	mPa.s	2.3732	2.3728	2.3726	2.3729
	Kinematic Vis.	cSt.	3.1070	3.1064	3.1061	3.1065
>210	Dynamic Vis.	mPa.s	2.5203	2.5201	2.5201	2.5202
	Kinematic Vis.	cSt.	3.2921	3.2919	3.2917	3.2919
>215	Dynamic Vis.	mPa.s	2.5781	2.5778	2.5780	2.5780
	Kinematic Vis.	cSt.	3.3638	3.3634	3.3637	3.3636

Table B-7 Flash point results for GTL Diesel heavy cuts

Cut No.	UOM	>130	>140	>150	>160	>170	>180	>190	>200	>210	>215
Flash Pt.	°C	59	63	70	77	82	91	96	103	110	113

Table B-8 Density results for GTL Diesel heavy cuts

Cut	Spec	UOM	Test1	Test2	Test3	Average
GTL Diesel	Density	kg/m3	767.346	767.346	767.55	767.4
>130	Density	kg/m4	767.652	767.754	767.754	767.7
>140	Density	kg/m5	768.672	768.672	768.774	768.7
>150	Density	kg/m6	770.4	770.406	770.406	770.4
>160	Density	kg/m7	772.242	772.344	772.344	772.3
>170	Density	kg/m8	773.772	773.772	773.67	773.7
>180	Density	kg/m9	776.016	776.016	776.016	776.0
>190	Density	kg/m10	777.342	777.444	777.444	777.4
>200	Density	kg/m11	779.076	779.076	779.076	779.1
>210	Density	kg/m12	780.81	780.81	780.81	780.8
>215	Density	kg/m13	781.728	781.728	781.728	781.7

APPENDIX C – LINGO PROGRAMMING

! Cloud Point estimation for New Regression Coeffiecent using Distillation Data;

```
CP = a + bT50 + cT90 + dT90-20 + eT50 * T90 + fSG + gSG * T90
!
Min = ((CPmeasuredGTL - CPcalcGTL)2 + (CPmeasured140 - CPcalc140)2 + (CPmeasured160 -
CPcalc160)2 + (CPmeasured180 - CPcalc180)2 + (CPmeasured200 - CPcalc200)2 +
(CPmeasured215 - CPcalc215)2)0.5;

@free(CPmeasuredGTL);
@free(CPmeasured140);
@free(CPmeasured160);
@free(CPmeasured180);
@free(CPmeasured200);
@free(CPmeasured215);
@free(CPcalcGTL);
@free(CPcalc130);
@free(CPcalc140);
@free(CPcalc150);
@free(CPcalc160);
@free(CPcalc170);
@free(CPcalc180);
@free(CPcalc190);
@free(CPcalc200);
@free(CPcalc210);
@free(CPcalc215);

@free(a);
@free(b);
@free(c);
@free(d);
@free(e);
@free(f);
```

```

@free(g);

CPmeasuredGTL= -5.7;
CPmeasured140= -5.1;
CPmeasured160= -4.6;
CPmeasured180= -2.8;
CPmeasured200= -1.3;
CPmeasured215= -0.2;

CPcalcGTL = a + b*D501 + c*D901 + d*(D901-D201) + e*D501*D901 + f*Den1+
g*Den1*D901;
CPcalc140 = a + b*D503 + c*D903 + d*(D903-D203) + e*D503*D903 + f*Den3+
g*Den3*D903;
CPcalc160 = a + b*D505 + c*D905 + d*(D905-D205) + e*D505*D905 + f*Den5+
g*Den5*D905;
CPcalc180 = a + b*D507 + c*D907 + d*(D907-D207) + e*D507*D907 + f*Den7+
g*Den7*D907;
CPcalc200 = a + b*D509 + c*D909 + d*(D909-D209) + e*D509*D909 + f*Den9+
g*Den9*D909;
CPcalc215 = a + b*D5011 + c*D9011 + d*(D9011-D2011) + e*D5011*D9011 +
f*Den11+ g*Den11*D9011;

a =      1195.917;
b =     -5.382029;
c =     -2.632678;
d =      0.1358335;
e =    0.1992243E-01;
f =      759.4667;
g =     -4.907416;

CPcalc130 = a + b*D502 + c*D902 + d*(D902-D202) + e*D502*D902 + f*Den2+
g*Den2*D902;
CPcalc150 = a + b*D504 + c*D904 + d*(D904-D204) + e*D504*D904 + f*Den4+
g*Den4*D904;
CPcalc170 = a + b*D506 + c*D906 + d*(D906-D206) + e*D506*D906 + f*Den6+
g*Den6*D906;
CPcalc190 = a + b*D508 + c*D908 + d*(D908-D208) + e*D508*D908 + f*Den8+
g*Den8*D908;
CPcalc210 = a + b*D5010 + c*D9010 + d*(D9010-D2010) + e*D5010*D9010 +
f*Den10+ g*Den8*D9010;

Den1 = 0.767414;
D201 = 202.3;
D501 = 260.7;
D901 = 331;

```

```
Den3 = 0.768706;
D203 = 205.8;
D503 = 261.1;
D903 = 329.4;

Den5 = 0.77231;
D205 = 221.9;
D505 = 268.0;
D905 = 331.9;

Den7 = 0.776016;
D207 = 235.3;
D507 = 273.7;
D907 = 332.1;

Den9 = 0.779076;
D209 = 249.5;
D509 = 280.7;
D909 = 335.6;

Den11 = 0.781728;
D2011 = 258.8;
D5011 = 285.6;
D9011 = 338.2;

Den2 = 0.76772;
D202 = 203.2;
D502 = 260.3;
D902 = 328.6;

Den4 = 0.770406;
D204 = 213.1;
D504 = 269.1;
D904 = 330.2;

Den6 = 0.773738;
D206 = 227.5;
D506 = 271.3;
D906 = 332.0;

Den8 = 0.77741;
D208 = 242;
D508 = 277.0;
D908 = 335.1;

Den10 = 0.78081;
D2010 = 257.1;
D5010 = 285.4;
D9010 = 335.5;
```

! Kinematic Viscosity Estimation for New Regression Coefficients using Distillation Data;

```
Min = ((KVmeasuredGTL - KVcalcGTL)^2 + (KVmeasured140 - KVcalc140)^2 + (KVmeasured160
- KVcalc160)^2 + (KVmeasured180 - KVcalc180)^2 + (KVmeasured200 - KVcalc200)^2 +
(KVmeasured215 - KVcalc215)^2)^0.5;

KVmeasuredGTL = 2.222;
KVmeasured140 = 2.2938;
KVmeasured160 = 2.5513;
KVmeasured180 = 2.8165;
KVmeasured200 = 3.1065;
KVmeasured215 = 3.3636;

@free(a);    @free(b);
@free(c);    @free(d);
@free(e);    @free(f);
@free(g);    @free(h);
@free(i);

KVcalcGTL = a*Den1 + b*Den1^2 + c*D101^2 + d/D101 + e*D501^2 + f/D501^2
+ g*D901^2 + h/D901 + i;
KVcalc140 = a*Den3 + b*Den3^2 + c*D103^2 + d/D103 + e*D503^2 + f/D503^2
+ g*D903^2 + h/D903 + i;
KVcalc160 = a*Den5 + b*Den5^2 + c*D105^2 + d/D105 + e*D505^2 + f/D505^2
+ g*D905^2 + h/D905 + i;
KVcalc180 = a*Den7 + b*Den7^2 + c*D107^2 + d/D107 + e*D507^2 + f/D507^2
+ g*D907^2 + h/D907 + i;
KVcalc200 = a*Den9 + b*Den9^2 + c*D109^2 + d/D109 + e*D509^2 + f/D509^2
+ g*D909^2 + h/D909 + i;
KVcalc215 = a*Den11 + b*Den11^2 + c*D1011^2 + d/D1011 + e*D5011^2 +
f/D5011^2 + g*D9011^2 + h/D9011 + i;

A = 69.6489;
B = 107.1539;
C = -0.5881154E-04;
D = 1382.238;
E = 0.1353130E-03;
F = 1.255967;
G = -0.7787119E-04;
H = 1.512452;
I = -120.3931;

KVcalc130 = a*Den2 + b*Den2^2 + c*D102^2 + d/D102 + e*D502^2 + f/D502^2
+ g*D902^2 + h/D902 + i;
KVcalc150 = a*Den4 + b*Den4^2 + c*D104^2 + d/D104 + e*D504^2 + f/D504^2
+ g*D904^2 + h/D904 + i;
KVcalc170 = a*Den6 + b*Den6^2 + c*D106^2 + d/D106 + e*D506^2 + f/D506^2
+ g*D906^2 + h/D906 + i;
KVcalc190 = a*Den8 + b*Den8^2 + c*D108^2 + d/D108 + e*D508^2 + f/D508^2
+ g*D908^2 + h/D908 + i;
```

```

KVcalc200 = a*Den10 + b*Den10^2 + c*D1010^2 + d/D1010 + e*D5010^2 +
f/D5010^2 + g*D9010^2 + h/D9010 + i;

Den1 = 0.767414;           D101 = 186.1;
D501 = 260.7;              D901 = 331;

Den3 = 0.768706;           D103 = 191.7;
D503 = 261.1;              D903 = 329.4;

Den5 = 0.77231;            D105 = 208.1;
D505 = 268.0;              D905 = 331.9;

Den7 = 0.776016;           D107 = 226.6;
D507 = 273.7;              D907 = 332.1;

Den9 = 0.779076;           D109 = 241.3;
D509 = 280.7;              D909 = 335.6;

Den11 = 0.781728;          D1011 = 253.1;
D5011 = 285.6;             D9011 = 338.2;

Den2 = 0.76772;            D102 = 187.9;
D502 = 260.3;              D902 = 328.6;

Den4 = 0.770406;           D104 = 199.5;
D504 = 264.1;              D904 = 330.2;

Den6 = 0.773738;           D106 = 215.3;
D506 = 271.3;              D906 = 332.0;

Den8 = 0.77741;             D108 = 232.7;
D508 = 277.0;              D908 = 335.1;

Den10 = 0.78081;            D1010 = 250.4;
D5010 = 285.4;              D9010 = 335.5;

```

! Calculating new regression Coefficients for the simple linear equation to calculate Cloud point using normal and *iso* Paraffins Data for Heavy GTL Diesel Cuts;

Min = ((DmeasuredGTL - DcalcGTL)^2 + (Dmeasured140 - Dcalc140)^2 + (Dmeasured160 - Dcalc160)^2 + (Dmeasured180 - Dcalc180)^2 + (Dmeasured200 - Dcalc200)^2 + (Dmeasured215 - Dcalc215)^2)^0.5;

```

@free (DmeasuredGTL);      @free (Dmeasured140);
@free (Dmeasured160);      @free (Dmeasured180);
@free (Dmeasured200);      @free (Dmeasured215);

```

```

@free(DcalcGTL);      @free(Dcalc140);
@free(Dcalc160);      @free(Dcalc180);
@free(Dcalc200);      @free(Dcalc215);
@free(Dcalc130);      @free(Dcalc150);
@free(Dcalc170);      @free(Dcalc190);
@free(Dcalc210);

DmeasuredGTL = -5.7;
Dmeasured140 = -5.1;
Dmeasured160 = -4.6;
Dmeasured180 = -2.8;
Dmeasured200 = -1.3;
Dmeasured215 = -0.2;

@free(a0);
@free(a1);
@free(a2);

DcalcGTL = a0 + a1*NP1 + a2*IP1;
Dcalc140 = a0 + a1*NP3 + a2*IP3;
Dcalc160 = a0 + a1*NP5 + a2*IP5;
Dcalc180 = a0 + a1*NP7 + a2*IP7;
Dcalc200 = a0 + a1*NP9 + a2*IP9;
Dcalc215 = a0 + a1*NP11 + a2*IP11;

a0 =      18.99043;
a1 =     -0.1217240;
a2 =     -0.4146445;

Dcalc130 = a0 + a1*NP2 + a2*IP2;
Dcalc150 = a0 + a1*NP4 + a2*IP4;
Dcalc170 = a0 + a1*NP6 + a2*IP6;
Dcalc190 = a0 + a1*NP8 + a2*IP8;
Dcalc210 = a0 + a1*NP10 + a2*IP10;

NP1= 57.3;
IP1= 42.7;
NP3= 69.12;
IP3= 30.88;
NP5= 86.5;
IP5= 31.5;
NP7= 67.97;
IP7= 32.03;
NP9= 68.15;
IP9= 31.85;

```

```
NP11= 69.53;
IP11= 30.47;
NP2= 70.35;
IP2= 29.65;
NP4= 69.1;
IP4= 30.9;
NP6= 68.12;
IP6= 31.88;
NP8= 68.46;
IP8= 31.54;
NP10= 69.52;
IP10= 30.48;
```

! Calculating new regression Coefficients for the simple linear equation to calculate Density using normal and *iso* Paraffins Data for Heavy GTL Diesel Cuts;

Min = ((DmeasuredGTL - DcalcGTL)^2 + (Dmeasured140 - Dcalc140)^2 + (Dmeasured160 - Dcalc160)^2 + (Dmeasured180 - Dcalc180)^2 + (Dmeasured200 - Dcalc200)^2 + (Dmeasured215 - Dcalc215)^2)^0.5;

```
DmeasuredGTL = 752.36667;
Dmeasured140 = 753.63333;
Dmeasured160 = 757.16667;
Dmeasured180 = 760.8;
Dmeasured200 = 763.8;
Dmeasured215 = 766.4;

@free(a0);
@free(a1);
@free(a2);

DcalcGTL = a0 + a1*NP1 + a2*IP1;
Dcalc140 = a0 + a1*NP3 + a2*IP3;
Dcalc160 = a0 + a1*NP5 + a2*IP5;
Dcalc180 = a0 + a1*NP7 + a2*IP7;
Dcalc200 = a0 + a1*NP9 + a2*IP9;
Dcalc215 = a0 + a1*NP11 + a2*IP11;

a0 = 806.1069;
a1 = -0.2120636;
a2 = -0.9713231;

Dcalc130 = a0 + a1*NP2 + a2*IP2;
Dcalc150 = a0 + a1*NP4 + a2*IP4;
Dcalc170 = a0 + a1*NP6 + a2*IP6;
Dcalc190 = a0 + a1*NP8 + a2*IP8;
```

```

Dcalc210 = a0 + a1*NP10 + a2*IP10;

NP1= 57.3;
IP1= 42.7;
NP3= 69.12;
IP3= 30.88;
NP5= 86.5;
IP5= 31.5;
NP7= 67.97;
IP7= 32.03;
NP9= 68.15;
IP9= 31.85;
NP11= 69.53;
IP11= 30.47;
NP2= 70.35;
IP2= 29.65;
NP4= 69.1;
IP4= 30.9;
NP6= 68.12;
IP6= 31.88;
NP8= 68.46;
IP8= 31.54;
NP10= 69.52;
IP10= 30.48;

```

! Calculating new regression Coefficients for the simple linear equation to calculate Dynamic Viscosity using normal and *iso* Paraffins Data for Heavy GTL Diesel Cuts;

Min = ((DmeasuredGTL - DcalcGTL)^2 + (Dmeasured140 - Dcalc140)^2 + (Dmeasured160 - Dcalc160)^2 + (Dmeasured180 - Dcalc180)^2 + (Dmeasured200 - Dcalc200)^2 + (Dmeasured215 - Dcalc215)^2)^0.5;

```

DmeasuredGTL = 1.67;
Dmeasured140 = 1.73;
Dmeasured160 = 1.93;
Dmeasured180 = 2.14;
Dmeasured200 = 2.37;
Dmeasured215 = 2.58;

@free(a0);
@free(a1);
@free(a2);

```

```

DcalcGTL = a0 + a1*NP1 + a2*IP1;
Dcalc140 = a0 + a1*NP3 + a2*IP3^2;
Dcalc160 = a0 + a1*NP5 + a2*IP5^2;
Dcalc180 = a0 + a1*NP7 + a2*IP7^2;

```

```

Dcalc200 = a0 + a1*NP9 + a2*IP9^2;
Dcalc215 = a0 + a1*NP11 + a2*IP11^2;

a0 =      2.485498;
a1 =      -0.1457566E-01;
a2 =      0.7278062E-03;

Dcalc130 = a0 + a1*NP2 + a2*IP2;
Dcalc150 = a0 + a1*NP4 + a2*IP4;
Dcalc170 = a0 + a1*NP6 + a2*IP6;
Dcalc190 = a0 + a1*NP8 + a2*IP8;
Dcalc210 = a0 + a1*NP10 + a2*IP10;

NP1= 57.3;
IP1= 42.7;
NP3= 69.12;
IP3= 30.88;
NP5= 86.5;
IP5= 31.5;
NP7= 67.97;
IP7= 32.03;
NP9= 68.15;
IP9= 31.85;
NP11= 69.53;
IP11= 30.47;
NP2= 70.35;
IP2= 29.65;
NP4= 69.1;
IP4= 30.9;
NP6= 68.12;
IP6= 31.88;
NP8= 68.46;
IP8= 31.54;
NP10= 69.52;
IP10= 30.48;

```

! Calculating new regression Coefficients for the simple linear equation to calculate Flash Point using normal and *iso* Paraffins Data for Heavy GTL Diesel Cuts;

```

Min = ((FmeasuredGTL - FcalcGTL)^2 + (Fmeasured140 - Fcalc140)^2 + (Fmeasured160 -
Fcalc160)^2 + (Fmeasured180 - Fcalc180)^2 + (Fmeasured200 - Fcalc200)^2 + (Fmeasured215 -
Fcalc215)^2)^0.5;

```

```

FmeasuredGTL = 58;
Fmeasured140 = 63;
Fmeasured160 = 77;
Fmeasured180 = 91;

```

```

Fmeasured200 = 103;
Fmeasured215 = 113;

@free(a0);
@free(a1);
@free(a2);

FcalcGTL = a0 + a1*NP1 + a2*IP1;
Fcalc140 = a0 + a1*NP3 + a2*IP3;
Fcalc160 = a0 + a1*NP5 + a2*IP5;
Fcalc180 = a0 + a1*NP7 + a2*IP7;
Fcalc200 = a0 + a1*NP9 + a2*IP9;
Fcalc215 = a0 + a1*NP11 + a2*IP11;

a0 = 267.9533;
a1 = -0.8230097;
a2 = -3.802000;

Fcalc130 = a0 + a1*NP2 + a2*IP2;
Fcalc150 = a0 + a1*NP4 + a2*IP4;
Fcalc170 = a0 + a1*NP6 + a2*IP6;
Fcalc190 = a0 + a1*NP8 + a2*IP8;
Fcalc210 = a0 + a1*NP10 + a2*IP10;

NP1= 57.3;
IP1= 42.7;
NP3= 69.12;
IP3= 30.88;
NP5= 86.5;
IP5= 31.5;
NP7= 67.97;
IP7= 32.03;
NP9= 68.15;
IP9= 31.85;
NP11= 69.53;
IP11= 30.47;
NP2= 70.35;
IP2= 29.65;
NP4= 69.1;
IP4= 30.9;
NP6= 68.12;
IP6= 31.88;
NP8= 68.46;
IP8= 31.54;
NP10= 69.52;
IP10= 30.48;

```

! Calculating new regression Coefficients for the simple linear equation to calculate Cloud point using individual carbon number for Heavy GTL Diesel Cuts;

Min = ((CmeasuredGTL - CcalcGTL)^2 + (Cmeasured140 - Ccalc140)^2 + (Cmeasured160 - Ccalc160)^2 + (Cmeasured180 - Ccalc180)^2 + (Cmeasured200 - Ccalc200)^2 + (Cmeasured215 - Ccalc215)^2)^0.5;

@free(CmeasuredGTL); @free(Cmeasured140);

@free(Cmeasured160); @free(Cmeasured180);

@free(Cmeasured200); @free(Cmeasured215);

@free(CcalcGTL); @free(Ccalc130);

@free(Ccalc140); @free(Ccalc150);

@free(Ccalc160); @free(Ccalc170);

@free(Ccalc180); @free(Ccalc190);

@free(Ccalc200); @free(Ccalc210);

@free(Ccalc215);

@free(a0); @free(a1); @free(a2);

@free(a3); @free(a4); @free(a5);

@free(a6); @free(a7); @free(a8);

@free(a9); @free(a10);

CmeasuredGTL= -5.7; Cmeasured140= -5.1;

Cmeasured160= -4.6; Cmeasured180= -2.8;

Cmeasured200= -1.3; Cmeasured215= -0.2;

CcalcGTL = a0 + a1*C91+ a2*C101 + a3*C111 + a4*C121 + a5*C131 + a6*C141 + a7*C151 + a8*C161 + a9*C171 + a10*C181;

Ccalc140 = a0 + a1*C93 + a2*C103 + a3*C113 + a4*C123 + a5*C133 + a6*C143 + a7*C153 + a8*C163 + a9*C173 + a10*C183;

Ccalc160 = a0 + a1*C95 + a2*C105 + a3*C115 + a4*C125 + a5*C135 + a6*C145 + a7*C155 +
a8*C165 + a9*C175 + a10*C185;

Ccalc180 = a0 + a1*C97 + a2*C107 + a3*C117 + a4*C127 + a5*C137 + a6*C147 + a7*C157 +
a8*C167 + a9*C177 + a10*C187;

Ccalc200 = a0 + a1*C99 + a2*C109 + a3*C119 + a4*C129 + a5*C139 + a6*C149 + a7*C159 +
a8*C169 + a9*C179 + a10*C189;

Ccalc215 = a0 + a1*C911 + a2*C1011 + a3*C1111 + a4*C1211 + a5*C1311 + a6*C1411 +
a7*C1511 + a8*C1611 + a9*C1711 + a10*C1811;

A0 =	1.234568;	A1 =	1.234568;
A2 =	0.7444774;	A3 =	1.234568;
A4 =	1.234568;	A5 =	-19.15653;
A6 =	163.7762;	A7 =	-110.8649;
A8 =	-211.2797;	A9 =	107.5923;
A10=	72.88011;		

Ccalc130 = a0 + a1*C92 + a2*C102 + a3*C112 + a4*C122 + a5*C132 +
a6*C142 + a7*C152 + a8*C162 + a9*C172 + a10*C182;
Ccalc150 = a0 + a1*C94 + a2*C104 + a3*C114 + a4*C124 + a5*C134 +
a6*C144 + a7*C154 + a8*C164 + a9*C174 + a10*C184;
Ccalc170 = a0 + a1*C96 + a2*C106 + a3*C116 + a4*C126 + a5*C136 +
a6*C146 + a7*C156 + a8*C166 + a9*C176 + a10*C186;
Ccalc190 = a0 + a1*C98 + a2*C108 + a3*C118 + a4*C128 + a5*C138 +
a6*C148 + a7*C158 + a8*C168 + a9*C178 + a10*C188;
Ccalc210 = a0 + a1*C910 + a2*C1010 + a3*C1110 + a4*C1210 + a5*C1310 +
a6*C1410 + a7*C1510 + a8*C1610 + a9*C1710 + a10*C1810;

C91 = 5.86;	C101 = 8.09;
C111 = 8.82;	C121 = 9.37;
C131 = 9.54;	C141 = 8.37;
C151 = 8.05;	C161 = 7.96;
C171 = 7.38;	C181 = 7.54;

C93 = 6.94;	C103 = 8.97;
C113 = 9.77;	C123 = 10.17;
C133 = 10.59;	C143 = 9.99;
C153 = 9.31;	C163 = 8.23;
C173 = 8.17;	C183 = 5.66;

C95 = 1.61;	C105 = 8.78;
C115 = 10.42;	C125 = 10.9;
C135 = 11.75;	C145 = 10.88;
C155 = 10.01;	C165 = 8.68;
C175 = 8.17;	C185 = 6.41;

C97 = 0.00;	C107 = 2.18;
C117 = 10.39;	C127 = 11.83;
C137 = 12.76;	C147 = 12.03;

C157 = 10.31;	C167 = 10.27;
C177 = 9.81;	C187 = 6.84;
C99 = 0.00;	C109 = 0.00;
C119 = 3.6;	C129 = 12.57;
C139 = 14.06;	C149 = 13.04;
C159 = 11.91;	C169 = 10.81;
C179 = 10.58;	C189 = 7.92;
C911 = 0.00;	C1011 = 0.00;
C1111 = 0.00;	C1211 = 7.03;
C1311 = 15.66;	C1411 = 15.4;
C1511 = 14.07;	C1611 = 11.87;
C1711 = 11.6;	C1811 = 8.06;
C92 = 7.73;	C102 = 9.26;
C112 = 9.6;	C122 = 10.17;
C132 = 10.4;	C142 = 9.95;
C152 = 9.15;	C162 = 8.12;
C172 = 7.52;	C182 = 5.46;
C94 = 4.19;	C104 = 8.91;
C114 = 9.85;	C124 = 10.4;
C134 = 11.16;	C144 = 10.3;
C154 = 9.52;	C164 = 8.39;
C174 = 8.08;	C184 = 6.29;
C96 = 0.00;	C106 = 6.83;
C116 = 11.05;	C126 = 11.81;
C136 = 12.0;	C146 = 11.0;
C156 = 10.30;	C166 = 9.21;
C176 = 8.64;	C186 = 6.57;
C98 = 0.00;	C108 = 0.57;
C118 = 7.89;	C128 = 12.49;
C138 = 13.26;	C148 = 12.3;
C158 = 11.2;	C168 = 10.57;
C178 = 10.2;	C188 = 7.28;
C910 = 0.00;	C1010 = 0.00;
C1110 = 0.78;	C1210 = 9.79;
C1310 = 15.22;	C1410 = 14.81;
C1510 = 12.87;	C1610 = 11.49;
C1710 = 10.75;	C1810 = 7.9;

! Calculating new regression Coefficients for the simple linear equation to calculate Density using individual carbon number for Heavy GTL Diesel Cuts;

Min = ((DmeasuredGTL - DcalcGTL)^2 + (Dmeasured140 - Dcalc140)^2 + (Dmeasured160 - Dcalc160)^2 + (Dmeasured180 - Dcalc180)^2 + (Dmeasured200 - Dcalc200)^2 + (Dmeasured215 - Dcalc215)^2)^0.5;

```
DmeasuredGTL = 752.4;
Dmeasured140 = 753.6;
Dmeasured160 = 757.2;
Dmeasured180 = 760.8;
Dmeasured200 = 763.8;
Dmeasured215 = 766.4;

@free(a0);          @free(a1);
@free(a2);          @free(a3);
@free(a4);          @free(a5);
@free(a6);          @free(a7);
@free(a8);          @free(a9);
@free(a10);

DcalcGTL = a0 + a1*C91 + a2*C101 + a3*C111 + a4*C121 + a5*C131 +
a6*C141 + a7*C151 + a8*C161 + a9*C171 + a10*C181;
Dcalc140 = a0 + a1*C93 + a2*C103 + a3*C113 + a4*C123 + a5*C133 +
a6*C143 + a7*C153 + a8*C163 + a9*C173 + a10*C183;
Dcalc160 = a0 + a1*C95 + a2*C105 + a3*C115 + a4*C125 + a5*C135 +
a6*C145 + a7*C155 + a8*C165 + a9*C175 + a10*C185;
Dcalc180 = a0 + a1*C97 + a2*C107 + a3*C117 + a4*C127 + a5*C137 +
a6*C147 + a7*C157 + a8*C167 + a9*C177 + a10*C187;
Dcalc200 = a0 + a1*C99 + a2*C109 + a3*C119 + a4*C129 + a5*C139 +
a6*C149 + a7*C159 + a8*C169 + a9*C179 + a10*C189;
Dcalc215 = a0 + a1*C911 + a2*C1011 + a3*C1111 + a4*C1211 + a5*C1311 +
a6*C1411 + a7*C1511 + a8*C1611 + a9*C1711 + a10*C1811;

a0 = 1.234568;
a1 = 1.234568;
a2 = 19.34361;
a3 = 1.234568;
a4 = 1.234568;
a5 = 28.96898;
a6 = 22.97483;
a7 = -63.20092;
a8 = -61.83823;
a9 = 107.5923;
a10 = 40.22408;

Dcalc130 = a0 + a1*C92 + a2*C102 + a3*C112 + a4*C122 + a5*C132 +
a6*C142 + a7*C152 + a8*C162 + a9*C172 + a10*C182;
```

```

Dcalc150 = a0 + a1*C94 + a2*C104 + a3*C114 + a4*C124 + a5*C134 +
a6*C144 + a7*C154 + a8*C164 + a9*C174 + a10*C184;
Dcalc170 = a0 + a1*C96 + a2*C106 + a3*C116 + a4*C126 + a5*C136 +
a6*C146 + a7*C156 + a8*C166 + a9*C176 + a10*C186;
Dcalc190 = a0 + a1*C98 + a2*C108 + a3*C118 + a4*C128 + a5*C138 +
a6*C148 + a7*C158 + a8*C168 + a9*C178 + a10*C188;
Dcalc210 = a0 + a1*C910 + a2*C1010 + a3*C1110 + a4*C1210 + a5*C1310 +
a6*C1410 + a7*C1510 + a8*C1610 + a9*C1710 + a10*C1810;

C91 = 5.86;          C101 = 8.09;
C111 = 8.82;         C121 = 9.37;
C131 = 9.54;         C141 = 8.37;
C151 = 8.05;         C161 = 7.96;
C171 = 7.38;         C181 = 7.54;

C93 = 6.94;          C103 = 8.97;
C113 = 9.77;         C123 = 10.17;
C133 = 10.59;        C143 = 9.99;
C153 = 9.31;         C163 = 8.23;
C173 = 8.17;         C183 = 5.66;

C95 = 1.61;          C105 = 8.78;
C115 = 10.42;        C125 = 10.9;
C135 = 11.75;        C145 = 10.88;
C155 = 10.01;        C165 = 8.68;
C175 = 8.17;         C185 = 6.41;

C97 = 0.00;          C107 = 2.18;
C117 = 10.39;        C127 = 11.83;
C137 = 12.76;        C147 = 12.03;
C157 = 10.31;        C167 = 10.27;
C177 = 9.81;         C187 = 6.84;

C99 = 0.00;          C109 = 0.00;
C119 = 3.6;          C129 = 12.57;
C139 = 14.06;        C149 = 13.04;
C159 = 11.91;        C169 = 10.81;
C179 = 10.58;        C189 = 7.92;

C911 = 0.00;         C1011 = 0.00;
C1111 = 0.00;        C1211 = 7.03;
C1311 = 15.66;       C1411 = 15.4;
C1511 = 14.07;       C1611 = 11.87;
C1711 = 11.6;        C1811 = 8.06;

C92 = 7.73;          C102 = 9.26;
C112 = 9.6;          C122 = 10.17;
C132 = 10.4;         C142 = 9.95;
C152 = 9.15;         C162 = 8.12;
C172 = 7.52;         C182 = 5.46;

C94 = 4.19;          C104 = 8.91;
C114 = 9.85;         C124 = 10.4;
C134 = 11.16;        C144 = 10.3;

```

```

C154 = 9.52;          C164 = 8.39;
C174 = 8.08;          C184 = 6.29;

C96 = 0.00;            C106 = 6.83;
C116 = 11.05;          C126 = 11.81;
C136 = 12.0;           C146 = 11.0;
C156 = 10.30;          C166 = 9.21;
C176 = 8.64;           C186 = 6.57;

C98 = 0.00;            C108 = 0.57;
C118 = 7.89;           C128 = 12.49;
C138 = 13.26;          C148 = 12.3;
C158 = 11.2;           C168 = 10.57;
C178 = 10.2;           C188 = 7.28;

C910 = 0.00;           C1010 = 0.00;
C1110 = 0.78;          C1210 = 9.79;
C1310 = 15.22;          C1410 = 14.81;
C1510 = 12.87;          C1610 = 11.49;
C1710 = 10.75;          C1810 = 7.9;

```

! Calculating new regression Coefficients for the simple linear equation to calculate dynamic Viscosity using individual carbon number for Heavy GTL Diesel Cuts;

```

Min = ((DVmeasuredGTL - DVcalcGTL)^2 + (DVmeasured140 - DVcalc140)^2 + (DVmeasured160
- DVcalc160)^2 + (DVmeasured180 - DVcalc180)^2 + (DVmeasured200 - DVcalc200)^2 +
(DVmeasured215 - DVcalc215)^2)^0.5;

DVmeasuredGTL = 1.672;
DVmeasured140 = 1.7287;
DVmeasured160 = 1.9317;
DVmeasured180 = 2.1428;
DVmeasured200 = 2.3729;
DVmeasured215 = 2.578;

@free(a0);           @free(a1);
@free(a2);           @free(a3);
@free(a4);           @free(a5);
@free(a6);           @free(a7);
@free(a8);           @free(a9);
@free(a10);

@free(DVcalc130);    @free(DVcalc150);
@free(DVcalc170);    @free(DVcalc190);
@free(DVcalc210);

DVcalcGTL = a1*C91 + a2*C101 + a3*C111 + a4*C121 + a5*C131 + a6*C141 +
a7*C151 + a8*C161 + a9*C171 + a10*C181;

```

```

DVcalc140 = a1*C93 +a2*C103 + a3*C113 + a4*C123 + a5*C133 + a6*C143 +
a7*C153 + a8*C163 + a9*C173 + a10*C183;
DVcalc160 = a1*C95 +a2*C105 + a3*C115 + a4*C125 + a5*C135 + a6*C145 +
a7*C155 + a8*C165 + a9*C175 + a10*C185;
DVcalc180 = a1*C97 +a2*C107 + a3*C117 + a4*C127 + a5*C137 + a6*C147 +
a7*C157 + a8*C167 + a9*C177 + a10*C187;
DVcalc200 = a1*C99 +a2*C109 + a3*C119 + a4*C129 + a5*C139 + a6*C149 +
a7*C159 + a8*C169 + a9*C179 + a10*C189;
DVcalc215 = a1*C911 +a2*C1011 + a3*C1111 + a4*C1211 + a5*C1311 +
a6*C1411 + a7*C1511 + a8*C1611 + a9*C1711 + a10*C1811;

A0 =      1.234568;
A1 =      1.234568;
A2 =      1.199324;
A3 =      1.234568;
A4 =      1.234568;
A5 =     -18.64817;
A6 =      160.7957;
A7 =     -109.7300;
A8 =     -207.3866;
A9 =      106.4914;
A10 =     71.95477;

DVcalc130 = a0 + a1*C92 + a2*C102 + a3*C112 + a4*C122 + a5*C132 +
a6*C142 + a7*C152 + a8*C162 + a9*C172 + a10*C182;
DVcalc150 = a0 + a1*C94 + a2*C104 + a3*C114 + a4*C124 + a5*C134 +
a6*C144 + a7*C154 + a8*C164 + a9*C174 + a10*C184;
DVcalc170 = a0 + a1*C96 + a2*C106 + a3*C116 + a4*C126 + a5*C136 +
a6*C146 + a7*C156 + a8*C166 + a9*C176 + a10*C186;
DVcalc190 = a0 + a1*C98 + a2*C108 + a3*C118 + a4*C128 + a5*C138 +
a6*C148 + a7*C158 + a8*C168 + a9*C178 + a10*C188;
DVcalc210 = a0 + a1*C910 + a2*C1010 + a3*C1110 + a4*C1210 + a5*C1310 +
a6*C1410 + a7*C1510 + a8*C1610 + a9*C1710 + a10*C1810;

C91 = 5.86;          C101 = 8.09;
C111 = 8.82;         C121 = 9.37;
C131 = 9.54;         C141 = 8.37;
C151 = 8.05;         C161 = 7.96;
C171 = 7.38;         C181 = 7.54;

C93 = 6.94;          C103 = 8.97;
C113 = 9.77;         C123 = 10.17;
C133 = 10.59;        C143 = 9.99;
C153 = 9.31;         C163 = 8.23;
C173 = 8.17;         C183 = 5.66;

C95 = 1.61;          C105 = 8.78;
C115 = 10.42;        C125 = 10.9;
C135 = 11.75;        C145 = 10.88;
C155 = 10.01;        C165 = 8.68;
C175 = 8.17;         C185 = 6.41;

```

C97 = 0.00;	C107 = 2.18;
C117 = 10.39;	C127 = 11.83;
C137 = 12.76;	C147 = 12.03;
C157 = 10.31;	C167 = 10.27;
C177 = 9.81;	C187 = 6.84;
C99 = 0.00;	C109 = 0.00;
C119 = 3.6;	C129 = 12.57;
C139 = 14.06;	C149 = 13.04;
C159 = 11.91;	C169 = 10.81;
C179 = 10.58;	C189 = 7.92;
C911 = 0.00;	C1011 = 0.00;
C1111 = 0.00;	C1211 = 7.03;
C1311 = 15.66;	C1411 = 15.4;
C1511 = 14.07;	C1611 = 11.87;
C1711 = 11.6;	C1811 = 8.06;
C92 = 7.73;	C102 = 9.26;
C112 = 9.6;	C122 = 10.17;
C132 = 10.4;	C142 = 9.95;
C152 = 9.15;	C162 = 8.12;
C172 = 7.52;	C182 = 5.46;
C94 = 4.19;	C104 = 8.91;
C114 = 9.85;	C124 = 10.4;
C134 = 11.16;	C144 = 10.3;
C154 = 9.52;	C164 = 8.39;
C174 = 8.08;	C184 = 6.29;
C96 = 0.00;	C106 = 6.83;
C116 = 11.05;	C126 = 11.81;
C136 = 12.0;	C146 = 11.0;
C156 = 10.30;	C166 = 9.21;
C176 = 8.64;	C186 = 6.57;
C98 = 0.00;	C108 = 0.57;
C118 = 7.89;	C128 = 12.49;
C138 = 13.26;	C148 = 12.3;
C158 = 11.2;	C168 = 10.57;
C178 = 10.2;	C188 = 7.28;
C910 = 0.00;	C1010 = 0.00;
C1110 = 0.78;	C1210 = 9.79;
C1310 = 15.22;	C1410 = 14.81;
C1510 = 12.87;	C1610 = 11.49;
C1710 = 10.75;	C1810 = 7.9;

! Calculating new regression Coefficients for the simple linear equation to calculate Flash using individual carbon number for Heavy GTL Diesel Cuts;

Min = ((FmeasuredGTL - FcalcGTL)^2 + (Fmeasured140 - Fcalc140)^2 + (Fmeasured160 - Fcalc160)^2 + (Fmeasured180 - Fcalc180)^2 + (Fmeasured200 - Fcalc200)^2 + (Fmeasured215 - Fcalc215)^2)^0.5;

```
FmeasuredGTL = 58;
Fmeasured140 = 63;
Fmeasured160 = 77;
Fmeasured180 = 91;
Fmeasured200 = 103;
Fmeasured215 = 113;
```

```
@free(a0);          @free(a1);
@free(a2);          @free(a3);
@free(a4);          @free(a5);
@free(a6);          @free(a7);
@free(a8);          @free(a9);
@free(a10);
```

```
FcalcGTL = a0 + a1*C71 + a2*C81 + a3*C91 + a4*C101 + a5*C111 + a6*C121
+ a7*C131 + a8*C141 + a9*C151 + a10*C161;
Fcalc140 = a0 + a1*C73 + a2*C83 + a3*C93 + a4*C103 + a5*C113 + a6*C123
+ a7*C133 + a8*C143 + a9*C153 + a10*C163;
Fcalc160 = a0 + a1*C75 + a2*C85 + a3*C95 + a4*C105 + a5*C115 + a6*C125
+ a7*C135 + a8*C145 + a9*C155 + a10*C165;
Fcalc180 = a0 + a1*C77 + a2*C87 + a3*C97 + a4*C107 + a5*C117 + a6*C127
+ a7*C137 + a8*C147 + a9*C157 + a10*C167;
Fcalc200 = a0 + a1*C79 + a2*C89 + a3*C99 + a4*C109 + a5*C119 + a6*C129
+ a7*C139 + a8*C149 + a9*C159 + a10*C169;
Fcalc215 = a0 + a1*C711 + a2*C811 + a3*C911 + a4*C1011 + a5*C1111 +
a6*C1211 + a7*C1311 + a8*C1411 + a9*C1511 + a10*C1611;
```

```
A0 = -116.8804;
A1 = 1.234568;
A2 = 1.234568;
A3 = 1.234568;
A4 = 0.2941847E-01;
A5 = 1.234568;
A6 = -0.9829783;
A7 = 31.51734;
A8 = -15.65735;
A9 = -3.409164;
A10 = 2.722776;
```

```
Fcalc130 = a0 + a1*C72 + a2*C82 + a3*C92 + a4*C102 + a5*C112 + a6*C122
+ a7*C132 + a8*C142 + a9*C152 + a10*C162;
```

```

Fcalc150 = a0 + a1*C74 + a2*C84 + a3*C94 + a4*C104 + a5*C114 + a6*C124
+ a7*C134 + a8*C144 + a9*C154 + a10*C164;
Fcalc170 = a0 + a1*C76 + a2*C86 + a3*C96 + a4*C106 + a5*C116 + a6*C126
+ a7*C136 + a8*C146 + a9*C156 + a10*C166;
Fcalc190 = a0 + a1*C78 + a2*C88 + a3*C98 + a4*C108 + a5*C118 + a6*C128
+ a7*C138 + a8*C148 + a9*C158 + a10*C168;
Fcalc210 = a0 + a1*C710 + a2*C810 + a3*C910 + a4*C1010 + a5*C1110 +
a6*C1210 + a7*C1310 + a8*C1410 + a9*C1510 + a10*C16

C91 = 5.86;          C101 = 8.09;
C111 = 8.82;         C121 = 9.37;
C131 = 9.54;         C141 = 8.37;
C151 = 8.05;         C161 = 7.96;
C171 = 7.38;         C181 = 7.54;

C93 = 6.94;          C103 = 8.97;
C113 = 9.77;         C123 = 10.17;
C133 = 10.59;        C143 = 9.99;
C153 = 9.31;         C163 = 8.23;
C173 = 8.17;         C183 = 5.66;

C95 = 1.61;          C105 = 8.78;
C115 = 10.42;        C125 = 10.9;
C135 = 11.75;        C145 = 10.88;
C155 = 10.01;        C165 = 8.68;
C175 = 8.17;         C185 = 6.41;

C97 = 0.00;          C107 = 2.18;
C117 = 10.39;        C127 = 11.83;
C137 = 12.76;        C147 = 12.03;
C157 = 10.31;        C167 = 10.27;
C177 = 9.81;         C187 = 6.84;

C99 = 0.00;          C109 = 0.00;
C119 = 3.6;          C129 = 12.57;
C139 = 14.06;        C149 = 13.04;
C159 = 11.91;        C169 = 10.81;
C179 = 10.58;        C189 = 7.92;

C911 = 0.00;         C1011 = 0.00;
C1111 = 0.00;        C1211 = 7.03;
C1311 = 15.66;       C1411 = 15.4;
C1511 = 14.07;       C1611 = 11.87;
C1711 = 11.6;        C1811 = 8.06;

C92 = 7.73;          C102 = 9.26;
C112 = 9.6;          C122 = 10.17;
C132 = 10.4;         C142 = 9.95;
C152 = 9.15;         C162 = 8.12;
C172 = 7.52;         C182 = 5.46;

```

```

C94 = 4.19;          C104 = 8.91;
C114 = 9.85;         C124 = 10.4;
C134 = 11.16;        C144 = 10.3;
C154 = 9.52;         C164 = 8.39;
C174 = 8.08;         C184 = 6.29;

C96 = 0.00;          C106 = 6.83;
C116 = 11.05;        C126 = 11.81;
C136 = 12.0;          C146 = 11.0;
C156 = 10.30;        C166 = 9.21;
C176 = 8.64;          C186 = 6.57;

C98 = 0.00;          C108 = 0.57;
C118 = 7.89;          C128 = 12.49;
C138 = 13.26;        C148 = 12.3;
C158 = 11.2;          C168 = 10.57;
C178 = 10.2;          C188 = 7.28;

C910 = 0.00;         C1010 = 0.00;
C1110 = 0.78;        C1210 = 9.79;
C1310 = 15.22;        C1410 = 14.81;
C1510 = 12.87;        C1610 = 11.49;
C1710 = 10.75;        C1810 = 7.9;

```

! Calculating new regression Coefficients for the simple linear equation to calculate Cloud point using carbon number Grouping for Heavy GTL Diesel Cuts;

Min = ((CmeasuredGTL - CcalcGTL)^2 + (Cmeasured140 - Ccalc140)^2 + (Cmeasured160 - Ccalc160)^2 + (Cmeasured180 - Ccalc180)^2 + (Cmeasured200 - Ccalc200)^2 + (Cmeasured215 - Ccalc215)^2)^0.5;

```

@free(CmeasuredGTL);      @free(Cmeasured140);
@free(Cmeasured160);      @free(Cmeasured180);
@free(Cmeasured200);      @free(Cmeasured215);
@free(CcalcGTL);          @free(Ccalc130);
@free(Ccalc140);          @free(Ccalc150);
@free(Ccalc160);          @free(Ccalc170);
@free(Ccalc180);          @free(Ccalc190);
@free(Ccalc200);          @free(Ccalc210);
@free(Ccalc215);

```

```

CmeasuredGTL= -5.7;
Cmeasured140= -5.1;
Cmeasured160= -4.6;
Cmeasured180= -2.8;
Cmeasured200= -1.3;
Cmeasured215= -0.2;

@free(a0);           @free(a1);
@free(a2);           @free(a3);
@free(a4);

CcalcGTL = a0 + a1*(C81+C91+C101+C111) + a2*(C121+C131+C141+C151) +
a3*(C161+C171+C181+C191) + a4*(C201+C211+C221+C231);
Ccalc140 = a0 + a1*(C83+C93+C101+C113) + a2*(C123+C133+C143+C153) +
a3*(C163+C173+C183+C193) + a4*(C203+C213+C223+C233);
Ccalc160 = a0 + a1*(C85+C95+C105+C115) + a2*(C125+C135+C145+C155) +
a3*(C165+C175+C185+C195) + a4*(C205+C215+C225+C235);
Ccalc180 = a0 + a1*(C87+C97+C107+C117) + a2*(C1217+C137+C147+C157) +
a3*(C167+C177+C187+C197) + a4*(C201+C211+C221+C237);
Ccalc200 = a0 + a1*(C89+C99+C109+C119) + a2*(C129+C139+C149+C159) +
a3*(C169+C179+C189+C199) + a4*(C209+C219+C229+C239);
Ccalc215 = a0 + a1*(C811+C911+C1011+C1111) +
a2*(C1211+C1311+C1411+C1511) + a3*(C1611+C1711+C1811+C1911) +
a4*(C2011+C2111+C2211+C2311);

a0    =      12.67685;
a1    =     -0.3166214;
a2    =     -0.1909169;
a3    =      0.1301971;
a4    =     -0.6788095;

Ccalc130 = a0 + a1*(C82+C92+C102+C112) + a2*(C122+C132+C142+C152) +
a3*(C162+C172+C182+C192) + a4*(C202+C212+C222+C232);
Ccalc150 = a0 + a1*(C84+C94+C104+C114) + a2*(C124+C134+C144+C154) +
a3*(C164+C174+C184+C194) + a4*(C204+C214+C224+C234);
Ccalc170 = a0 + a1*(C86+C96+C106+C116) + a2*(C126+C136+C146+C156) +
a3*(C166+C176+C186+C196) + a4*(C206+C216+C226+C236);
Ccalc190 = a0 + a1*(C88+C98+C108+C118) + a2*(C128+C138+C148+C158) +
a3*(C168+C178+C188+C198) + a4*(C208+C218+C228+C238);
Ccalc210 = a0 + a1*(C810+C910+C1010+C1110) +
a2*(C1210+C1310+C1410+C1510) + a3*(C1610+C1710+C1810+C1910) +
a4*(C2010+C2110+C2210+C2310);

C91 = 5.86;          C101 = 8.09;
C111 = 8.82;          C121 = 9.37;

```

C131 = 9.54;	C141 = 8.37;
C151 = 8.05;	C161 = 7.96;
C171 = 7.38;	C181 = 7.54;
C93 = 6.94;	C103 = 8.97;
C113 = 9.77;	C123 = 10.17;
C133 = 10.59;	C143 = 9.99;
C153 = 9.31;	C163 = 8.23;
C173 = 8.17;	C183 = 5.66;
C95 = 1.61;	C105 = 8.78;
C115 = 10.42;	C125 = 10.9;
C135 = 11.75;	C145 = 10.88;
C155 = 10.01;	C165 = 8.68;
C175 = 8.17;	C185 = 6.41;
C97 = 0.00;	C107 = 2.18;
C117 = 10.39;	C127 = 11.83;
C137 = 12.76;	C147 = 12.03;
C157 = 10.31;	C167 = 10.27;
C177 = 9.81;	C187 = 6.84;
C99 = 0.00;	C109 = 0.00;
C119 = 3.6;	C129 = 12.57;
C139 = 14.06;	C149 = 13.04;
C159 = 11.91;	C169 = 10.81;
C179 = 10.58;	C189 = 7.92;
C911 = 0.00;	C1011 = 0.00;
C1111 = 0.00;	C1211 = 7.03;
C1311 = 15.66;	C1411 = 15.4;
C1511 = 14.07;	C1611 = 11.87;
C1711 = 11.6;	C1811 = 8.06;
C92 = 7.73;	C102 = 9.26;
C112 = 9.6;	C122 = 10.17;
C132 = 10.4;	C142 = 9.95;
C152 = 9.15;	C162 = 8.12;
C172 = 7.52;	C182 = 5.46;
C94 = 4.19;	C104 = 8.91;
C114 = 9.85;	C124 = 10.4;
C134 = 11.16;	C144 = 10.3;
C154 = 9.52;	C164 = 8.39;
C174 = 8.08;	C184 = 6.29;
C96 = 0.00;	C106 = 6.83;
C116 = 11.05;	C126 = 11.81;
C136 = 12.0;	C146 = 11.0;
C156 = 10.30;	C166 = 9.21;
C176 = 8.64;	C186 = 6.57;
C98 = 0.00;	C108 = 0.57;

```

C118 = 7.89;          C128 = 12.49;
C138 = 13.26;         C148 = 12.3;
C158 = 11.2;          C168 = 10.57;
C178 = 10.2;          C188 = 7.28;

C910 = 0.00;          C1010 = 0.00;
C1110 = 0.78;         C1210 = 9.79;
C1310 = 15.22;        C1410 = 14.81;
C1510 = 12.87;        C1610 = 11.49;
C1710 = 10.75;        C1810 = 7.9;

```

! Calculating new regression Coefficients for the simple linear equation to calculate Density using carbon number Grouping for Heavy GTL Diesel Cuts;

```

Min = ((DmeasuredGTL - DcalcGTL)^2 + (Dmeasured140 - Dcalc140)^2 + (Dmeasured160 -
Dcalc160)^2 + (Dmeasured180 - Dcalc180)^2 + (Dmeasured200 - Dcalc200)^2 +
(Dmeasured215 - Dcalc215)^2)^0.5;

```

```

DmeasuredGTL = 752.4;
Dmeasured140 = 753.6;
Dmeasured160 = 757.2;
Dmeasured180 = 760.8;
Dmeasured200 = 763.8;
Dmeasured215 = 766.4;

```

```

@free(a0);           @free(a1);
@free(a2);           @free(a3);
@free(a4);

```

```

DcalcGTL = a0 + a1*(C81+C91+C101+C111) + a2*(C121+C131+C141+C151) +
a3*(C161+C171+C181+C191) + a4*(C201+C211+C221+C231);
Dcalc140 = a0 + a1*(C83+C93+C101+C113) + a2*(C123+C133+C143+C153) +
a3*(C163+C173+C183+C193) + a4*(C203+C213+C223+C233);
Dcalc160 = a0 + a1*(C85+C95+C105+C115) + a2*(C125+C135+C145+C155) +
a3*(C165+C175+C185+C195) + a4*(C205+C215+C225+C235);
Dcalc180 = a0 + a1*(C87+C97+C107+C117) + a2*(C1217+C137+C147+C157) +
a3*(C167+C177+C187+C197) + a4*(C201+C211+C221+C237);
Dcalc200 = a0 + a1*(C89+C99+C109+C119) + a2*(C129+C139+C149+C159) +
a3*(C169+C179+C189+C199) + a4*(C209+C219+C229+C239);
Dcalc215 = a0 + a1*(C811+C911+C1011+C1111) +
a2*(C1211+C1311+C1411+C1511) + a3*(C1611+C1711+C1811+C1911) +
a4*(C2011+C2111+C2211+C2311);

```

```

A0 =      477.8303;
A1 =      2.502963;
A2 =      2.736700;
A3 =      3.638611;
A4 =      1.134588;

```

```

Dcalc130 = a0 + a1*(C82+C92+C102+C112) + a2*(C122+C132+C142+C152) +
a3*(C162+C172+C182+C192) + a4*(C202+C212+C222+C232);
Dcalc150 = a0 + a1*(C84+C94+C104+C114) + a2*(C124+C134+C144+C154) +
a3*(C164+C174+C184+C194) + a4*(C204+C214+C224+C234);
Dcalc170 = a0 + a1*(C86+C96+C106+C116) + a2*(C126+C136+C146+C156) +
a3*(C166+C176+C186+C196) + a4*(C206+C216+C226+C236);
Dcalc190 = a0 + a1*(C88+C98+C108+C118) + a2*(C128+C138+C148+C158) +
a3*(C168+C178+C188+C198) + a4*(C208+C218+C228+C238);
Dcalc210 = a0 + a1*(C810+C910+C1010+C1110) +
a2*(C1210+C1310+C1410+C1510) + a3*(C1610+C1710+C1810+C1910) +
a4*(C2010+C2110+C2210+C2310);

C91 = 5.86;          C101 = 8.09;
C111 = 8.82;         C121 = 9.37;
C131 = 9.54;         C141 = 8.37;
C151 = 8.05;         C161 = 7.96;
C171 = 7.38;         C181 = 7.54;

C93 = 6.94;          C103 = 8.97;
C113 = 9.77;         C123 = 10.17;
C133 = 10.59;        C143 = 9.99;
C153 = 9.31;         C163 = 8.23;
C173 = 8.17;         C183 = 5.66;

C95 = 1.61;          C105 = 8.78;
C115 = 10.42;        C125 = 10.9;
C135 = 11.75;        C145 = 10.88;
C155 = 10.01;        C165 = 8.68;
C175 = 8.17;         C185 = 6.41;

C97 = 0.00;          C107 = 2.18;
C117 = 10.39;        C127 = 11.83;
C137 = 12.76;        C147 = 12.03;
C157 = 10.31;        C167 = 10.27;
C177 = 9.81;         C187 = 6.84;

C99 = 0.00;          C109 = 0.00;
C119 = 3.6;           C129 = 12.57;
C139 = 14.06;         C149 = 13.04;
C159 = 11.91;         C169 = 10.81;
C179 = 10.58;         C189 = 7.92;

C911 = 0.00;         C1011 = 0.00;
C1111 = 0.00;         C1211 = 7.03;
C1311 = 15.66;        C1411 = 15.4;
C1511 = 14.07;        C1611 = 11.87;
C1711 = 11.6;          C1811 = 8.06;

C92 = 7.73;          C102 = 9.26;
C112 = 9.6;           C122 = 10.17;
C132 = 10.4;          C142 = 9.95;
C152 = 9.15;          C162 = 8.12;
C172 = 7.52;          C182 = 5.46;

```

```

C94 = 4.19;          C104 = 8.91;
C114 = 9.85;         C124 = 10.4;
C134 = 11.16;        C144 = 10.3;
C154 = 9.52;         C164 = 8.39;
C174 = 8.08;         C184 = 6.29;

C96 = 0.00;          C106 = 6.83;
C116 = 11.05;        C126 = 11.81;
C136 = 12.0;          C146 = 11.0;
C156 = 10.30;        C166 = 9.21;
C176 = 8.64;          C186 = 6.57;

C98 = 0.00;          C108 = 0.57;
C118 = 7.89;         C128 = 12.49;
C138 = 13.26;        C148 = 12.3;
C158 = 11.2;          C168 = 10.57;
C178 = 10.2;          C188 = 7.28;

C910 = 0.00;         C1010 = 0.00;
C1110 = 0.78;        C1210 = 9.79;
C1310 = 15.22;       C1410 = 14.81;
C1510 = 12.87;       C1610 = 11.49;
C1710 = 10.75;       C1810 = 7.9;

```

! Calculating new regression Coefficients for the simple linear equation to calculate Dynamic Viscosity using carbon number Grouping for Heavy GTL Diesel Cuts;

**Min = ((DVmeasuredGTL - DVcalcGTL)^2 + (DVmeasured140 - DVcalc140)^2 +
(DVmeasured160 - DVcalc160)^2 + (DVmeasured180 - DVcalc180)^2 + (DVmeasured200 -
DVcalc200)^2 + (DVmeasured215 - DVcalc215)^2)^0.5;**

```

DVmeasuredGTL = 1.672;
DVmeasured140 = 1.7287;
DVmeasured160 = 1.9317;
DVmeasured180 = 2.1428;
DVmeasured200 = 2.3729;
DVmeasured215 = 2.578;

@free(a0);           @free(a1);
@free(a2);           @free(a3);
@free(a4);

DVcalcGTL = a0 + a1*(C81+C91+C101+C111) + a2*(C121+C131+C141+C151) +
a3*(C161+C171+C181+C191) + a4*(C201+C211+C221+C231);
DVcalc140 = a0 + a1*(C83+C93+C101+C113) + a2*(C123+C133+C143+C153) +
a3*(C163+C173+C183+C193) + a4*(C203+C213+C223+C233);
DVcalc160 = a0 + a1*(C85+C95+C105+C115) + a2*(C125+C135+C145+C155) +
a3*(C165+C175+C185+C195) + a4*(C205+C215+C225+C235);

```

```

DVcalc180 = a0 + a1*(C87+C97+C107+C117) + a2*(C1217+C137+C147+C157) +
a3*(C167+C177+C187+C197) + a4*(C201+C211+C221+C237);
DVcalc200 = a0 + a1*(C89+C99+C109+C119) + a2*(C129+C139+C149+C159) +
a3*(C169+C179+C189+C199) + a4*(C209+C219+C229+C239);
DVcalc215 = a0 + a1*(C811+C911+C1011+C1111) +
a2*(C1211+C1311+C1411+C1511) + a3*(C1611+C1711+C1811+C1911) +
a4*(C2011+C2111+C2211+C2311);

a0 = -15.04641;
a1 = 0.1514898;
a2 = 0.1578198;
a3 = 0.2443232;
a4 = 0.4089467E-01;

DVcalc130 = a0 + a1*(C82+C92+C102+C112) + a2*(C122+C132+C142+C152) +
a3*(C162+C172+C182+C192) + a4*(C202+C212+C222+C232);
DVcalc150 = a0 + a1*(C84+C94+C104+C114) + a2*(C124+C134+C144+C154) +
a3*(C164+C174+C184+C194) + a4*(C204+C214+C224+C234);
DVcalc170 = a0 + a1*(C86+C96+C106+C116) + a2*(C126+C136+C146+C156) +
a3*(C166+C176+C186+C196) + a4*(C206+C216+C226+C236);
DVcalc190 = a0 + a1*(C88+C98+C108+C118) + a2*(C128+C138+C148+C158) +
a3*(C168+C178+C188+C198) + a4*(C208+C218+C228+C238);
DVcalc210 = a0 + a1*(C810+C910+C1010+C1110) +
a2*(C1210+C1310+C1410+C1510) + a3*(C1610+C1710+C1810+C1910) +
a4*(C2010+C2110+C2210+C2310);

C91 = 5.86; C101 = 8.09;
C111 = 8.82; C121 = 9.37;
C131 = 9.54; C141 = 8.37;
C151 = 8.05; C161 = 7.96;
C171 = 7.38; C181 = 7.54;

C93 = 6.94; C103 = 8.97;
C113 = 9.77; C123 = 10.17;
C133 = 10.59; C143 = 9.99;
C153 = 9.31; C163 = 8.23;
C173 = 8.17; C183 = 5.66;

C95 = 1.61; C105 = 8.78;
C115 = 10.42; C125 = 10.9;
C135 = 11.75; C145 = 10.88;
C155 = 10.01; C165 = 8.68;
C175 = 8.17; C185 = 6.41;

C97 = 0.00; C107 = 2.18;
C117 = 10.39; C127 = 11.83;
C137 = 12.76; C147 = 12.03;
C157 = 10.31; C167 = 10.27;
C177 = 9.81; C187 = 6.84;

C99 = 0.00; C109 = 0.00;
C119 = 3.6; C129 = 12.57;
C139 = 14.06; C149 = 13.04;

```

```

C159 = 11.91;      C169 = 10.81;
C179 = 10.58;      C189 = 7.92;

C911 = 0.00;        C1011 = 0.00;
C1111 = 0.00;        C1211 = 7.03;
C1311 = 15.66;        C1411 = 15.4;
C1511 = 14.07;        C1611 = 11.87;
C1711 = 11.6;        C1811 = 8.06;

C92 = 7.73;          C102 = 9.26;
C112 = 9.6;          C122 = 10.17;
C132 = 10.4;          C142 = 9.95;
C152 = 9.15;          C162 = 8.12;
C172 = 7.52;          C182 = 5.46;

C94 = 4.19;          C104 = 8.91;
C114 = 9.85;          C124 = 10.4;
C134 = 11.16;          C144 = 10.3;
C154 = 9.52;          C164 = 8.39;
C174 = 8.08;          C184 = 6.29;

C96 = 0.00;          C106 = 6.83;
C116 = 11.05;          C126 = 11.81;
C136 = 12.0;          C146 = 11.0;
C156 = 10.30;          C166 = 9.21;
C176 = 8.64;          C186 = 6.57;

C98 = 0.00;          C108 = 0.57;
C118 = 7.89;          C128 = 12.49;
C138 = 13.26;          C148 = 12.3;
C158 = 11.2;          C168 = 10.57;
C178 = 10.2;          C188 = 7.28;

C910 = 0.00;          C1010 = 0.00;
C1110 = 0.78;          C1210 = 9.79;
C1310 = 15.22;          C1410 = 14.81;
C1510 = 12.87;          C1610 = 11.49;
C1710 = 10.75;          C1810 = 7.9;

```

! Calculating new regression Coefficients for the simple linear equation to calculate Flash Point using carbon number Grouping for Heavy GTL Diesel Cuts;

Min = ((FmeasuredGTL - FcalcGTL)^2 + (Fmeasured140 - Fcalc140)^2 + (Fmeasured160 - Fcalc160)^2 + (Fmeasured180 - Fcalc180)^2 + (Fmeasured200 - Fcalc200)^2 + (Fmeasured215 - Fcalc215)^2)^0.5;

```

FmeasuredGTL = 58;
Fmeasured140 = 63;
Fmeasured160 = 77;
Fmeasured180 = 91;
Fmeasured200 = 103;

```

```

Fmeasured215 = 113;

@free(a0);          @free(a1);
@free(a2);          @free(a3);
@free(a4);

FcalcGTL = a0 + a1*(C81+C91+C101+C111) + a2*(C121+C131+C141+C151) +
a3*(C161+C171+C181+C191) + a4*(C201+C211+C221+C231);
Fcalc140 = a0 + a1*(C83+C93+C101+C113) + a2*(C123+C133+C143+C153) +
a3*(C163+C173+C183+C193) + a4*(C203+C213+C223+C233);
Fcalc160 = a0 + a1*(C85+C95+C105+C115) + a2*(C125+C135+C145+C155) +
a3*(C165+C175+C185+C195) + a4*(C205+C215+C225+C235);
Fcalc180 = a0 + a1*(C87+C97+C107+C117) + a2*(C1217+C137+C147+C157) +
a3*(C167+C177+C187+C197) + a4*(C201+C211+C221+C237);
Fcalc200 = a0 + a1*(C89+C99+C109+C119) + a2*(C129+C139+C149+C159) +
a3*(C169+C179+C189+C199) + a4*(C209+C219+C229+C239);
Fcalc215 = a0 + a1*(C811+C911+C1011+C1111) +
a2*(C1211+C1311+C1411+C1511) + a3*(C1611+C1711+C1811+C1911) +
a4*(C2011+C2111+C2211+C2311);

a0 =      -985.1677;
a1 =      9.469443;
a2 =      10.45296;
a3 =      13.81209;
a4 =      4.253735;

Fcalc130 = a0 + a1*(C82+C92+C102+C112) + a2*(C122+C132+C142+C152) +
a3*(C162+C172+C182+C192) + a4*(C202+C212+C222+C232);
Fcalc150 = a0 + a1*(C84+C94+C104+C114) + a2*(C124+C134+C144+C154) +
a3*(C164+C174+C184+C194) + a4*(C204+C214+C224+C234);
Fcalc170 = a0 + a1*(C86+C96+C106+C116) + a2*(C126+C136+C146+C156) +
a3*(C166+C176+C186+C196) + a4*(C206+C216+C226+C236);
Fcalc190 = a0 + a1*(C88+C98+C108+C118) + a2*(C128+C138+C148+C158) +
a3*(C168+C178+C188+C198) + a4*(C208+C218+C228+C238);
Fcalc210 = a0 + a1*(C810+C910+C1010+C1110) +
a2*(C1210+C1310+C1410+C1510) + a3*(C1610+C1710+C1810+C1910) +
a4*(C2010+C2110+C2210+C2310);

C91 = 5.86;          C101 = 8.09;
C111 = 8.82;         C121 = 9.37;
C131 = 9.54;         C141 = 8.37;
C151 = 8.05;         C161 = 7.96;
C171 = 7.38;         C181 = 7.54;

C93 = 6.94;          C103 = 8.97;
C113 = 9.77;         C123 = 10.17;
C133 = 10.59;        C143 = 9.99;
C153 = 9.31;         C163 = 8.23;
C173 = 8.17;         C183 = 5.66;

C95 = 1.61;          C105 = 8.78;
C115 = 10.42;        C125 = 10.9;
C135 = 11.75;        C145 = 10.88;

```

C155 = 10.01;	C165 = 8.68;
C175 = 8.17;	C185 = 6.41;
C97 = 0.00;	C107 = 2.18;
C117 = 10.39;	C127 = 11.83;
C137 = 12.76;	C147 = 12.03;
C157 = 10.31;	C167 = 10.27;
C177 = 9.81;	C187 = 6.84;
C99 = 0.00;	C109 = 0.00;
C119 = 3.6;	C129 = 12.57;
C139 = 14.06;	C149 = 13.04;
C159 = 11.91;	C169 = 10.81;
C179 = 10.58;	C189 = 7.92;
C911 = 0.00;	C1011 = 0.00;
C1111 = 0.00;	C1211 = 7.03;
C1311 = 15.66;	C1411 = 15.4;
C1511 = 14.07;	C1611 = 11.87;
C1711 = 11.6;	C1811 = 8.06;
C92 = 7.73;	C102 = 9.26;
C112 = 9.6;	C122 = 10.17;
C132 = 10.4;	C142 = 9.95;
C152 = 9.15;	C162 = 8.12;
C172 = 7.52;	C182 = 5.46;
C94 = 4.19;	C104 = 8.91;
C114 = 9.85;	C124 = 10.4;
C134 = 11.16;	C144 = 10.3;
C154 = 9.52;	C164 = 8.39;
C174 = 8.08;	C184 = 6.29;
C96 = 0.00;	C106 = 6.83;
C116 = 11.05;	C126 = 11.81;
C136 = 12.0;	C146 = 11.0;
C156 = 10.30;	C166 = 9.21;
C176 = 8.64;	C186 = 6.57;
C98 = 0.00;	C108 = 0.57;
C118 = 7.89;	C128 = 12.49;
C138 = 13.26;	C148 = 12.3;
C158 = 11.2;	C168 = 10.57;
C178 = 10.2;	C188 = 7.28;
C910 = 0.00;	C1010 = 0.00;
C1110 = 0.78;	C1210 = 9.79;
C1310 = 15.22;	C1410 = 14.81;
C1510 = 12.87;	C1610 = 11.49;
C1710 = 10.75;	C1810 = 7.9;

APPENDIX D – LINGO CALCULATIONS RESULTS

Table D-1 Cloud point calculation using LINGO with various methods

Cloud Point	Measured	Distillation	(i-n)Paraffin	Individual CN	CN Grouping
GTL	-5.7	-5.69	-5.69	-5.70	-5.70
>130	-5.7	-3.98	-1.87	-50.56	-5.95
>140	-5.1	-5.09	-2.23	-5.10	-5.10
>150	-4.9	-4.81	-2.23	10.84	-4.84
>160	-4.6	-4.59	-4.60	-4.60	-4.60
>170	-3.5	-3.98	-2.52	-73.17	-3.91
>180	-2.8	-2.79	-2.56	-2.80	-2.80
>190	-2.1	-2.63	-2.42	-59.65	-2.13
>200	-1.3	-1.29	-2.51	-1.30	-1.30
>210	-0.4	-0.63	-2.11	26.18	-0.63
>215	-0.2	-0.19	-2.11	-0.20	-0.20

Table D-2 Density calculation using LINGO with various methods

Density	Measured	(i-n)Paraffin	Individual CN	CN Grouping
GTL	767.4	767.5	767.4	767.4
>130	767.7	777.6	706.3	769.5
>140	768.7	776.7	768.7	768.7
>150	770.4	776.7	780.9	771.8
>160	772.3	772.3	772.3	772.3
>170	773.7	775.9	750.0	773.7
>180	776.0	775.8	776.0	776.0
>190	777.4	776.2	747.6	777.4
>200	779.1	775.9	779.1	779.1
>210	780.8	777.0	760.8	780.6
>215	781.7	777.0	781.7	781.7

Table D-3 Dynamic viscosity calculation using LINGO with various methods

Dynamic Viscosity	Measured	(i-n)Paraffin	Individual CN	CN Grouping
GTL	1.67	1.68	767.4	1.67
>130	1.68	1.48	706.3	1.75
>140	1.73	2.17	768.7	1.73
>150	1.81	1.50	780.9	1.92
>160	1.93	1.95	772.3	1.93
>170	2.01	1.52	750	2.02
>180	2.14	2.24	776	2.14
>190	2.24	1.51	747.6	2.27
>200	2.37	2.23	779.1	2.37
>210	2.52	1.49	760.8	2.47
>215	2.58	2.15	781.7	2.58

Table D-4 Flash point calculation using LINGO with various methods

Flash Point	Measured	(i-n)Paraffin	Individual CN	CN Grouping
GTL	58	58.4	58.0	58.0
>130	59	97.3	59.9	66.0
>140	63	93.7	63.0	63.0
>150	70	93.6	70.3	75.0
>160	77	77.0	77.0	77.0
>170	82	90.7	81.3	82.3
>180	91	90.2	91.0	91.0
>190	96	91.7	96.5	96.4
>200	103	90.8	103.0	103.0
>210	110	94.9	109.7	108.8
>215	113	94.9	113.0	113.0